

出國報告（出國類別：進修）

97 年國外進修出國報告

英國諾丁漢大學 大地工程碩士課程及專題研究報告

服務機關：台灣電力公司 輸變電工程處 南區施工處

姓名職稱：土木工程師 蔡明達

派赴國家：英國

出國期間：97 年 09 月 15 日 ~ 98 年 08 月 29 日

報告日期：98 年 10 月 30 日

摘要

近來因溫室氣導致之全球暖化可能性提高，隨之而來的劇烈天候變化，將對基礎建設造成重大影響，本公司為台灣基礎建設重要的一環，基礎建設中最先開始要面對的就是基礎工程的問題，大地工程所研究的範圍以此為主軸，這也是土木工程中較為新興的範疇。

本次進修的科目選擇諾丁漢大學(The University of Nottingham)土木工程系之大地工程。課程包含大地工程(Geotechnical Engineering)、海岸工程(Coastal Engineering)、營建規劃與風險(Construction Planning & Risk)、有限元素分析法在結構力學之應用(Finite element analysis in Structure Mechanics)、土木工程之研究準備(Civil Engineering Research Preparation)、在春季的學期有土壤力學(Soil mechanics)、版與殼(Plates and shells)、鐵路工程(Railway Engineering)、交通工程(Traffic engineering)、研究計畫之組織與設計(Civil Engineering Research Project Organisation and Design)，暑期則執行專案計畫，主題為 Stress-strain behaviour of cemented sand。

英國之大地工程之設計規範與我國之建築物基礎構造設計規範，設計之原理及考量大致相同，但在細節上仍有值得借鏡之處，如擋土牆設計時加入非預期之開挖狀況，可有效提高施工時之安全性。

目錄

第壹章 進修目的與過程	1
1.1 進修目的.....	1
1.2 進修過程.....	1
1.2.1 進修時程.....	1
1.2.2 進修前準備.....	2
1.2.3 進修國家、學制與學校概述.....	3
1.2.4 進修課程摘述.....	5
1.2.5 專題研究: Stress-strain behaviour of cemented sand.....	8
第貳章 進修心得、感想與出國期間遭逢之事項	10
2.1 語言學習.....	10
2.2 課程學習.....	10
2.3 專題研究.....	11
2.4 文化與生活.....	13
第參章 具體建議	15
附錄—專題報告: Stress-strain behaviour of cemented sand	

第壹章

進修目的與過程

1.1 進修目的

筆者於 96 年底經資格篩選及本處主管同意推薦，參與「97 年度『菁英留學計畫推動方案』選派人員赴國外進博、碩士學位實施方案」之甄選。該方案係配合行政院「菁英留學計畫推動方案」選送人員出國進修碩士以上學位，為培育具有潛力人員，並鼓勵研究發展風氣，以提高營運績效。

在 97 年 3 月 26 日參加評選委員會議簡報面試，且於 97 年 4 月 2 日獲通知為正取人員。申請進修國家為英國，申請進修學校為諾丁漢大學 (The University of Nottingham)，申請進修學位為大地工程碩士 (Master of Science in Civil Engineering : Geotechnical Engineering)。

奉准進修人員可獲得的協助有：(1)、於進修期間帶職帶薪，(2)、補助申請學校(3 所)所需之測驗及申請費，(3)、學雜費檢據核實補助，(4)、生活費補助(1150 美金/月)，(5)、綜合補助及健康保險補助 (150 美金/月)，(6)、進修所需往返機票。

奉准進修人員應配合履行之義務及限制為：(1)、97 年 12 月 31 日前成行。(2)、進修年限為 2 年。(3)、每學期將撰寫心得及成績單寄回人力資源處。(4)、返國 2 個月內提出進修報告。(5)、返國後義務服務期限按出國支領公費期間加 2 倍計算。(6)、遭學校開除、非因重大事故自行中止、或逾進修年限或學期成績 2 科以上不及格且未即返國服務以及進修期工作將遭追償費用。

1.2 進修過程

1.2.1 進修時程

進修由 97 年 09 月 15 日出發起至 98 年 8 月 29 日返國，總計 349 天。第一星期之 Welcome program 為環境介紹及環境適應課程。正式課程由 97 年 9 月 22 日至 98 年 8 月 29 日，分為秋季、春季、夏季三個學期及暑假期間四個部份。詳細之時程內容詳表 1.1。

表 1.1 進修時程表

時程	名稱	內容
97.09.15	出發	
97.09.16~97.09.21	Welcome Program	環境介紹及環境適應
97.09.22~97.12.12	秋季學期	教學
97.12.13~98.01.11	聖誕節假期	課程復習自修及評量準備
98.01.12~98.03.20	春季學期	教學及評量
98.03.21~98.04.19	復活節假期	課程復習自修及評量準備
98.04.20~98.06.19	夏季學期	教學及評量
98.06.20~98.08.28	暑期	專案及論文撰寫
97.08.29	返國	

1.2.2 進修前準備

進修前準備概分為: (1)、語言考試準備。 (2)、學校申請。 (4)、財務安排。分述如下:

(1)、語言考試 IELTS 準備

申請英國學校需要準備的為 IELTS 考試成績。其原是英國當局針對留學生而設的英語能力檢定測驗，自 1990 年更名為 The International English Language Testing System, 簡稱為 IELTS(雅思)。在英國澳紐等英語為主要語言的國家就學、移民、工作等，都需在申請時提供 IELTS 成績證明英文能力。IELTS 測驗內容涵蓋聽、說、讀、寫四個項目，分別以 0~9 分來評定程度，愈高愈佳。再依四個分項結果平均後得總體的結果。經查詢土木工程相關科系所需 IELTS 成績約在 6~6.5 分間。

(2)、學校申請

此部份則請英國留學代辦協助，因其以收取學校傭金為主，故所有諮詢及服務基本是免費的，可請其提供相關學校申請之資料，並請其預作篩選，亦可提供申請時程

之規劃與申請文件之撰寫修改服務。此外也會幫忙線上申請文件及簽證申請文件之代填、學校宿舍申請，生活及學習經驗亦可提供諮詢。

學校申請應準備之主要文件有成績單、自傳及二封推薦信。筆者以符合申請規定之相關科系、取得之語言成績要求及學校排名在前 20 名內等兩大要件為主要考量，經篩選後正式提出申請者有四間，為 Imperial College London、The University of Nottingham、Newcastle University Upon Tyde 及 University College London，相關排名詳如表 1.2 所示。

表 1.2 正式申請學校及排名

申請學校(土木工程相關研究所)	全英研究排名 (RAE 2008)	全英排行 (Guardian/2009)	全英排行 (Times/2009)
Imperial College London	1	1	2
The University of Nottingham	4	5	10
Newcastle University Upon Tyde	5	15	14
University College London	14	12	17

上述初期均取得條件核可函(Conditional offer)，惟 The University of Nottingham 於語言成績提供後，同意給予無條件核可函(Unconditional offer)，故最後決定前往該校就讀。

(3)、財務安排

主要感謝公司提供出國費用借支，方便申請人著手安排作業前期計畫，申請人可於出國前 3 工作天辦理出國旅費借支，待相關文件核可後，至人力資源處辦理出國計畫行程核可及預借旅費借據。其後至會計處開立傳單，至台銀領取借支支票，可借支費用包含其後辦理保險、學雜費、一年生活費及往返機票費用。

1.2.3 進修國家、學制與學校概述

進修國家:英國

英國主要由四個構成國家組成，分別是英格蘭、蘇格蘭、威爾斯和北愛爾蘭，加上一系列附屬島嶼共同組成。距台灣約 9700 餘公里，飛機航程約 14 小時。人口約 6120 萬，約為台灣的 2.7 倍，面積 244,820 平方公里，約為台灣的 6.8 倍，與台灣時差 7 至 8 小時。

學制及進修學位

英國高等教育修業年限為大學 3 年、碩士(教學型)1 年、博士 3 年以上。

本次申請為教學式碩士課程(by course work)，其修業期間為一年，課程結合課堂授課制，研討會，導師教學制的授課方式，最後三個月用來做研究並撰寫畢業論文(Dissertation)或研究報告(Project)(約一萬到一萬五千字)。至於評分方面包括每學期的短篇報告(Essays, 3000-5000 字)及期末考試。

研究所時程分為秋季、春季、夏季及暑期四個階段，詳表 1.3。秋季及春季各修習 60 個學分，每門課 10~20 個學分。暑期執行專案計畫 60 個學分。總計 180 個學分。

表 1.3 課程時程表

學期	期間	內容
秋季	97 年 09 月 22 日 97 年 12 月 12 日	教學
春季	98 年 01 月 12 日 98 年 03 月 20 日	教學及評量
夏季	98 年 04 月 20 日 98 年 06 月 19 日	教學及評量
暑期	98 年 06 月 20 日 98 年 08 月 28 日	專案及論文

就讀學校

此次就讀學校為諾丁漢大學，位於中英格蘭地區。全校約有 36,000 名學生，含超過來自 145 個國家的 7,500 的國際學生。原中國上海復旦大學校長楊福家現為該校校長，而副校長則由 Colin Campbell 擔任。學校有 6 個學院，包括有文學院、工學院、教育學院、法學暨社會學院、理學院、醫學暨健康學院。教職員有 5000 人。海外有兩所分校，分別位於馬來西亞吉隆坡及中國寧波市。

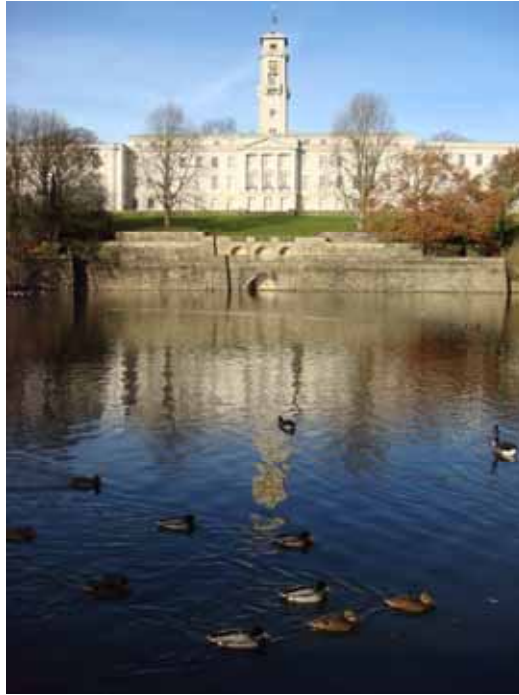


圖 1.1 諾丁罕大學校園一隅

1.2.4 進修課程摘述

本次總計修習之課程在秋季的學期有大地工程(Geotechnical Engineering)、海岸工程(Coastal Engineering)、營建規劃與風險(Construction Planning & Risk)、有限元素分析法在結構力學之應用(Finite element analysis in Structure Mechanics)、土木工程之研究準備(Civil Engineering Research Preparation)、在春季的學期有土壤力學(Soil mechanics)、版與殼(Plates and shells)、鐵路工程(Railway Engineering)、交通工程(Traffic engineering)、研究計畫之組織與設計(Civil Engineering Research Project Organisation and Design)，各課程詳細說明如下。

大地工程 (Geotechnical Engineering) :

本課程包含探討基礎工程中之淺基礎，深基礎，擋框架式和加勁土壤擋土牆，堤岸及堤岸壩之各項概念。授課內容包含淺基礎承載力、基礎底面之應力分佈分析、沈陷量分析、現地試驗、側向土壓力、懸臂式擋土牆、加勁擋土牆、加勁邊坡、堤岸壩、單樁基礎軸向承載力、群樁基礎設計、單樁側向支承力、試樁、基樁施工瑕疵等。

海岸工程 (Coastal Engineering) :

本課程包含探討波浪與潮汐，漂沙及海浪復育以及海岸工程概念及管理。授課目標為了解實際波浪運動及模擬方式、實際的海岸變遷、如何簡化及解決海岸工程問題以及建構海岸工程之概念。授課內容為淺水波流體力學、波浪理論與設計、海岸變遷與形成、沙灘復育、引潮力、大潮小潮循環、氣象潮、潮汐共振、潮汐發電等。

營建規劃管理及風險評估 (Construction Planning & Risk) :

本課程包含進階營建管理技巧包含網圖(precedence networks)，平衡作業線(line-of-balance method)，時間-空間圖(space-time diagrams)，不確定性管理流程(management of uncertain processes)，風險管理(Risk management)等的各項概念及案例說明。本課程目標為了解網圖專案排程之技巧，線性及重複性工作之排程技巧，不確定性工作排程技巧及營建工程之風險管理之意義。授課主要分為進階網圖技巧，多種日曆工作排程技巧，工作排程中的不確定性，重複性專案規畫(如大樓興建)，線性專案規畫(如管線工程)，風險評估。

有限元素分析法在結構力學之應用 (Finite element analysis in Structure Mechanics) :

本課程包含介紹有限元素法且與其他數值方法比較，2D 應力、2D 應變、樑理論、潛能等之有限元素法之模擬方式。此外，平面元素之考量及 3D 有限元素法與實際設計應用之探討亦在授課範圍，另教導使用套裝軟體 ANSYS 及 MATLAB 進行有限元素法之模擬。

土木工程研究準備 (Civil Engineering Research Preparation)

本課程屬導師教學制(Tutorials)的授課方式，配合暑期專案進行，為其準備工作。主要內容為：(1)、回顧由導師提供與專案相關之三篇論文。(2)、利用文獻回顧提出現存的問題或須研究的議題及可能之解決方案。

土壤力學 (Soil mechanics)

本課程以討論土壤力學的極限狀態的準則及用來預測土壤行為的模型(Cam clay)，其可對土壤之彈性與塑性行為提供一個構架準則，並說明實務上應用。課程目標為發展土壤行為的構架準則，建立土壤行為的模型，並利用該模型解釋觀察到的試驗結果，進而利用該模型去預測土壤行為。授課內容包含：(1)、相關概念之複習。(2)、直剪試驗與三軸試驗。(3)、摩擦力與黏結力。(4)、發展彈性與塑性模型。(5)、彈塑性土壤模型--Cam clay 之推導。(6)、三軸應力路徑及採 Cam clay 模型預測。(7)、破裂與拉力破壞。(8)、砂土之行為。(9)、CSSM 和 Cam Clay 模型的應用。(10)、土壤之自然歷史。(11)土壤極限狀態之應用。

版與殼 (Plates and shells)

本課程包含二個部份，一是殼構造之薄膜理論，包含理論之推導及分析，亦介紹許多薄殼建築及實際薄殼模型的製作。二是板構造理論，亦包含理論之推導及分析、演算。

鐵路工程 (Railway Engineering) :

此課程主要為介紹軌道結構，包含實務上之應用在施工、監測及維護保養，相關之材料性質及行為模式如道渣及鐵軌，和軌道分析及軌道路線布設技巧亦一併介紹。最後，輕軌、捷運及運轉操作等皆在授課的範圍內。

交通工程 (Traffic engineering)

此課程主要目標為介紹管理控制都市路網之相關理論基礎，包含形成都市交通流量理論之基礎、交通流量資料之收集、交通訊號控制及決定交通流量分布之運輸模型。授課內容包含：(1)、基礎交通參數。(2)、基礎交通參數間之關係。

(3)、起點-目的之資料蒐集。(4)、交通號誌控制。(5)、運輸模擬。(6)、交通流量模擬。

研究計畫之組織與設計(Civil Engineering Research Project Organisation and Design)

此課程為土木工程研究準備之延伸，主要讓學生發展且界定暑期之專案研究計畫。本課程亦讓學生學習如何發表成果。包含在暑期會議時簡報及製作海報。

1.2.5 專題研究：Stress-Strain behaviours of cemented sands

本專題研究於 98 年 6 月至 8 月底，進行約三個月，內容包含文獻回顧、試驗儀器之學習及試驗流程之確定、研究範圍之界定以及論文之撰寫。以下概述研究內容，完整之論文請詳附錄 A。相關研究之內容，計畫發表於 2010 年 第 17 屆東南亞大地工程研討會中發表，目前已通過摘要審查。

論文摘述

依據文獻回顧發現，大部份的研究已經清楚指出了解天然及人工的膠結性沙土的重要性在各方面之應用。添加膠結性材料來改良現地的土壤的方式已廣泛的被使用，例如地盤改良以防止土壤液化，壩體之邊坡保護等。雖然有了各式各樣的實際應用，但迄今仍無合理的準則來評估強度。在自然界中存在的膠結性沙土，卻常常造成工程上的問題，尤其是膠結性碳酸沙土廣泛分布在熱帶及亞熱帶大陸棚區域，且該區域存在豐富石化原料的儲藏，故其相關之工程性質近來引起更多的關注。膠結性碳酸沙土通常有高壓縮性與相對低的密度，如此易造成非常低的打樁摩擦力，以及基礎發生較理論預估之沈陷量，例如 1982 年時西澳的西北處之 North Rankin 平台，在基樁設置時，即發生低於預期之摩擦力 (King & Lodge, 1988)。

有部份的研究取用現地天然膠結性碳酸沙土，但取樣過程容易擾動且現地的天然膠結性碳酸沙土分布，在膠結性及顆粒尺寸有很大差異性，故造成在研究方面的困難。為了避免上述困難，由人工調配的膠結性沙土已成為模擬天然膠結沙土的替代方案，此部份已有許多的研究證實。在最近的研究中，主要集中在傳統的圍壓範圍內 (< 1 MPa)，在較高的圍壓下的試驗結果大部份是在非膠結性沙土上。在不排水的狀況下，孔隙水壓力會大幅地增加進而造成液化、不穩定和破壞。在此狀況下的破壞常為驟然的，若此種破壞發生在重大的公共建設上，將造成人員傷亡及嚴重財物損失，故不排水狀況下之膠結性土壤行為十分重要。目前在高圍壓不排水狀況下的相關研究依

然十分欠缺，為進一步了解在高圍壓狀況下膠結土壤不排水行為與大地工程之應用，相關的試驗結果頗為需要。

本研究總共提出 8 組膠結性與非膠性結土壤分別在壓密不排水下進行三軸試驗。研究中採用之土壤為 Portaway 砂，膠結材料為波特蘭水泥。試驗主要利用諾丁漢大地力學中心(Nottingham Centre of Geomechanics) 的高圍壓三軸試驗系統(如圖 1.1)。

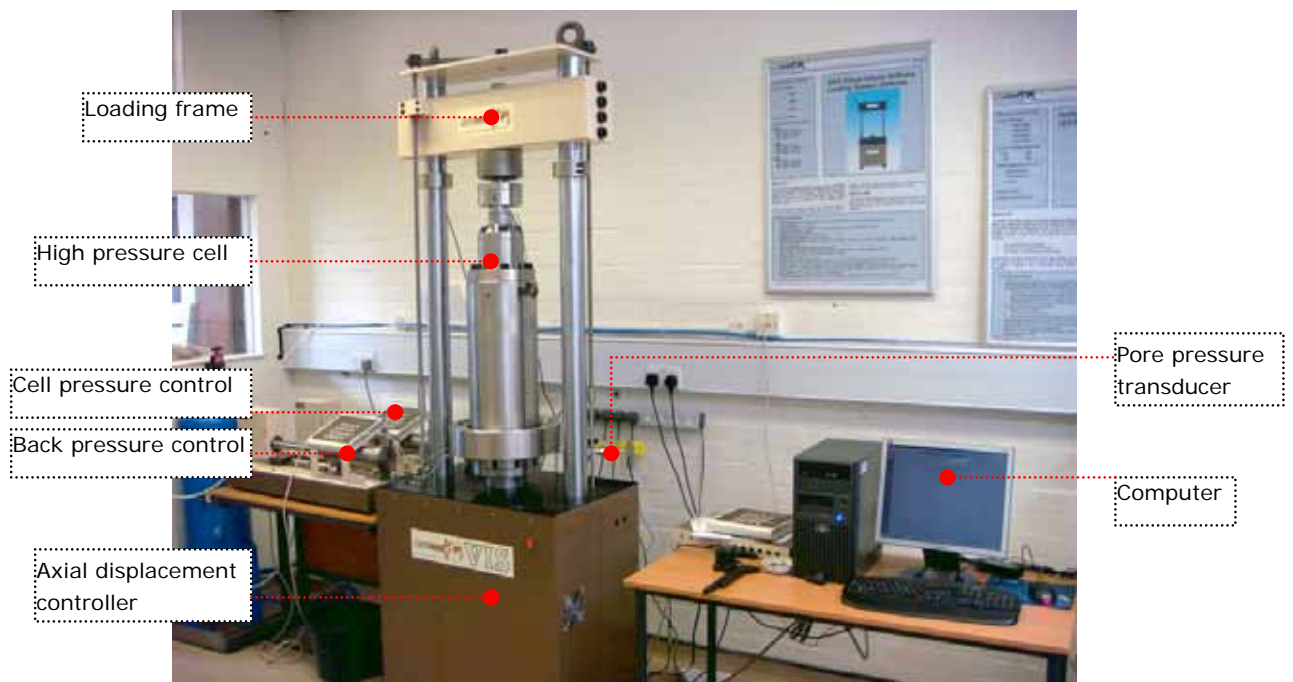


圖 1.1 高圍壓三軸系統

從研究結果中可以觀察到，較高的膠結材料含量、相對密度、圍壓和排水的狀況會導致較高的軸差應力及應力比。較高的膠結材料含量除了導致較高的軸差應力外，亦會讓尖峰之軸差應力較早發生。而土樣的相對密度、膠結材料之含量、及施加之圍壓大小及會影響超額孔隙水壓。

第貳章

進修心得與感想及出國期間遭逢事項

2.1 語言學習

出國進修，語言係重要因素，本次進修國家為英國，想當然爾英文為主要語言。惟國內所修習之英語，相關之教材其實是以美式之字彙及口音為主。期初誤以為二者均為英語，應無差異，但事實上仍有差距。如以聽、說、讀、寫來區分，聽與讀屬輸入端，說與寫為輸出端。一開始預期輸出端會有比較大的提昇的空間，但事實上輸入端亦有加強的空間。除字彙上拼法約略不同外，英式口音與美式口音的不同，在即時溝通上也會產生障礙，故在前期生活適應上，花費了一段時間才克服這些困擾。

由於申請出國時程上緊迫，並無餘裕的時間，安排提前一個月或二週來參加語言課程以進一步提昇語言之能力。惟學校學期中仍有免費的語言課程供國際學生參加。故在專業課程之外的時間，安排了學術寫作、學術簡報及論文寫作等課程。學期中的語言課程課堂上有來自不同地方之國際學生一同學習，配合申請的學生宿舍中的國際學生同住的生活環境，語言能力之提昇效果確較為顯著。故語言學習，其實不單單只是單字、文法或句型的記誦，其實是文化、生活溶入，學習才有意義。

2.2. 課程學習

在英國的授課方式，大致可概分為二個部份，一是課堂授業，針對某個專題開課供選讀，另一個是導師制度。

課堂授業

教學的型態其實與國內並無二致，課前之授課講義，上課時之投影片或POWERPOINT，課堂中之討論，課後作業及期末評量，除了是用英文書寫、進行之外，大致上皆與國內之教學型態相仿，但下列幾項除外。

所有的課程，教授均自行編寫教材及投影片進行教學，與國內指定教科書不同。好處是可不受單一本教科書之限制亦對相同的議題可以提供不同的觀點，且可減輕學生購買教科書之負擔。

此外，教育上十分關注重抄襲作弊等不公平的行為，每一份作業均要求學生於繳交前簽名，確認自己繳交的作業並無違反學校之抄襲條款。這一點在學術精神上的要求，由日常點滴來養成，與筆者以往之經驗亦較不同。由於現今之網路發達，相關之資料取得便利，常見學生為一時之便而摘取他人心血又不說明來源於何處，有違學術傳承之用意，故如此之作法，或可扼止抄襲，進而鼓勵研究創作。

課程本身包含了複習，且如同正式授課一般，除課程概要提示之外，教授逐一講解前幾年的考試題目(考古題)，此點與國內教學大相逕庭。國內的教學，通常在講授之後，除課後作業之外，授課老師幾乎不會花時間說明考古題，國外在課程內排入且授課教授重視複習及評量的作法，會引導學生重新去重視必要的課程內容。另一個要點，教授亦會花費時間，說明題目背後想要評試的要點為何，且詳述解題之程序及作法，讓學生可以清楚的明白面對問題應如何考量且何為正確的思考路徑，此為筆者體驗到與過去所受教育差異較大之處。

課程中，尚有機會去接觸英國的大地工程相關之設計規範(British Standard)，大致上與我國的建築物基礎構造設計規範範圍相仿，但有幾個細節上，筆者認為有值得借鏡之處，如擋土牆設計時加入非預期之開挖狀況，可有效提高施工時之安全性。

導師制度

現今之教育方式，主要是肇因於一百多年前工業革命之後產生的型態，讓大量的人可以在短時間內，獲取足夠的知識及技能後，馬上可以應付實際上之工作需求。但在工業革命之前，學問之傳授則是類似導師制度，這是值得注意的一點，英國是工業革命的發源地，但其教育系統中仍保有工業革命前的特徵。可以推論這是十分重要制度。

甫一開學，選課指導教授就說明學生與導師的相處是十分重要的事。導師在學期中，約略每週和學生見面一次，每次見面，學生針對導師所開書目或指定問題，準備研究心得或摘要，在師生研討過程中就文章論點進行討論，導師亦會進一步指示後續之研討方向。就筆者而言，初期在語言表達尚未融入英式英語時，導師給予許多直接的指正，對於語言之學習有明顯提昇的效果，另外亦可訓練邏輯思考及臨場反應能力。此外對於英國密集學期制的而言，導師可以隨時清晰的瞭解學生研習的情況，給予必要且即時的協助。

2.3 專題研究

專題研究相關之學分(100 credits)占有學分逾一半(180 credits)，可見專題研究為課程中的主軸，研究的主題在開學時可以選擇某個範疇，待其範疇選定後，學校會指定某教授為導師，其後之專題研究即與導師與學生商討訂定，但仍與教授目前仍進行之主題為主。

專題在第一個學期時的主要內容，由導師提供與專案相關之三篇論文開始，導師擇定之三篇，包含了與該項研究相關之十年內重要論文，目的是讓學生了解目前該項研究進行狀況。進而希望學生利用文獻回顧提出現存的問題或須研究的議題及可能之解決方案。在第二學期時要求學生發展且界定專案研究計畫，同時亦讓學生學習如何發表成果，包含簡報及製作海報。

筆者專題研究之主題為膠結性砂土之行為，同時有一名相關之博士班學生已在進行相關之研究，範圍集中在膠結性砂土之排水行為，故本次研究擇定在不排水的行為以期可擴展研究之範圍，及與排水行為比較。

研究儀器如圖 1.1 所示，因其發展為進行高圍壓之三軸為主，可達 64MPa，故其與一般之三軸室最大的不同為其三軸室為不銹鋼製，也因此二個比較危險的地方，其一是三軸室較重，需由天車吊運。其二是高圍壓本身即隱含危險成份存在。故在進行時需有實驗室技工或博士班學生在場。

暑期專期部份，主要分為三個主要的部份。第一是儀器學習使用及試體之製作，約略三週。第二個部份為實驗及結果分析，最後一個部份為論文撰寫。儀器是向博士班學生學習如果操作及使用，但仍有主要的差異在排水狀況。除筆者之外，另外仍有二名博士班學生要利用同樣的試驗儀器進行相關試驗，故有利於初期之學習，但期後自身的試驗時間安排反倒不易。

暑期專題時間的原本就捉襟見肘，每一個試驗試體製作完成及養護需二週，每一組試驗要二天，且試驗室不容許碩士生單獨待超過下午五點，所幸另二名博士生均十分勤奮，幾乎每日都在研究室中待至晚上才離開，周六日亦不例外。筆者大部份均配合他們在試驗室時間作息，如此得以完成大部份的試驗。二名博士班學生均來自巴基斯坦，皆為回教徒，一日要祈禱五次，故常在試驗中就必需離開試驗室，回到他們的研究室進行祈禱。與來自不同的國家的學生交流討論，有許多特別的感受。二人均十分珍惜進修的機會，但對未來有不同的規劃，一個是積極的完成學業想返國服務，一是想留下來在英國工作，落地生根。二個人均十分和善且對宗教十分虔誠，打破中東人即為恐怖分子的刻板印象。不同文化之某些思維亦有相通之處，某次在準備試驗

前，筆者問其中一人：「我的準備工作如何？這個試驗會成功嗎？」他回答：「Ishiala」筆者再問：「這是什麼意思？」他回答：「God wish.」意思是，我已經完成我應該做的事了，接下來成不成功就看真主阿拉的旨意了。有點像是我們常說的：「盡人事聽天命。」

後來仍有部份試驗無法完成，主因是儀器出現不明的漏水原因。加上已超過預計研究試驗的時間，且導師有於研討會發表的計畫，故在請示導師之後，同意就現有的資料分析及撰寫論文。

首次長篇英文論文(約 12,000 字)的撰寫，花費相當大的功夫。除了前期陸陸續續整理的資料，論文主體的撰寫花費 5~6 週的時間。過程中，與導師密切的討論並且其給予筆者充份的協助，讓筆者可以在時限內論文撰寫。撰寫長篇論文主要的訓練除了學術寫作本身以外，仍包含架構長篇論文的訓練及就既有資料之表達及論述能力。

2.4 文化與生活

由於課業十分的緊湊，故大部份生活的經驗來自宿舍生活。筆者所選擇的宿舍是學校與當地租賃公司合作辦理的，是六個人一個平面的。另外五個室友，分別來自義大利、印度、蘇丹、肯亞。這幾個國家在來英國唸書之前，對筆者而言只是地理名詞。

與我同住的義大利人有二個，一個叫 Nicola 修習法律，一個叫 Matteo 修習建築。就如同一般人對義大利的刻板印象一樣，兩人均十分熱情健談，常常帶著不同的朋友前來用餐。其中 Matteo 相當喜愛日本文化，甚至在手腕上刺上自己名字的片假名，每個星期也會閱讀日本的漫畫。印度人 Syed 是進修資管，他則是我學習英文的好對象，因為英文是印度的官方語言，常常和他對話讓我生活方面的英語會話有很大的進步，因為父親的工作關係，他其實是在沙烏地阿拉伯長大。來自蘇丹的 Ashiraf，是個醫生，是來自非洲大陸的黑人，一開始他不同的生活習慣，讓我十分的痛苦，後來才知道他在家中是有佣人，打掃、煮飯完全不用他動手，初期不同的衛生習慣，煮飯習慣常發生衝突，也會發生燒黑整個廚房之類的情形，但後來 Ashiraf 已經可以燒一手好菜，也偶而會把廚房打掃的一塵不染。來自肯亞 Azar 是進修商管，他其實是印度裔的肯亞人，住在我的隔壁，是個虔誠的回教徒，常常在不同的時刻聽他在祈禱。

在我們一個小小的宿舍中，就可以體會不同國家之間的文化衝突，這些衝突常常是許多不了解所造成，只要了解之後就會開始欣賞甚至喜歡。例如，我不一開始並不喜歡義大利人的 espresso 咖啡，覺得像在喝藥一般，後來經過幾次嘗試後，開始喜愛

其風味，甚至去買了摩卡壺自己每天煮二杯喝。而蘇丹人與眾不同的生活習慣，讓所有人不諒解，卻沒有人願意當面跟他溝通，取而代之的是背後不斷的抱怨，但是後來他慢慢的轉變，反而是他看不慣廚房客廳的髒亂而自己捲起袖子打掃一番。另一個地方就班級也可以看到，班上有十多個來自中國同學，一開始我不說，他們覺得我也是來自大陸。有些人對於某些兩岸的話題較為敏感，但長期下來，覺得大部份的人還是可以透過交流，增加了解來降低一些誤會的發生。

全球化的影響也在這兒可以看到影子，超市中可以便宜買到來自全世界的商品，來這兒進修的人，說著同樣的語言，大都想留下來工作。文化上的差異依然存在，但可以發現區域化的特色正慢慢消失。

居住的地區是 Raleigh Park 亦是體現這樣的變化，早期是著名的來禮自行車的生產地，頂盛時雇用了 8000 人，每年生產 200 萬台自行車，而我在現地除了雕塑或碑文之外，一點也感受不到任何有關的事物，值得一提是我們學校的一個校區 Jubilee campus，就是利用他的廠區復育後改建的，兼固自然景觀，十分優美怡人。



第肆章

具體建議

一、參考 BS 8002 Code practice for Earth retaining structures 相關之擋土設計規範考量加入非預期之開挖及加載。

此點國內建築物基礎構告規範擋土牆設計中，並無加入非預期之開挖及加載之考量，考量本公司之建設時程長及重視工安水準，於設計階段多方考量興建過程中非預期的狀況，可以降低非預期事項造成之損壞。

BS 規範中提及之二點略述如下：

(1)、非預期開挖深度：不得小於 $0.1H$ 或 $0.5M$ 。

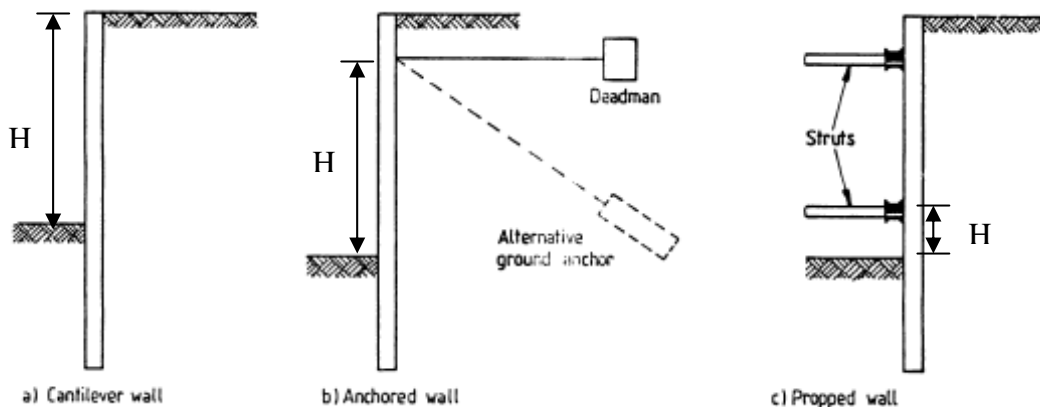


圖 3.1 擋土牆非預期開挖深度考量 (修改自 BS 8002)

(2)、最小地表加載： 10KN/m^2 。

二、公司常採用 MS Project 作各工作排程時時應注意該軟體之限制。

在二個活動之間通常有四種關係，(1)開始->開始，(2)結束->結束，(3)開始->結束，(4)結束->開始。但 MS Project 套裝軟體二個活動間，只容許一種方式連接。而且它不支援工作-延遲方式之排程方式。以擋土牆施工排程為例，如圖 3.2 之施工網圖是無法利用 MS Project 繪製，只可能繪製出圖 3.3、圖 3.4、圖 3.5 等圖。表示該套裝軟體無法在單一圖表完整的表達出所有的可能性，可能會誤導或影響決策考量，故在使用時應注意工具本身的限制。

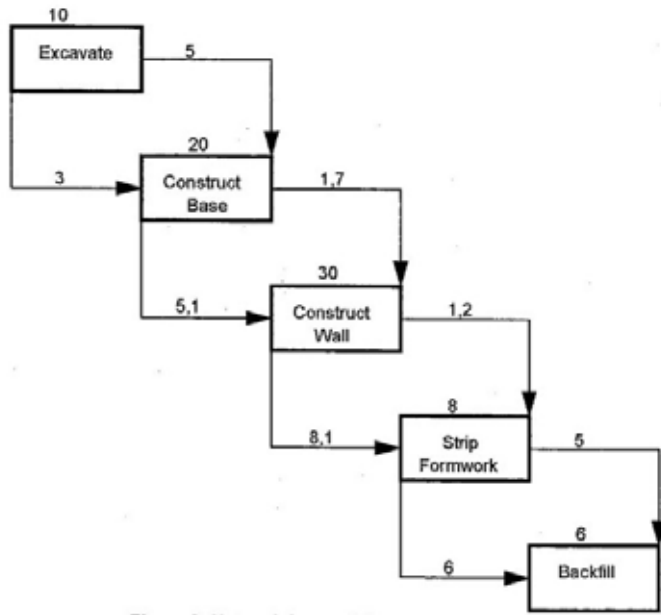


圖 3.2 擋土牆施工網圖

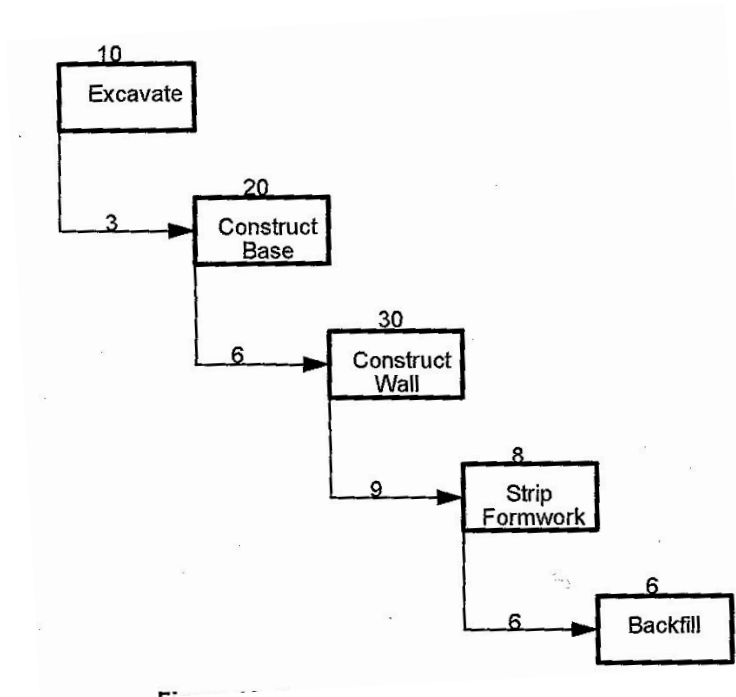


圖 3.3 圖 3.2 可能的版本

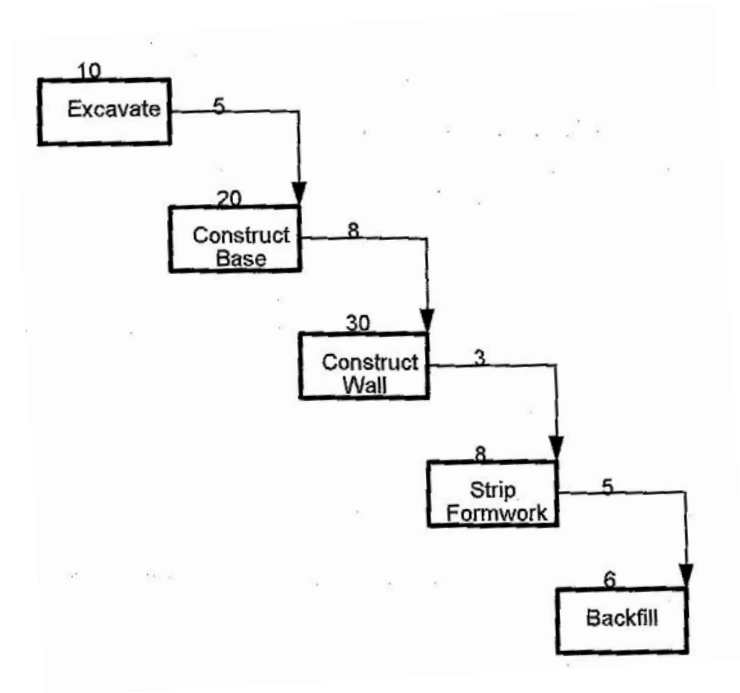


圖 3.4 圖 3.2 可能的版本

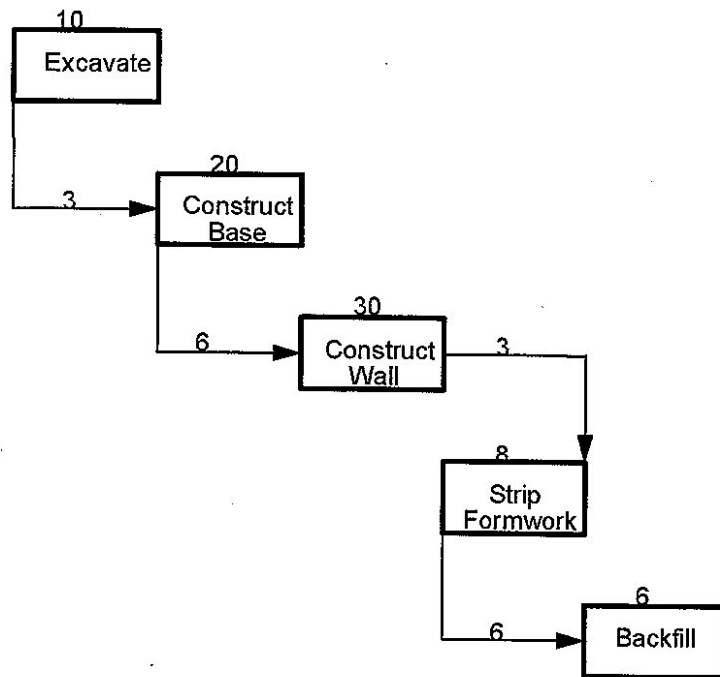


圖 3.5 圖 3.2 可能的版本

三、氣候變遷衝擊的因應

近來因為人為因素造成溫室氣體增加，導致全球暖化的可能性愈來愈高，間接造成劇烈的氣候變化，將對基礎建設造成重大影響。尤其是輸變電線路之建設，以點線而形成之網絡，所面臨的考驗將益加嚴峻。原本依照之設計規範是按氣候變遷前資料所研訂，是否有足多的裕度來面對日後的衝擊，仍需要進一步的證實。氣候變遷研究本身即充滿不確定，但較佳的設計規範仍可讓建物或構造物承受天然災害的考驗。故建議應積極且有系統的收集及歸納氣候變遷相關的資訊，定期辦理研討活動，即時修定相關之規範，以期在新建之設施可避免重蹈覆轍，以降低日後災後的復舊或重建工作。

附錄

專題報告

Stress-strain behaviour of cemented sand



The University of
Nottingham

Department of Civil Engineering

Stress-strain behaviour of cemented sand

By **TSAI, MING-TA**

Supervisor: **Dr. Dariusz Wanatowaski**

Date: **August 2009**

Dissertation submitted to the University of Nottingham in partial fulfilment of the degree of Master of Science in Civil Engineering : Geotechnical Engineering.

Abstract

Most prior studies have noted the importance of understanding behaviour of naturally and artificially cemented granular materials. However, artificially cemented which is an alternative to simulate the natural cemented sandy soil materials were tested mostly under conventional pressure (1 MPa) and most of the studies carried out at high pressures were focused on uncemented granular materials. In undrained conditions, pore pressure may increase significantly to lead to liquefaction, instability and failure which are hard to be avoided and cause casualties and heavy loss of properties easily. This study therefore aim to achieve better understanding of behaviour of cemented granular materials at high pressures under the undrained conditions

A total of 8 consolidated undrained triaxial tests including uncemented and cemented Portaway sand CIU triaxial tests of at high pressures and conventional pressure are carried out. Portland cement was used as cementation agent for preparing artificially cemented specimens. A high pressure triaxial cell which can provide up to 64MPa confining pressure in Nottingham Centre of Geomechanics was used to conduct the high confining pressure triaxial test.

It was observed that higher cement content, relative density, confining pressure, and drained condition cause higher maximum deviatoric stress and stress ratio. Furthermore, the higher cement content leads to higher maximum deviatoric stress and let the peak deviatoric stress show earlier. The excess pore water pressure is affected by relative density, confining pressure, and cement content.

KEYWORDS: High-pressure triaxial test, undrained test, excess pore pressure, cemented sand, stress-strain behaviour

Acknowledgements

The work described in this dissertation was carried out at the Department of Civil Engineering, The University of Nottingham during the period of January 2009 to August 2009.

My sincere thanks are due to my supervisor Dr. Dariusz Wanatowski, for his supervision, guidance and support throughout this research. Furthermore, he spent his precious time for examining the experimental results and proof reading this dissertation. Without his support, this dissertation would not have been possible.

Amanullah Marri and Sarah Ud-din, PhD students, provided crucial guidance and assistance while I was involved in experimental work in laboratory. I would also like to thank my colleague and classmate Yong Zhao for his help and discussion for learning the triaxial test system. He also offered unique experience in experimental work. I would also like to thank all the technicians in the School of Civil Engineering for their help and advice with the experimentation, in particular Ian Richardson.

Last but not least, I am grateful to my parents and girlfriend for their constant support and encouragement during my study.

Contents

List of figures.....	iv
List of tables.....	vii
Nomenclature	viii
Acronym	ix
Chapter 1 Introduction	
1.1 Background	1
1.2 Research objectives	3
1.3 Organisation of the dissertation	4
Chapter 2 Literature review	
2.1 Introduction.....	5
2.2 Background	5
2.3 Cement type.....	8
2.4 Isotropic compression behaviour.....	9
2.5 Shear behaviour.....	12
2.5.1 Isotropically consolidated drained test in cemented specimen	12
2.5.2 Isotropically consolidated undrained test in cemented specimen	14
2.5.3 Isotropically consolidated undrained test at high pressures	20
2.6 Summary	22
Chapter 3 Methodology	
3.1 Introduction.....	24
3.2 Materials	24
3.2.1 Portaway sand	24
3.2.2 Cementing agent.....	25
3.3 Molding and curing of cemented specimens	27

3.4 High Pressure Triaxial test system	29
3.4.1 Conventional triaxial testing system	29
3.4.2 High pressure triaxial testing system	31
3.4.3 High pressure triaxial cell.....	33
3.4.4 Loading frame	34
3.4.5 Advanced digital pressure / volume controller	35
3.5 Testing procedures.....	37
3.5.1 Uncemented specimen preparation.....	37
3.5.2 Cemented specimen preparation	38
3.5.3 Setting up the high pressure cell.....	40
3.5.4 Procedures of triaxial test	42
3.5.4.1 Saturation	43
3.5.4.2 Isotropic consolidation.....	44
3.5.4.3 Undrained Shearing	44
3.6 Experimental Program	45
3.7 Summary	46

Chapter 4 Experimental results and discussion

4.1 Introduction.....	47
4.2 Undrained behaviour of uncemented sand	47
4.2.1 Effect of density	47
4.2.2 Effect of confining pressure	51
4.3 Undrained behaviour of cemented sand	54
4.3.1 Effect of cement content.....	54
4.3.2 Effect of confining pressure	61
4.4 Comparison between drained and undrained behavior	64
4.4.1 Uncemented sand.....	64
4.4.2 Cemented sand	66

List of figures

Figure 2.1	Idealized behaviour of cemented soils: (a) stress path; (b) stress-strain behaviour	8
Figure 2.2	Typical stress-strain curve	9
Figure 2.3	Schematic comparison of the isotropic compression of weakly and strongly cemented carbonate sand.	10
Figure 2.4	Isotropic compression responses for the 0% to 3% cement content specimens. (a) 0% and 1% cement content. (b) 0% and 2% cement content. (c) 0% and 3% cement content. .	11
Figure 2.5	Stress-strain-volumetric response for: (a) 0% cement; (b) 1% cement; (c) 3% cement; (d) 5% cement.	13
Figure 2.6	Stress-strain-volumetric response for a constant initial mean effective stress $p'=60 \text{ kN/m}^2$	14
Figure 2.7	Prevailing failure modes of specimens: (a) barreling in uncemented specimens, (b) shear zone in cemented specimens.	15
Figure 2.8	Responses of Stress-strain, excess pore pressure-strain and stress ratio-strain for: (a) uncemented, (b) 1.5% cement.	16
Figure 2.9	Responses of Stress-strain, excess pore pressure-strain and stress ratio-strain for: (a) 4.5% cement, (b) 9% cement	17
Figure 2.10	Stress paths: (a) uncemented, (b) 1.5% cement, (c) 4.5% cement, (d) 9% cement	18
Figure 2.11	Variation of ultimate stress ratio (M) versus cement content	19
Figure 2.12	Undrained compression tests between 6.4 and 68.9 MPa initial confining pressure on dense Cambria sand: (a) deviatoric stress; and (b) excess pore pressure relationship.	20
Figure 2.13	Effective stress paths of undrained compression tests on dense Cambria sand shown on p' - q diagram.	21

Figure 2.14 Effect of different high-pressure stress paths of drained and undrained tests that fall at common effective mean normal stress..	23
Figure 3.1 Grain size distribution curve of Portaway sand	25
Figure 3.2 The process of mixing sample: (a) Adding and measuring sand. (b) Adding and measuring cement. (c) Shaking the box to mix. (d) Mixed cemented sand.....	28
Figure 3.3 Moulds: (a) The mould of 5cm in diameter and 10 cm in height. (b) The mould of 3.8cm in diameter and 7.6cm in height.....	28
Figure 3.4 The conventional triaxial test system.....	29
Figure 3.5 Conventional triaxial test apparatus: (a) schematic; (b) hydraulically operated cell.....	30
Figure 3.6 The complete triaxial test system (up to 1.7 MPa).....	31
Figure 3.7 Schematic diagram of the high pressure apparatus.....	32
Figure 3.8 Overall setup of high pressure triaxial system.	32
Figure 3.9 Cross-section of high pressure triaxial cell	33
Figure 3.10 Cell base connections.....	34
Figure 3.11 Overall setup of high pressure triaxial apparatus in the loading frame.....	35
Figure 3.12 Advanced Digital Pressure/Volume Controller.....	36
Figure 3.13 Control of Advanced Digital Pressure/Volume Controller	37
Figure 3.14 Uncemented specimen preparation before removing the split membrane stretcher.....	39
Figure 3.15 Prepared cemented specimen.....	40
Figure 3.16 Assemble the Clamp Ring(a) and retaining ring(b)	41
Figure 3.17 The Trolley	42
Figure 3.18 Fitting the triaxial cell into the loading frame.....	42
Figure 3.19 Typical back volume against time during the process of consolidation	44
Figure 4.1 Results of CIU triaxial test on medium dense and dense sand: (a)	

	stress-strain behaviour; (b) Δu versus ϵ_1 curves; (c) q/p' versus ϵ_1 curves; (d) effective stress paths.	48
Figure 4.2	Location of instability line for loose sand	49
Figure 4.3	Results of CIU triaxial test in uncemented specimens at different confining pressures: (a) stress-strain behaviour; (b) Δu versus ϵ_1 curves; (c) q/p' versus ϵ_1 curves; (d) effective stress paths.	43
Figure 4.4	Results of CIU triaxial test in of different cement content at conventional confining pressure(500 kPa): (a) stress-strain behaviour; (b) Δu versus ϵ_1 curves; (c) q/p' versus ϵ_1 curves; (d) effective stress paths.....	56
Figure 4.5	Results of CIU triaxial test in of different cement content at high confining pressure(4000 kPa): (a) stress-strain behaviour; (b) Δu versus ϵ_1 curves; (c) q/p' versus ϵ_1 curves; (d) effective stress paths.	59
Figure 4.6	The relationship between cement content and intercept	61
Figure 4.7	Results of CIU triaxial test in different confining pressure : (a) stress-strain behaviour; (b) Δu versus ϵ_1 curves; (c) q/p' versus ϵ_1 curves; (d) effective stress paths.	62
Figure 4.8	Results of uncemented specimens in CIU and CID triaxial test: (a) stress-strain behaviour; (b) q/p' versus ϵ_1 curves; (c) effective stress paths.....	65
Figure 4.9	Results of cemented specimens in CIU and CID triaxial test: (a) stress-strain behaviour; (b) q/p' versus ϵ_1 curves; (c) effective stress paths.....	67

List of tables

Table 3.1 Index Properties of Portaway sand	25
Table 3.2 The composition of CEM II /B-V 32, 5 N Portland cement.....	26
Table 3.3 The strength of CEM II /B-V 32, 5 N Portland cement.....	26
Table 3.4 The composition of type A.....	27
Table 3.5 The composition of type B.....	27
Table 3.6 Summary of test conducted	45
Table 4.1 Peak deviatoric stresses, Peak effective mean stresses and peak stress ratios of three confining pressure.	53

Nomenclature

B	=B value
e	=Void ratio
e_{\max}	=Maximum void ratio
e_{\min}	=Minimum void ratio
L_o	=Original specimen length
M_s	=Mass of solids
p'	=Mean effective depth
p'_f	=Peak mean effective depth
q	=Deviator stress
q_c'	=Effective confining stress
q_f	=Peak deviator stress
q/p'	=Effective stress ratio
V_T	=Total volume
V_o	=Original specimen volume
W_s	=Weight of solids
ϵ_a	=Axial strain
σ_1	=Axial stress
σ_3	=Confining pressure
σ_1'	=Effective axial stress
σ_3'	=Effective confining pressure
ρ_d	=Dry density
ΔL	=Change in specimen length
Δu	=Excess pore water pressure
ΔV	=Change in specimen volume
ϕ_p	=Peak friction angle

Acronym

ADPVC	=Advanced digital pressure/volume controller
CID	=Isotropically consolidated drained test
CIU	=Isotropically consolidated undrained test
UC	=Unconfined compression test
GDS	=Global Digital Systems

Chapter 1 Introduction

1.1 Background

Adding cemented materials artificially to improve local soil has been used successfully in considerable areas, such as ground improvement to increase soil strength or prevent liquefaction, pavement base layers, and slope protection for earth dams. In spite of extensive applications, there are still no reliable criteria to evaluate their strength.

Naturally cemented granular soils often cause engineering problems. For instance, the cemented carbonate soils are generally composed of the skeletal remains of marine organisms, and have various particle sizes from sand to silt size. Cemented carbonate sediments are widely distributed on the continental shelves in temperate and tropical area of the world, and exist in many regions where are substantial petrochemical reserves (e.g., the Arabian Gulf and around the coastal of Australia and India). Therefore, the interest in the behaviour of carbonate soils has increased in recent years, owing to difficulties on these sediments (McLelland, 1988). The engineering behaviours of carbonate soils are quite different from the carbonate soils with similar grain sizes. These cemented carbonate soils are highly compressible and relative low densities. These features may cause very low skin friction to be mobilized on driven piles and cause much greater settlements under footings than expected from theoretical settlement analysis. For example, on the North Rankin Platform installed off North West Australia in 1982, unexpected low driving resistance indicated the piles might not provide the design shaft friction capacity (King & Lodge, 1988).

Several studies investigating the behaviour of carbonate soil were based on laboratory testing of nature soil specimens retrieved from the field. These approaches presented some difficulties resulting from the disturbance to the structure that can

occur during the sampling process. A loss of stiffness was caused by the disturbance of interparticle contacts and breakage of cement bonds. The other principal problem associated with the testing of naturally cemented sands is its high variability, both in the degree of cementation and in the nature of the particle. Therefore, the variability and the difficulty of sampling without disturbance make it difficult to study the fundamental behaviour of natural cemented materials.

In order to avoid above difficulties, artificially cemented soils have been used to approach the naturally cemented soils. The appropriateness of the approach is concerned as follow. Although the behaviour of the naturally cemented soil is different from sandy soils, it has been demonstrated by Coop (1990) that uncemented carbonate sand exhibit all the features of conventional sands. The engineering responses of noncarbonated and carbonate sands at similar void ratios show similar behaviours (Semple, 1988). Clough et. al (1981) also indicated the general features shown by the artificially cemented specimens are identical to cemented noncarbonated sands. Thus, artificial cemented specimen is an alternative simulation of natural cemented soils in the laboratory to achieve qualitative understanding of the behaviour of cemented soils without excessive sample variability of sampling disturbance.

Soils needed to add cement artificially are generally important or in poor soil conditions. The behaviour of cemented or uncemented granular materials can normally be characterized for practical applications from the results of drained tests because in many situations the material can be considered as drained. However, if the loading rate is fast, such as those caused by explosions or earthquakes, or if the permeability of the soil is relative low, as in fine sands, silts, or carbonate sand, and undrained condition can exist. In undrained condition, pore pressure may increase significantly to lead to liquefaction, instability and failure. If these catastrophic failures occur in important infrastructures, causalities and heavy loss of properties cannot be

avoided. These illustrate the importance of understanding the undrained behaviour in cemented granular materials.

In recent studies, artificially cemented materials were tested mostly under low pressures and most of the studies carried out at high pressures were focused on uncemented granular materials. There is a lack of data on cemented granular materials tested at high pressures under undrained conditions. Thus, for future geotechnical applications, more experimental studies are required to improve understanding of undrained behaviour of cemented soils at high pressure.

1.2 Research objectives

The goal of this research is to achieve better understanding of behaviour of cemented granular materials at high pressures under the undrained conditions. This involves a detailed literature review and the laboratory testing.

Specific tasks of the project include:

- (1) A literature review on the effects of cement type, cement content, effective confining pressure, and drainage on behaviours of the cemented granular materials.
- (2) To conduct a series of undrained triaxial tests of uncemented Portaway sand at high pressures and conventional pressure.
- (3) To conduct a series of undrained triaxial tests of cemented Portaway sand at high pressures and conventional pressure.
- (4) To analyses and compare the results with previous studies.

The data obtained could be used to examine or improve existing constitutive models to simulate behaviour of cemented materials more accurately.

1.3 Organisation of the dissertation

This thesis is divided into five chapters. The brief outline of each chapter is given below.

Chapter 1 gives an introduction to this research work. In Chapter 2, a review of background knowledge and literature relevant to this work is presented. The literature review is divided into three parts: background, the effect of cement type, isotropic compression behaviour, and shear behaviour.

Chapter 3 describes methodology including the apparatus and experimental procedures. Initially, the properties of the Portaway sand and cementing agent are described. Secondly, the sample moulding and curing procedures are presented. Thirdly, the high pressure triaxial testing system is introduced. Then, the isotropically concentrated undrained triaxial testing procedures are illustrated. Finally, the testing program is given.

Chapter 4 consists of the results and interpretations of the undrained high pressure triaxial tests on cemented specimens. .

Chapter 5 presents the conclusions of the work and recommendations for further research. The effects of confining pressure and cement content on the behaviour of cemented Portaway sand are discussed. Comparison of drained and undrained behaviour of cemented sand at high pressures is also presented.

Appendix A is the short paper related to the work carried out for the project. Appendix B contains two risk assessments for experimental works carried out on specimen preparation and assembling the high pressure triaxial apparatus. Appendix C and D are the paper submitted to the winter and summer conferences.

Chapter 2 Literature review

2.1 Introduction

Cemented and bonded materials are often encountered in geotechnical field. Cementation plays an important role in stress–strain, stiffness, bearing capacity and mechanical parameters of cemented soils. However, from a mechanical point of view, cemented soils, weak rocks, and similar bonded materials constitute an intermediate class of geomaterials placed between classical soil mechanicals and rock mechanicals (Schnaid et al.2001).

This chapter presents a literature review, divided into five sections: (1) background, (2) cement type, (3) isotropic compression behaviour and (4) shear behaviour. The first part, section 2.2, presents a general review of behaviour of naturally and artificially cemented soils. Next, section 2.3, the effect of cement type is discussed briefly. Following this, isotropic compression behaviour in cemented soils is reviewed. Finally, in section 2.5, the shear behaviour is discussed.

2.2 Background

Cementation in naturally cemented sands can be attributed to several sources as follows: (i) existence of agents such as silica, hydrous silicates, hydrous iron oxides and carbonate deposits between grains, (ii) cold welding between the soil grains, (iii) presence of a matrix of silts and clays between sand and gravel particles (Haeri et al. 2005). Experimental research on naturally cemented soils is rare because acquiring undisturbed specimens from naturally cemented coarse grained soils is extremely difficult. The other problem associated with the testing of naturally cemented sands is that, depending on their geological origin, there can be high spatial variability, on the degree of cementation, the nature of particles and the density. An alternative is therefore to use artificially cemented specimens made up through the addition to the soil of a cementing agent, such as Portland cement, gypsum, or lime. This allow the

simulation of natural cemented soils in the laboratory and the qualitative understanding of the behaviour of cemented sands without excessive sample variability and any uncertainty due to sampling disturbance (Rotta et al. 2003). These supported by Coop (1990) demonstrated that uncemented carbonate sand exhibits all the features of conventional soil. In addition, the engineering response of noncarbonated and carbonate sand at similar void ratios shows similar behaviour (Semple 1988). Furthermore, Boey (1990) also demonstrated that artificially and naturally cemented soils show similar behaviour.

In last three decades, a number of researchers have been giving important experimental contributions in this area. Some of them are reviewed below to identify some significant characteristics of the cemented granular soils.

Clough et al. (1981) reported a set of triaxial and unconfined compression tests to examine the effects of cementation and density on the behaviour of naturally and artificially cemented sands. Test results showed that stiffness and peak strength increased with density and the amount of cementing agent. They suggested that in addition to cementation and density, grain size distribution and grain size arrangement (fabric) have an important role on the behaviour of cemented sands.

Leroueil and Vaughan (1990) reviewed studies that had been carried out by others on cemented and structured soils. They suggested that structure in soils such as stiff over consolidated clays, clay-shales, cemented sands, residual soils, artificially bonded soils and weak rocks may arise from many different sources but they have similar features. They have shown that the yield in structured soils can occur under compression, shear and swelling stresses and the stress-strain behaviour of naturally and artificially cemented soils to be basically dependent on their initial state, and its position in relation to the yield curve and the critical state line of the uncemented remoulded soil.

Airey (1993) carried out conventional and stress path triaxial tests to examine the

behaviour of natural calcarenite soils. He used tension testing for estimating of the degree of cementation of naturally cemented specimens. He reported the responses of the naturally cemented soils were found to be similar to those of other cemented soils. He suggested that the cementation increases the shear modulus and the size of the yield locus; however, its effects on the volumetric response are negligible.

Coop and Atkinson (1993) conducted tests on artificially cemented carbonate sands. Test results showed that the direction of the stress path, the drainage conditions and the confining pressure affect the peak strength. They showed that the stress-strain behaviour of cemented specimens depends on the position of the initial state of the stress of the soil with respect to the yield locus of the bonding. They also described the idealized behaviour of cemented soils, which is divided into three different classes, as illustrated in figure 2.1. The first class shown in line 1 of figure 2.1 occurs when the soil reaches its yield stress during isotropic compression; in this case, shearing will produce a similar behaviour to that observed for an equivalent uncemented soil. The second class shown in line 2 of figure 2.1 occurs for intermediate stress states, in which the bonds will be broken during shear; the strength is controlled by the frictional component of the equivalent uncemented soil and the stress-strain curve shows a well-defined yield point after an apparent linear behaviour. In the third class shown in line 3 of figure 2.1 the soil is sheared at low confining stresses, when compared to the bond strength; a peak in the stress-strain curve occurs at small strains and for stresses outside the limit state surface of the equivalent uncemented soil.

Das et al. (1995) carried out unconfined compression tests on the artificially cemented sands. They reported that unconfined compression strength increase with cement content and compressive strains at failure decrease with cement content.

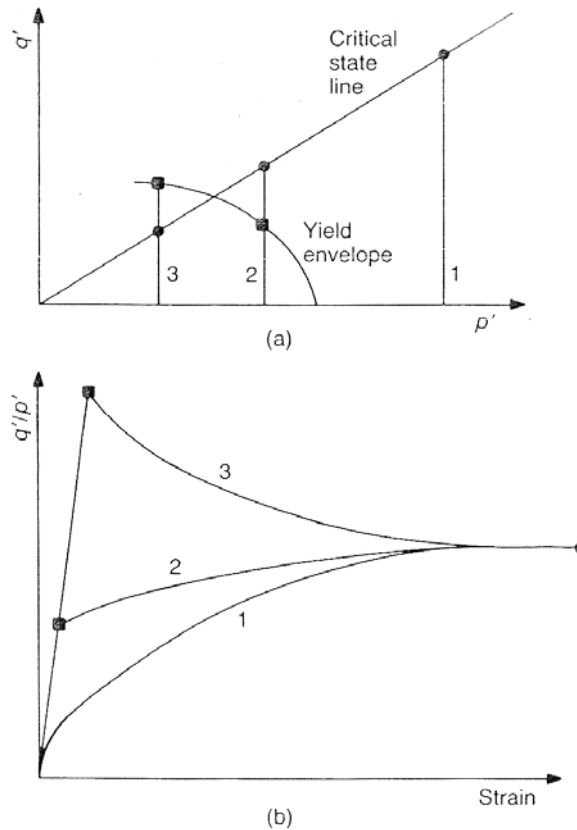


Figure 2.1 Idealized behaviour of cemented soils: (a) stress path; (b) stress-strain behaviour (after Coop & Atkinson, 1993)

2.3 Cement type

Ismail et al. (2002) studied the effect of cement type on the shear behaviour of cemented calcareous sand. They used three different types of cement agent (Portland cement, gypsum and calcite) for preparing artificially cemented specimens. Triaxial tests on specimens of different cementation type with similar unconfined compression strength and density, showed different effective stress paths and post yield responses. The Portland cemented specimens showed ductile behaviour while calcite and gypsum cemented specimens exhibited brittle yield. Their typical behaviours are shown in figure 2.2.

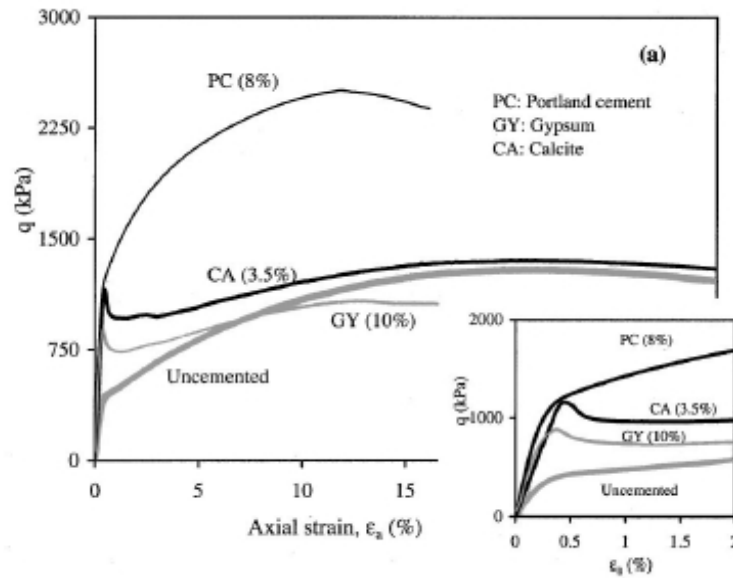


Figure 2.2 Typical stress-strain curve (Modified after Ismail et al. 2002)

2.4 Isotropic compression behaviour

The compression behaviour of the cemented sands is similar to that of other compressive soils. In isotropic consolidation, the specimens show a stiff response up to pre-consolidation pressure and then follow the normal compression lines (NCL). The normal compression line can be expressed as:

$$v = N - \lambda \ln p' \quad (2.1)$$

Cuccovillo and Coop (1999) described the idealized isotropic compression behaviour of calcarenite of various degrees of bonding shown in figure 2.3.

Rotta et al. (2003) reported a series isotropical compression test shown in figure 2.4. It presents the results obtained from the isotropic compression tests carried out on specimens cured under different confining stresses and for cement contents of 1%, 2% and 3% respectively. The identification of the tests follows the general nomenclature ISO(x)y-z, where x is the cement content, y is the curing confining stress, and z is the maximum isotropic stress reached in the test. They found that, for the artificially cemented specimens, the primary yield stress in isotropic compression

is a function of the curing void ratio and cement content; it is also dependent on the curing stresses, but is independent of any increase in the OCR after curing. Indeed, the relative contribution of cementation to the soil behaviour in isotropic compression reduces with decreasing curing void ratio. At similar void ratios, the curing confining stress influences the primary yield stress, but does not affect the incremental yield stress.

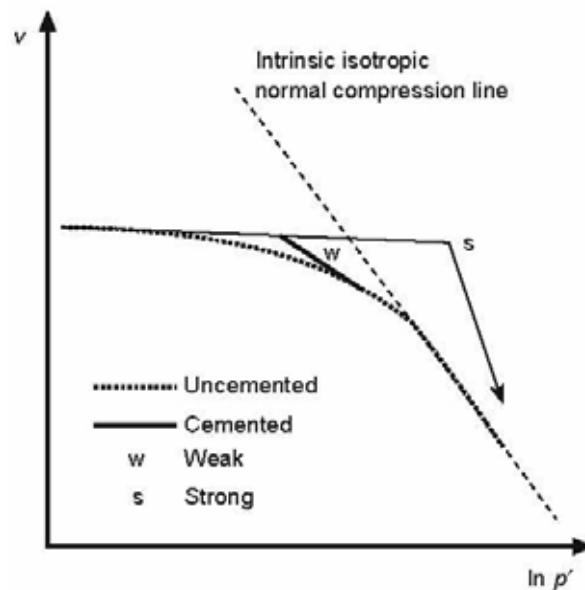
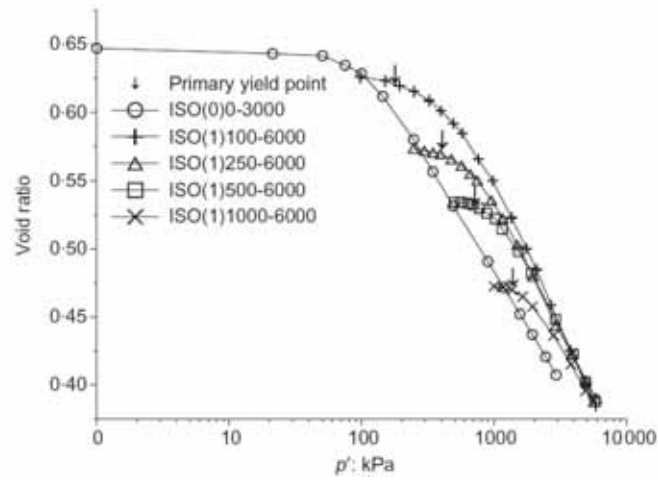
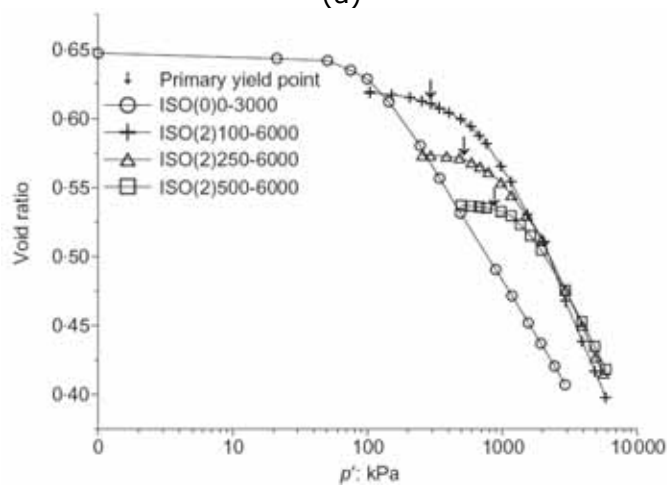


Figure 2.3 Schematic comparison of the isotropic compression of weakly and strongly cemented carbonate sand (after Coop and Atkinson 1993)

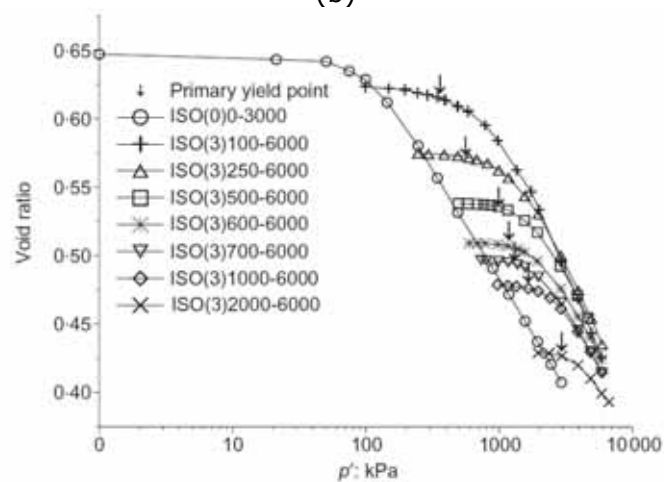
The results also demonstrates the coupled effect of density and cementation on the cemented soils. Huang and Airey (1998) reported that, the effects of the cementation are only significant for stresses below an apparent preconsolidation stress for the artificial soil. The strength and stiffness increase with increasing density and cement content, but the influence of the cementation decreases as the density increases.



(a)



(b)



(c)

Figure 2.4 Isotropic compression responses for the 0% to 3% cement content specimens. (a) 0% and 1% cement content. (b) 0% and 2% cement content. (c) 0% and 3% cement content (Modified after Rotta et al. 2003).

2.5 Shear behaviour

Triaxial test is widely used to investigate the stress-strain behaviour of soils. Isotropically consolidated drained (CID) test and undrained (CIU) test are normally used to accurately characterize the behaviour of uncemented and cemented materials. In this section, both of them will be reviewed. All undrained behaviour of sand at high pressures is also discussed at the end of this section.

2.5.1 Drained behaviour

Schnaid et al. (2001) had carried out CID tests on artificially cemented sand. The specimens were prepared with cemented content of 1, 3, and 5% respectively. The soil specimens were derived from weathered sandstone and obtained from the region of Porto Alegre in southern Brazil, and the cement type was ordinary Portland cement. Their results, shown in figure 2.5, illustrate typical trend of deviatoric stress versus axial strain and volumetric strain versus axial strain for specimens with different cement content.

Figure 2.5 (a) shows the results on uncemented specimens and figures 2(b-d) shows the artificially cemented specimens with cemented content of 1, 3, and 5% respectively. Figure 2.6 illustrates the changes in soil behaviour, resulting from the addition of cement, by comparing the stress-strain curves obtained for different cement contents and a constant initial mean effective stress.

An initial examination of the curves presented in figures 2.5 and 2.6 clearly shows the soil behaviour to be strongly dependent on the cement content. As the cement content increases, both peak strength and initial stiffness increase. Unlike the uncemented soil, cemented specimens show a brittle behaviour at failure with well defined shear planes being formed. This brittle response increases with increasing cement content and decreases as the initial mean effective stress increases. The axial strain at failure decreases with increasing cement content and it also decreases

with increasing initial mean effective stresses. As for the volumetric response, the cemented specimens show an initial compression followed by a strong expansion with the maximum dilation rate taking place right after the peak strength. Subsequently, the dilation rate decreases as the soil approaches an ultimate stable condition. Therefore the existence of an ultimate state was suggested. In figure 2.6, the deviatoric stress approaches a constant value with increasing axial strain, which does not seem to be affected by cementation.

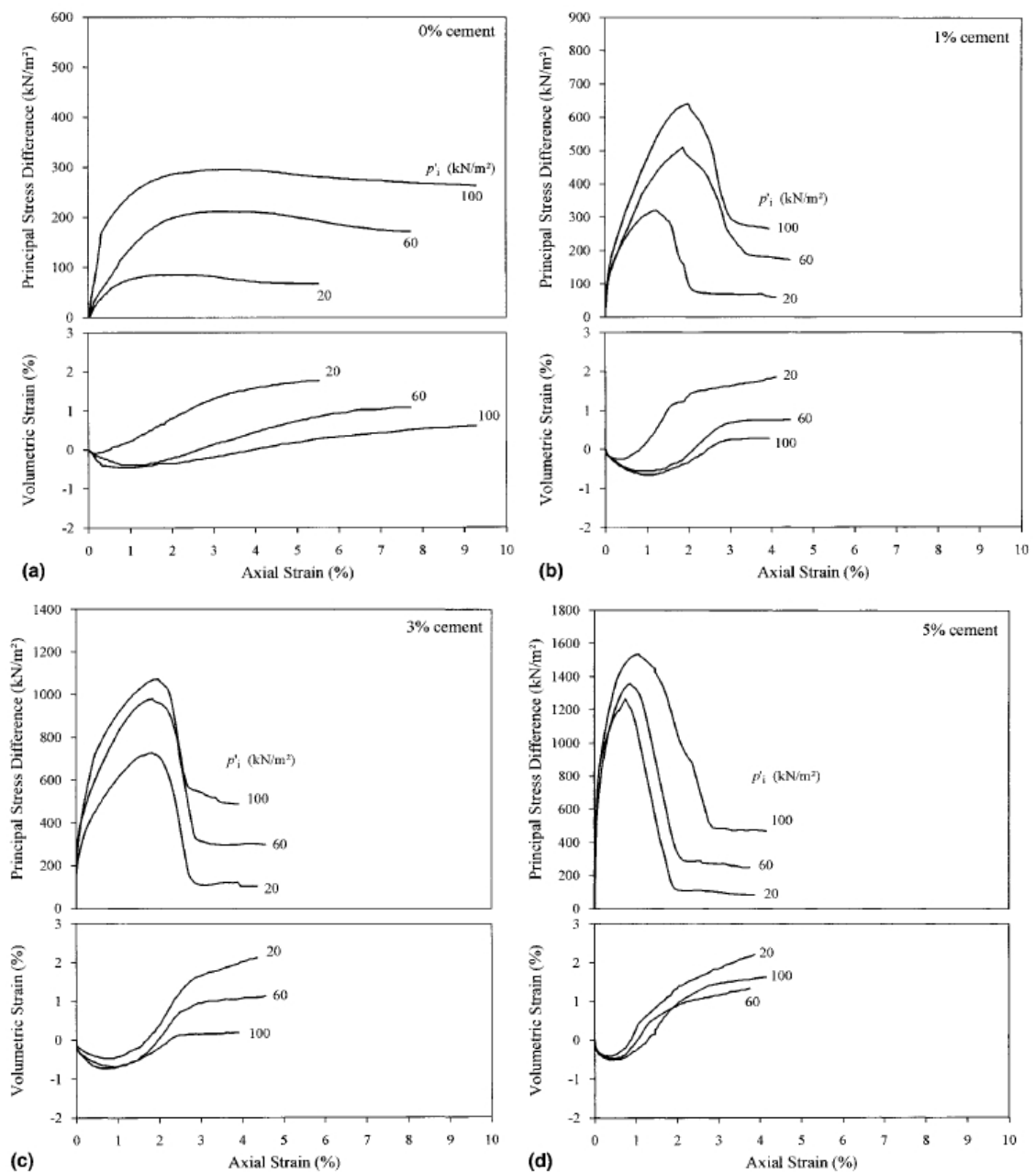


Figure 2.5 Stress-strain-volumetric response for: (a) 0% cement; (b) 1% cement; (c) 3% cement; (d) 5% cement (after Schnaid et al. 2001).

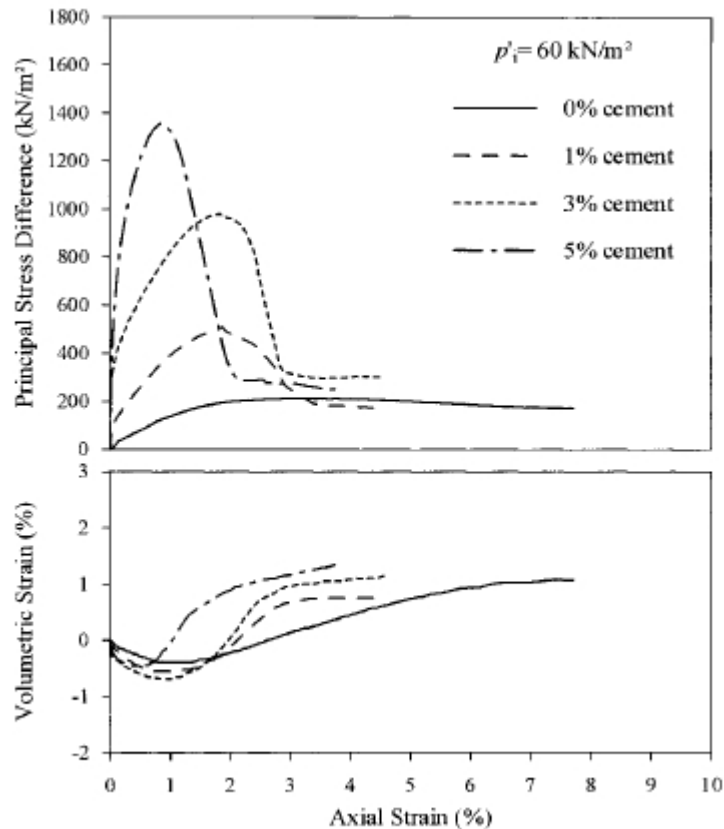


Figure 2.6 Stress-strain-volumetric response for a constant initial mean effective stress $p'_i = 60 \text{ kN/m}^2$ (after Schnaid et al. 2001).

2.5.2 Undrained behaviour

Haeri et al. (2005) conducted a series of isotropically consolidated undrained tests (CIU) on artificially cemented sandy gravel. The typical failure modes of uncemented and cemented specimens are shown in figure 2.7. They observed that the specimens tested at confining pressures higher than 100 kPa showed barreling failure modes during shear. However, shear zones formed in specimens tested at the low confining pressure (25 kPa). Uncemented specimens at confining pressures from 50 and 100 kPa and relative density of 70% showed barreling failure mode at low strain levels of up to 10% and then shear zones were formed after 10% strain. Lightly cemented specimens (1.5% cement) showed a brittle failure mode accompanied by shear zones at low confining pressures. The same specimens tested at higher pressures showed a barreling failure mode at small strain followed by shear zones at strains greater than about 8%. Other cemented specimens (3%, 4.5%, 6% and 9% cement) showed a

brittle failure mode accompanied by shear zones. The brittle behaviour increased with increasing of cementation and density and decreased with an increase in confining pressure. They also found that the thickness of the shear zone in cemented specimens varied between 2 and 5 cm and the inclination angle of the shear zones with respect to horizontal varied between 60 and 70 degrees.

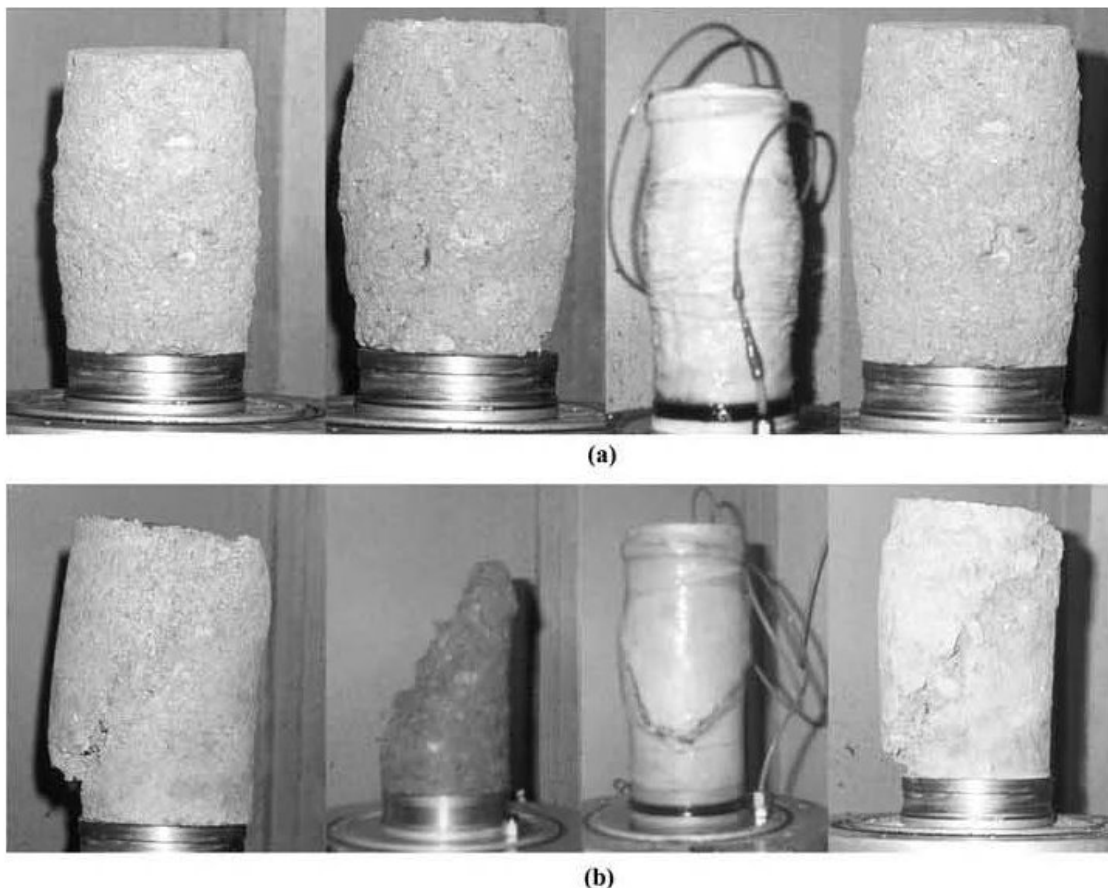


Figure 2.7 Prevailing failure modes of specimens: (a) barreling in uncemented specimens, (b) shear zone in cemented specimens (after Haeri et al. 2005)

Results from Haeri et al. (2005) carried out on dense specimen prepared with cemented content of 0, 1.5, 4.5, and 9% and performed at different confining pressures including 25, 50, 100, 300, and 400, or 500 kN are shown below. Response of stress-strain, excess pore pressure-strain and stress ratio-strain are shown in figures 2.8 and 2.9 and the stress paths are shown in figure 2.10.

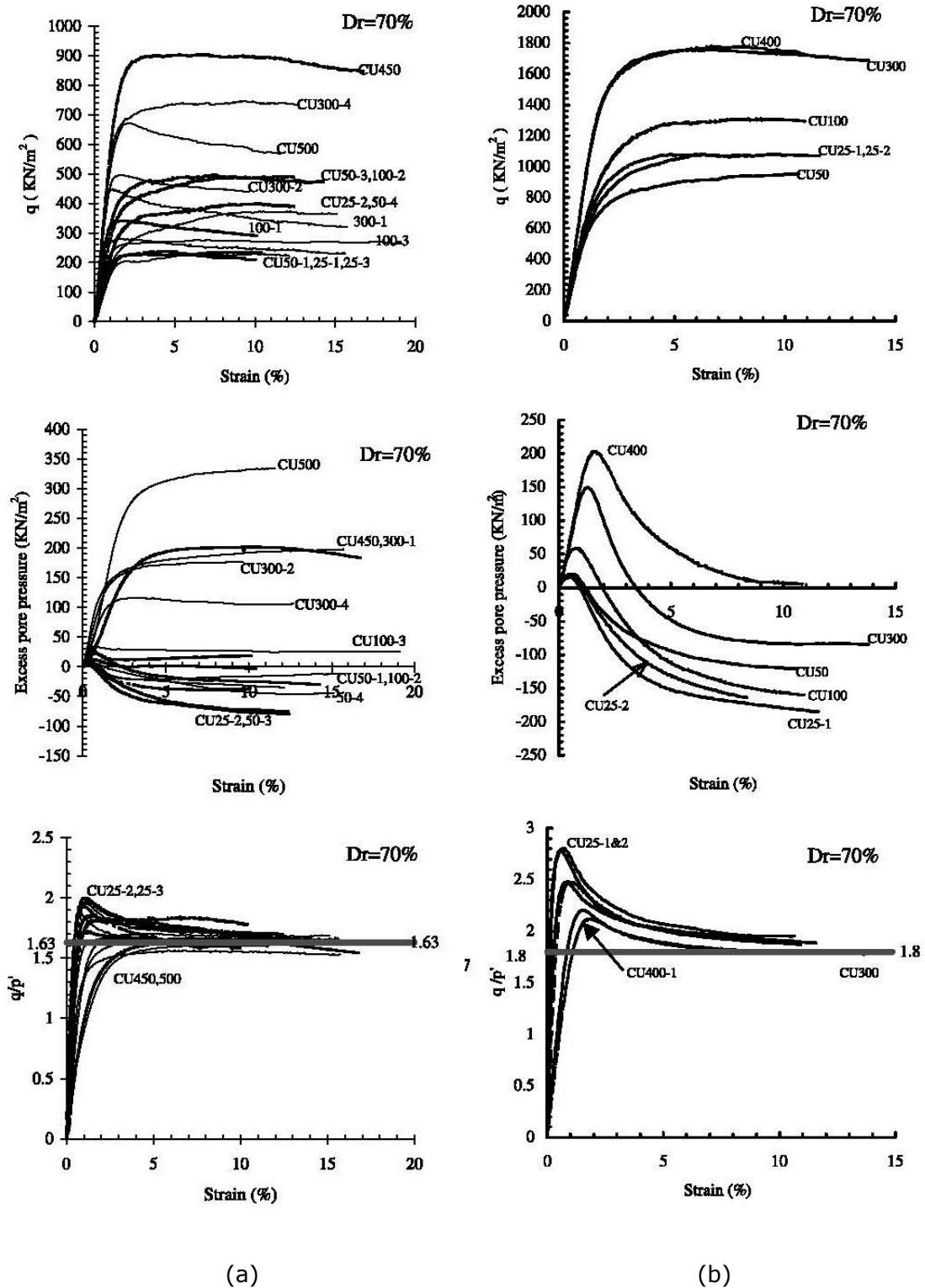


Figure 2.8 Responses of Stress-strain, excess pore pressure-strain and stress ratio-strain for: (a) uncemented, (b) 1.5% cement (modified after Haeri et al. 2005)

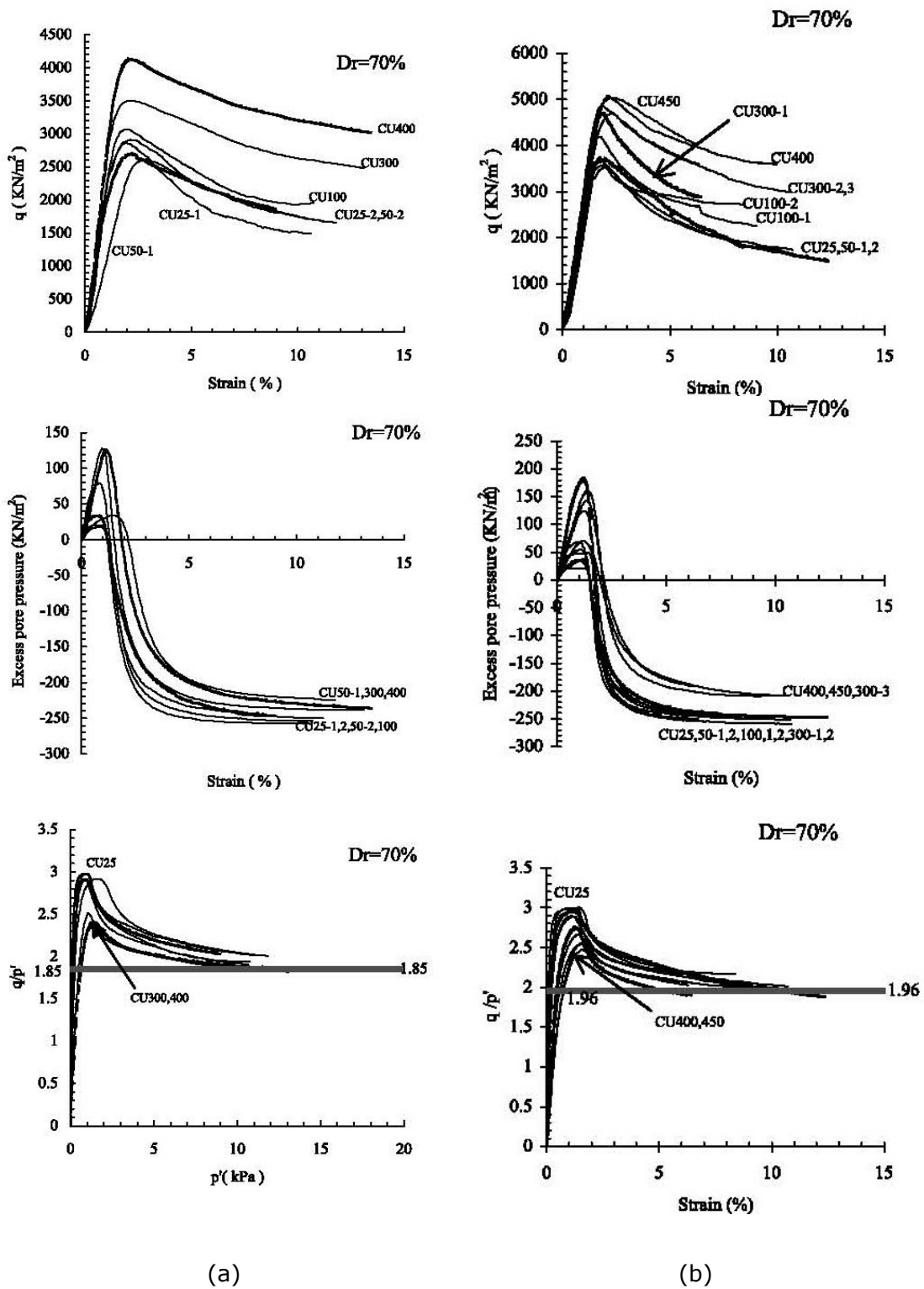


Figure 2.9 Responses of Stress-strain, excess pore pressure-strain and stress ratio-strain for: (a) 4.5% cement, (b) 9% cement (modified after Haeri et al. 2005)

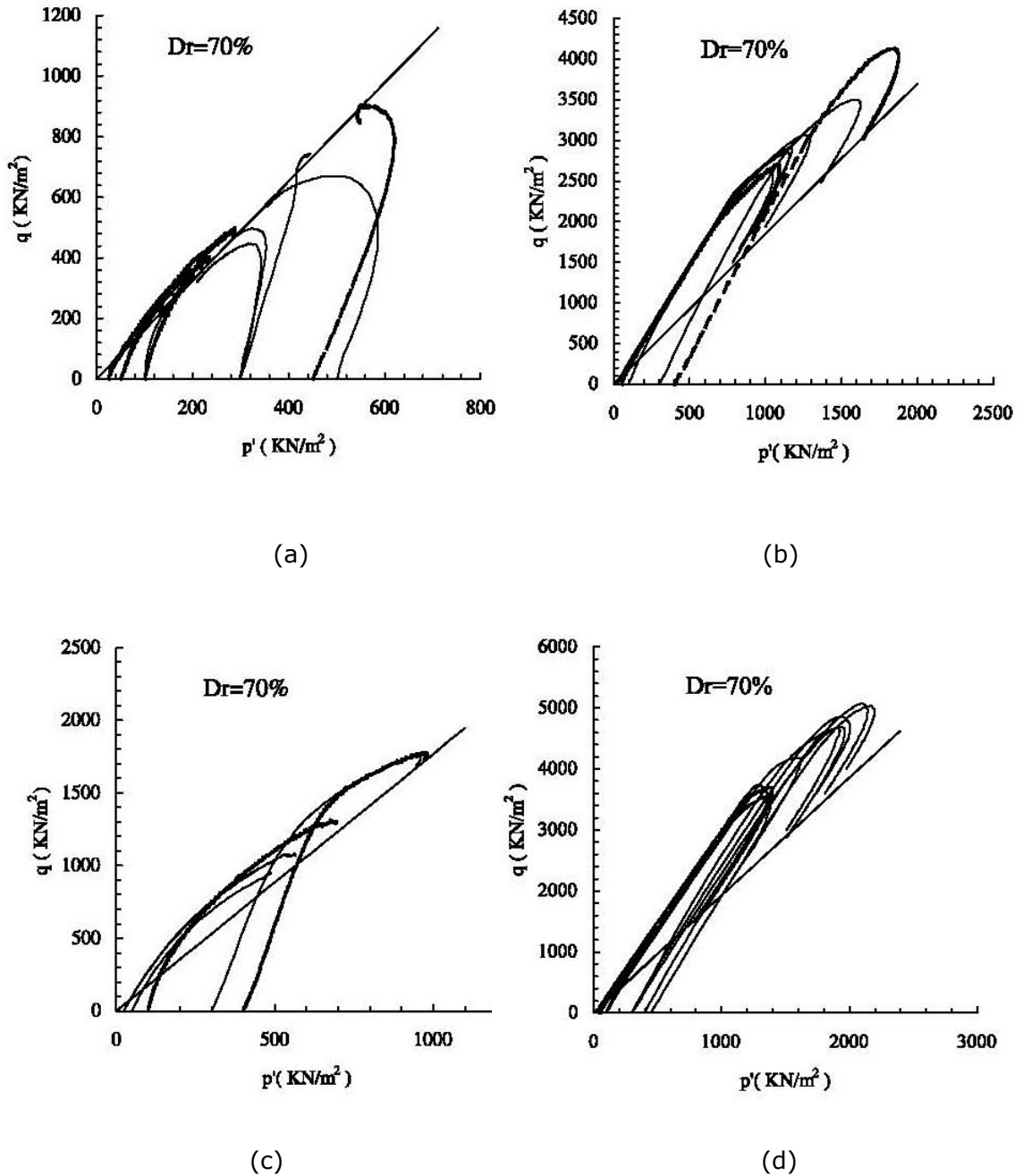


Figure 2.10 Stress paths: (a) uncemented, (b) 1.5% cement, (c) 4.5% cement, (d) 9% cement (modified after Haeri et al. 2005)

In these figures, the test results are named based on test conditions. CU stands for consolidated undrained tests. A two or three digit number indicating confining pressure follows the CU caption. This number is followed by a dash and a one-digit number showing the number of repeated tests on a specific sample with specific cement content tested under the same confining pressure.

Test results for uncemented and lightly cemented samples shown in figure 2.8 indicate that the stiffness increases with an increase in confining pressure for such soils. However, the effect of confining pressure on the stiffness is much less significant for strongly cemented specimens shown in figure 2.9. As can be observed from figures 2.8 and 2.9, stiffness increases with the increase in cement content. The stress–strain curves for uncemented and lightly cemented samples shown in figure 2.8 do not have any peak strength, while those for highly cemented samples present clear peak strength shown in figure 2.9. The maximum stress ratio, $(q/p')_{\max}$, decreases with an increase in confining pressure are shown in figure 2.8 and 2.9. However, the value increases with relative density and cement content.

Consider the maximum value of $(q/p')_{\max}$ which is associated with the lowest confining pressure. In triaxial tests, the stress ratio usually approaches a constant value at ultimate state. The ultimate stress ratio is the slope of critical state line in q – p' space. The variation of slope with respect to cement content is plotted in Figure 2.11. The value increases for cemented samples with increase in cement content and density (Haeri et al. 2005).

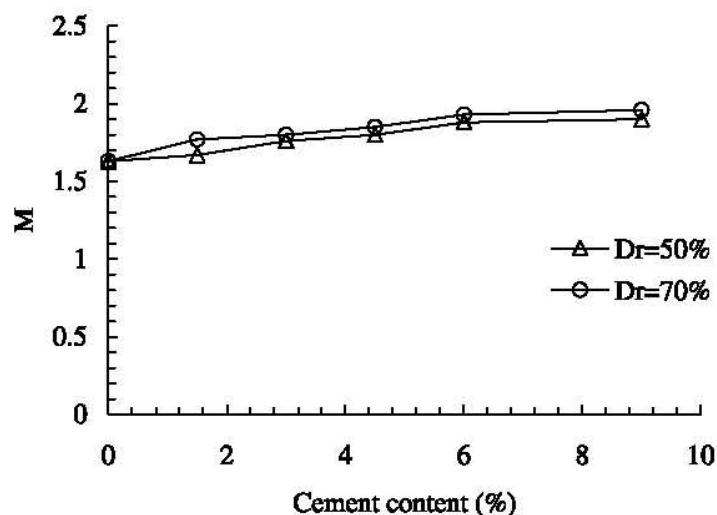


Figure 2.11 Variation of ultimate stress ratio (M) versus cement content (modified after Haeri et al. 2005)

2.5.3 Undrained behaviour at high pressures

Lade and Yamamuro (1996) reported a series of isotropically consolidated undrained tests (CIU) on Cambria sand at high pressure. The initial effective confining pressure was between 6.4 MPa and 68.9 MPa. Their results shown in figure 2.12, illustrate the deviatoric stress versus axial strain and excess pore pressure versus axial strain. The results of effective stress paths are shown in figure 2.13.

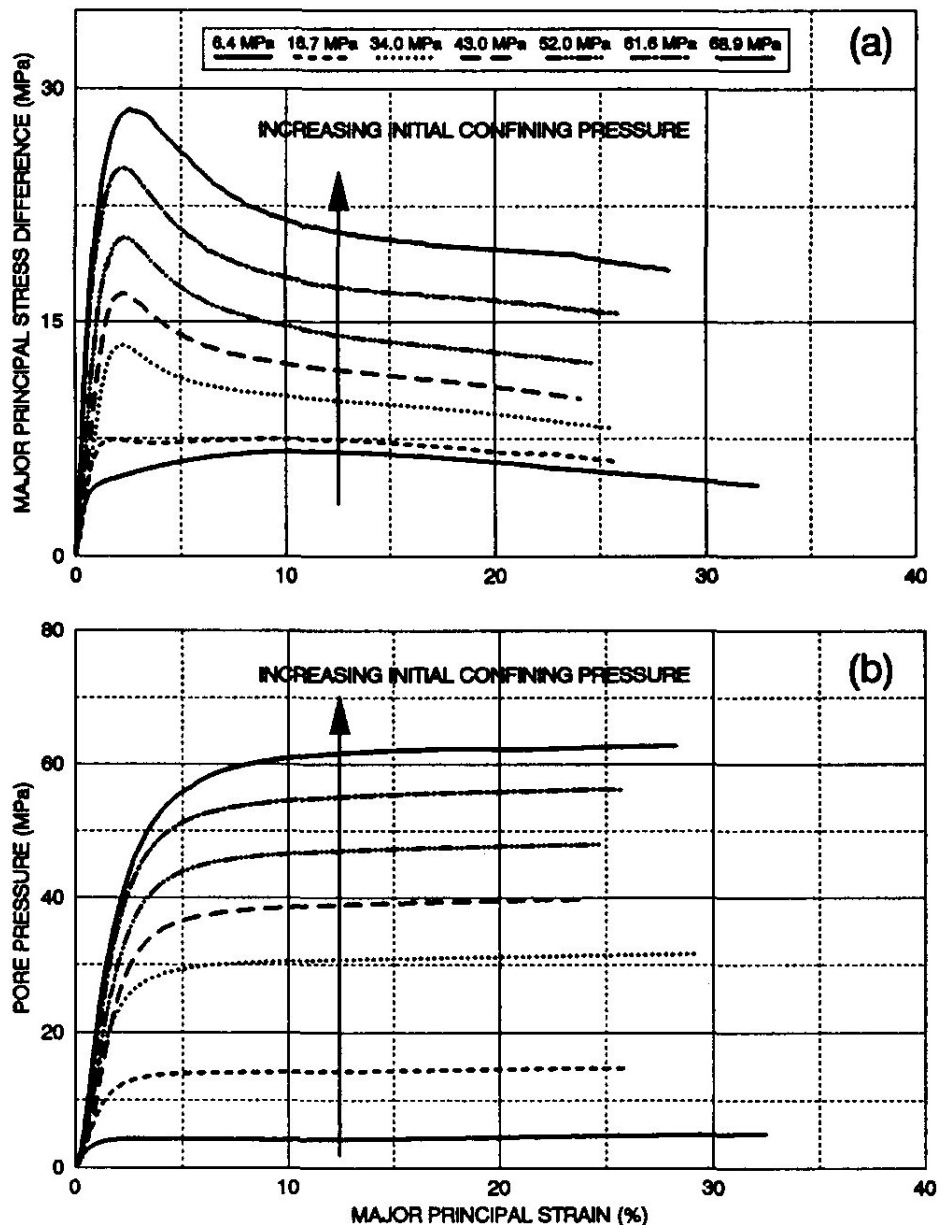


Figure 2.12 Undrained compression tests between 6.4 and 68.9 MPa initial confining pressure on dense Cambria sand: (a) deviatoric stress; and (b) excess pore pressure relationship. (after Lade and Yamamuro 1996)

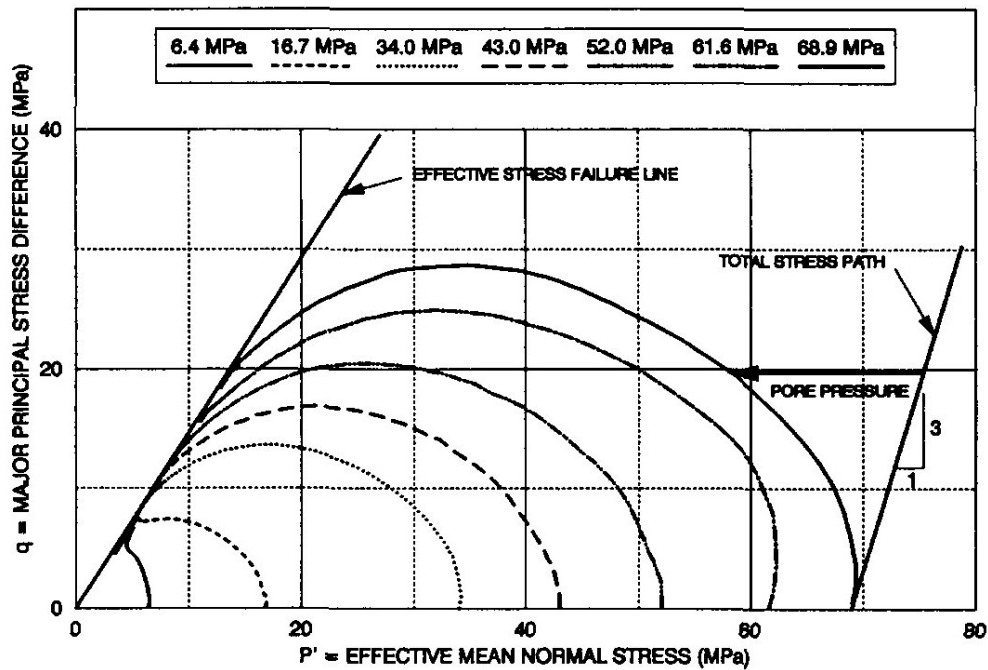


Figure 2.13 Effective stress paths of undrained compression tests on dense Cambria sand shown on p' - q diagram. (after Lade and Yamamuro 1996)

Lade and Yamamuro (1996) found that the initial slopes of stress-strain curves are steeper as the initial confining pressures increase. At low initial confining pressures, such as 6.4 MPa, the maximum deviatoric stresses occurs at large strains. The test at 16.7 MPa confining pressure shows the different behaviour. It increases to a peak, following by a decrease, but then rise again to its maximum value at failure. The tests at confining pressures higher than 16.7 MPa increase to a peak, then following by a decrease to the end of test. At large strains the effective confining pressure has decreased to allow the specimen to present volumetrically dilatant tendencies, leading to the pore pressure to decrease, therefore, increasing the effective stress. This can be observed clearly in figure 2.13.

The excess pore pressures shown in figure 2.12 (b) indicate that all tests shows tendencies for overall net compressive volumetric behaviour, because the generated pore pressure are all positive. As the initial confining pressure is above 16.7 MPa, the pore pressure which induced quickly results in a rapid decrease in the effective confining pressure. Hence, the deviatoric stress reaches to a peak soon after shearing

begins. After the peak, the magnitude of the deviatoric stress declines with increasing strain. This is caused by pore pressure which continues to increase with additional shearing. In figure 2.13, the tests of initial confining pressures above 16.7 MPa show in effective stress paths that rise up, and then move toward the origin due to increasing pore pressure. Then, the maximum deviatoric stress is reached, and it decreases with continuing pore pressure increase until it become tangential to the effective stress failure line. These effective stress paths exhibit contractive volumetric change behaviour. However, the lower initial confining pressure, such as 6.4 MPa, shows different behaviour. It increases upward, but it moves only slightly to the left, because the pore pressure generated is not as significant as that at higher confining pressure. This test shows a tendency toward volumetric dilation before the maximum deviatoric stress, and this result in decreasing pore pressure. The specimen continues to strengthen, the stress path moves upward with increasing deviatoric stress and effective mean stress. In the end, it reaches the maximum deviatoric stress and follows the effective stress failure line.

Lade and Yamamuro (1996) also discussed the differences between high pressure stress paths for drained and undrained tests which are shown as figure 2.14. The specimen in the undrained test, first undergoes large isotropic compression under drained conditions. Following this, it experiences undrained shearing, in which induced large positive pore pressures occurs rapidly. Therefore, the effective confining pressure in the specimen decreases. In figure 2.14, the drained test shows a smaller isotropic compression and the most of the particle crushing and corresponding densification occurs during the shearing.

2.6 Summary

In this chapter, the relationship between artificially and naturally cemented soils is reviewed. Because of their similar behaviours at similar void ratio and initial state, using artificially cemented specimens is an alternative to understand the behaviour of cemented sands without excess sample variability or sampling disturbance. It has

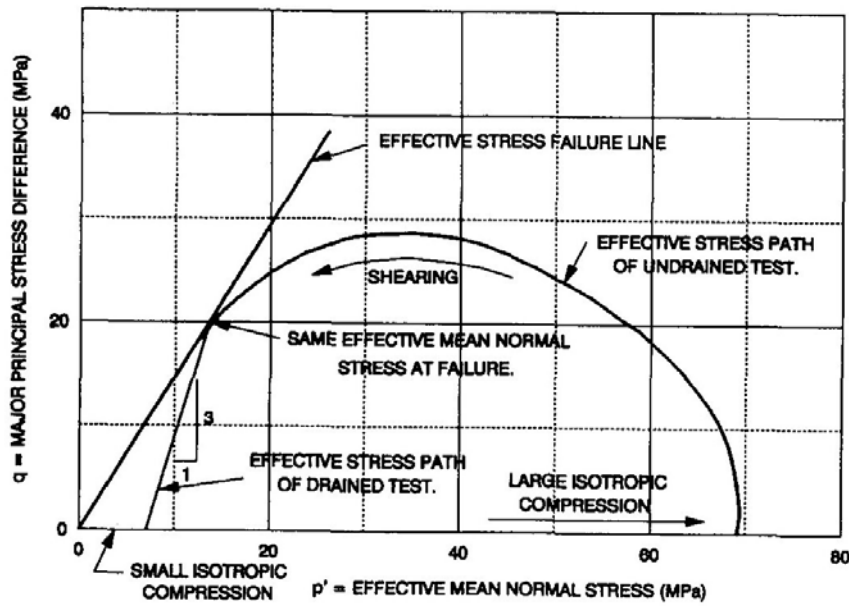


Figure 2.14 Effect of different high-pressure stress paths of drained and undrained tests that fall at common effective mean normal stress. (after Lade and Yamamuro 1996)

been shown that the stress-strain behaviours of cemented soils depend on the combined effects of dry density, effective confining pressure and percentage of cement content. However there is a lack of understanding on the stress-strain undrained behaviour of cemented granular materials at high pressure.

Chapter 3 Methodology

3.1 Introduction

The focus of this chapter is to describe the materials, equipments and procedures that were used in this research work. Firstly, the properties of the Portaway sand and Portland cement are described. Secondly, the sample moulding and curing procedures are presented. Thirdly, the high pressure triaxial testing system is introduced. Then, the isotropically concentrated undrained triaxial testing procedures are illustrated. Finally, the testing program is presented.

3.2 Materials

The granular material used in this study is Portaway sand. Portland cement (CEM II /B-V 32, 5 N) used as cementing agent. Detailed description of both materials is given below.

3.2.1 Portaway sand

The sand tested was Portaway sand which was used in previous experimental projects at Nottingham Centre for Geomechanics (Wang 2005). It is well-graded, medium quartz sand from Sheffield, England. Before using the Portaway sand for specimen preparation, the sand was washed and oven dried, and then sieved passing through 2.0mm and retaining on 63 μ m. Portaway sand has a specific gravity G_s of 2.65, a mean grain size D_{50} of 0.4mm, a effective grain size D_{10} of 0.22mm, a coefficient of uniformity C_u of 2.05. The maximum void ratios e_{min} and e_{max} are 0.46 and 0.79, respectively (Wang 2005). The size gradation curve is shown in figure 3.1 and the index properties are listed in table 3.1.

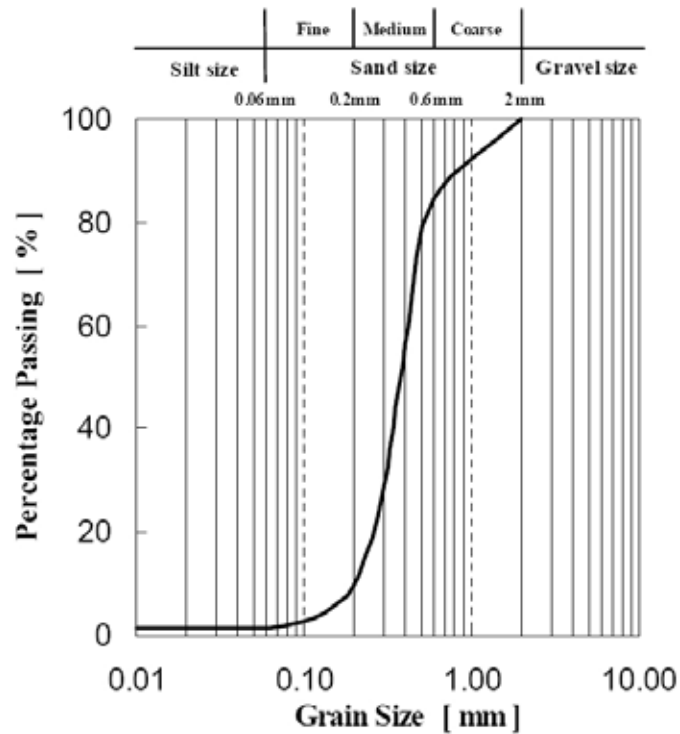


Figure 3.1 Grain size distribution curve of Portaway sand

Table 3.1 Index Properties of Portaway sand

Portaway sand index properties	
Effective grain size, D ₁₀ : mm	0.22
Mean grain size, D ₅₀ : mm	0.40
Uniformity coefficient: D ₆₀ / D ₁₀	2.05
Specific Gravity, G _s	2.65
Maximum void ratio e _{max}	0.79
Minimum void ratio e _{min}	0.46

3.2.2 Cementing agent

Portland cement (BS EN 197-1 CEM II /B-V 32, 5 N) is used for cementing agent in this study in order to compare the previous study. According to BS EN 197-1, CEM II is Portland-composite cement. It contains Portland cement and up to 35% of other single constituents. It mainly contains 65-79% of Clinker and 21-35% of siliceous fly ash. Its composition and strength are shown in tables 3.2 and 3.3, respectively.

Table 3.2 The composition of CEM II /B-V 32, 5 N Portland cement (Modified from BS EN 197-1)

Main types	Notation of the 27 products (types of)		Composition [percentage by mass ^{a)}]										Minor additional constituents
			Main constituents										
			Clinker K	Blast-furnace slag S	Silica fume D ^{b)}	Pozzolana		Fly ash		Burnt shale T	Limestone		
natural P	natural calcined Q	siliceous V				calcareous W	L	LL					
CEM I	Portland cement	CEM I	95-100	-	-	-	-	-	-	-	-	-	0 to 5
CEM II	Portland-slag cement	CEM I/A-S	80 to 94	6 to 20	-	-	-	-	-	-	-	-	0 to 5
		CEM I/B-S	65 to 79	21 to 35	-	-	-	-	-	-	-	-	0 to 5
	Portland-silica fume cement	CEM I/A-D	90 to 94	-	6 to 10	-	-	-	-	-	-	-	0 to 5
		Portland-pozzolana cement	CEM I/A-P	80 to 94	-	-	6 to 20	-	-	-	-	-	-
	CEM I/B-P		65 to 79	-	-	21 to 35	-	-	-	-	-	-	0 to 5
	CEM I/A-Q		80 to 94	-	-	-	6 to 20	-	-	-	-	-	0 to 5
	CEM I/B-Q		65 to 79	-	-	-	21 to 35	-	-	-	-	-	0 to 5
	Portland-fly ash cement	CEM I/A-V	80 to 94	-	-	-	-	6 to 20	-	-	-	-	0 to 5
		CEM I/B-V	65 to 79	-	-	-	-	21 to 35	-	-	-	-	0 to 5
		CEM I/A-W	80 to 94	-	-	-	-	-	6 to 20	-	-	-	0 to 5
	Portland-burnt shale cement	CEM I/A-T	80 to 94	-	-	-	-	-	-	6 to 20	-	-	0 to 5
		CEM I/B-T	65 to 79	-	-	-	-	-	-	21 to 35	-	-	0 to 5
	Portland-limestone cement	CEM I/A-L	80 to 94	-	-	-	-	-	-	-	6 to 20	-	0 to 5
		CEM I/B-L	65 to 79	-	-	-	-	-	-	-	21 to 35	-	0 to 5
		CEM I/A-LL	80 to 94	-	-	-	-	-	-	-	-	6 to 20	0 to 5
		CEM I/B-LL	65 to 79	-	-	-	-	-	-	-	-	21 to 35	0 to 5

Table 3.3 The strength of CEM II /B-V 32, 5 N Portland cement (Modified from BS EN 197-1)

Strength class	Compressive strength MPa				Initial setting time min	Soundness (expansion) mm
	Early strength		Standard strength			
	2 days	7 days	28 days			
32,5 N	-	≥ 16,0	≥ 32,5	≤ 52,5	≥ 75	≤ 10
32,5 R	≥ 10,0	-				
42,5 N	≥ 10,0	-	≥ 42,5	≤ 62,5	≥ 60	
42,5 R	≥ 20,0	-				
52,5 N	≥ 20,0	-	≥ 52,5	-	≥ 45	
52,5 R	≥ 30,0	-				

3.3 Moulding and curing of cemented specimens

Two types, A and B, of cemented samples were used in the isotropically consolidated undrained triaxial tests. Type A was 5cm in diameter and 10cm in height and type B was 3.8cm in diameter and 7.6cm in height. The dry density of all the cemented specimens was 17.4kN/m^3 .

At the beginning of moulding, the soil, cement and water were weighted as shown in table 3.4 and table 3.5, and the soil and cement were mixed until the mixture acquired a uniform consistency. The water was then added continuously to the mixing process until a homogeneous paste was created. After mixing sufficient material for one specimen, the mixture was placed in the box to avoid moisture losses as shown in figure 3.2.

Table 3.4 The composition of type A

The composition of type A				
Dimension= 5cm(Diameter) x 10cm(Height) $r_d=17.4\text{ kN/m}^3$				
Cement content (%)	weight of sand (g)	Weight of cement (g)	Weight of water (g)	Total weight (g)
5%	334.25	16.71	35.10	386.06
10%	321.24	32.12	35.34	388.71
15%	309.24	46.39	35.56	391.18

Table 3.5 The composition of type B

The composition of type B				
Dimension= 3.8cm(Diameter) x 7.6cm(Height) $r_d=17.4\text{ kN/m}^3$				
Cement content (%)	weight of sand (g)	Weight of cement (g)	Weight of water (g)	Total weight (g)
5%	146.73	7.34	15.41	169.47
10%	141.02	14.10	15.51	170.63
15%	135.75	20.36	15.61	171.72

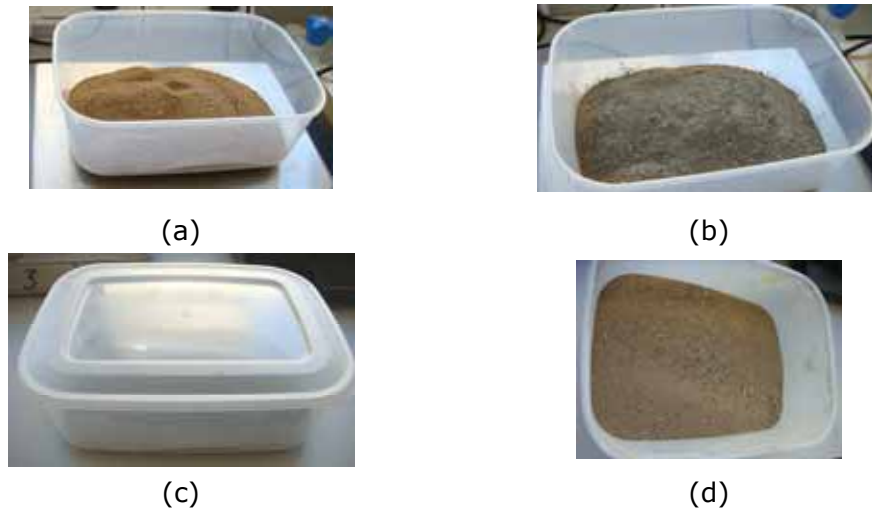


Figure 3.2 The process of mixing sample: (a) Adding and measuring sand. (b) Adding and measuring cement. (c) Shaking the box to mix. (d) Mixed cemented sand.

The specimen was then compacted in three layers into split cylindrical mould shown in figure 3.3, which was lubricated. For the purpose of decreasing unevenness of the specimen surface, two transparencies were placed into the mould. One is placed on the bottom of the mould, and the other is placed on the side. In order to increase the consistency of the specimen, the weight of mixture and the thickness of each layer were kept the same. Prior to place next layer, the top of each layer was slightly scarified to avoid discontinuity. After moulding process, the specimens were left in the mould for 24 hours for curing. Then, the specimens were taken out from the mould and were stored in relative humidity above 95% for 14 days.



Figure 3.3 Moulds: (a) The mould of 5cm in diameter and 10 cm in height. (b) The mould of 3.8cm in diameter and 7.6cm in height.

3.4 High pressure triaxial system

The high pressure triaxial testing is the main area in this study. However, the conventional triaxial tests were also conducted to compare the stress-strain behaviours of sand at conventional and high pressures. Hence, before introducing high pressure triaxial test system, conventional triaxial test system will be described. Detailed description of high pressure triaxial test system is given in following sections.

3.4.1 Conventional triaxial testing system

The conventional triaxial test system used in this project is shown in figure 3.4. The conventional apparatus and control system schematic diagram are also illustrated in figure 3.5 and figure 3.6 respectively. The system is based on the classic Bishop & Wesley-type stress path triaxial cell, and the GDS pressure/volume controllers. Three of these pressure controllers link the computer to the test cell as follows:

- one for axial stress and axial displacement control.
- one for cell pressure control.
- one for setting back pressure and measuring volume change.

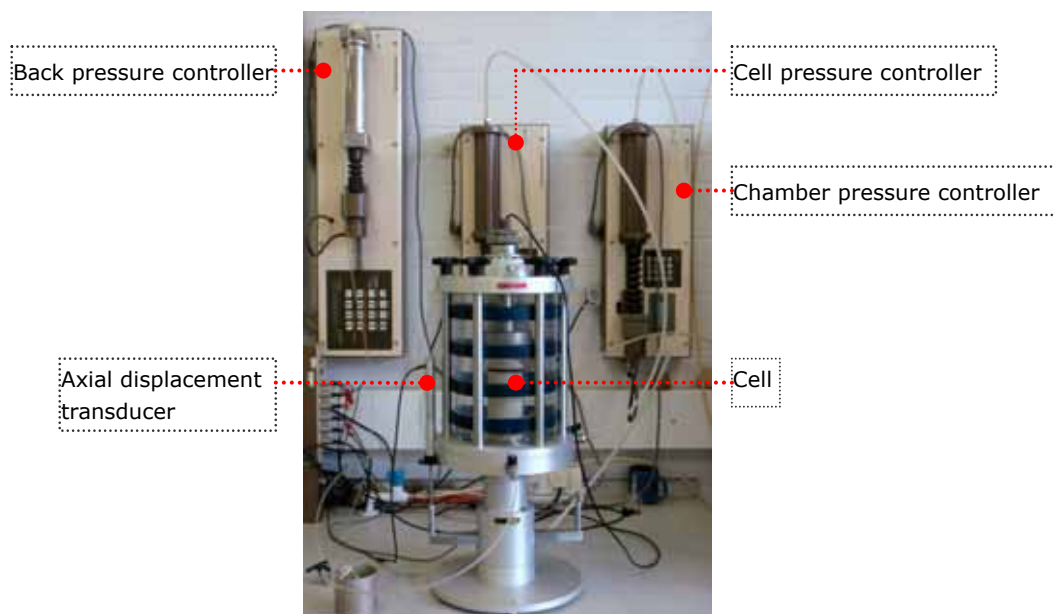


Figure 3.4 The conventional triaxial test system

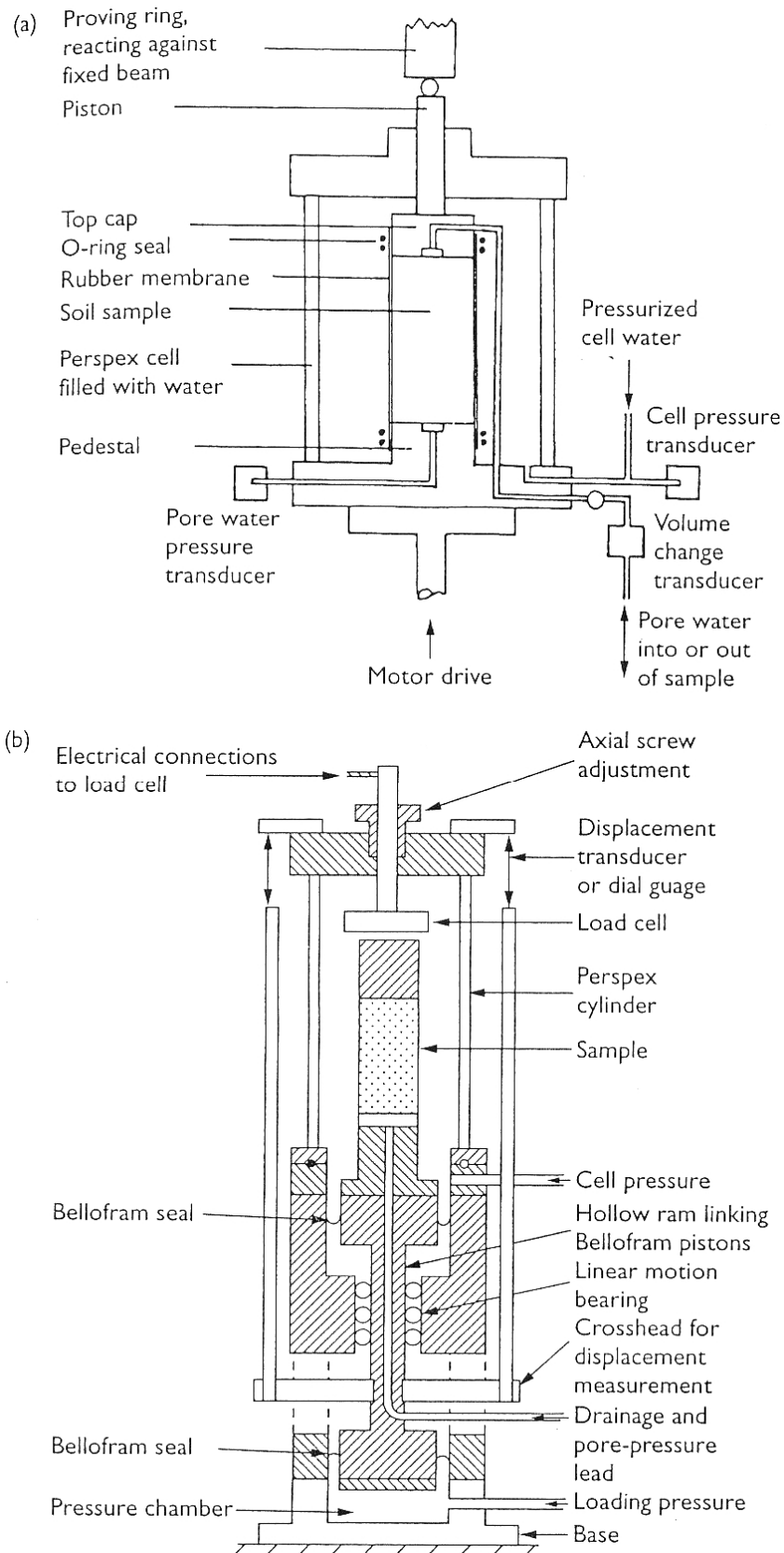


Figure 3.5 Conventional triaxial test apparatus: (a) schematic; (b) hydraulically operated cell (after Powrie 2004)

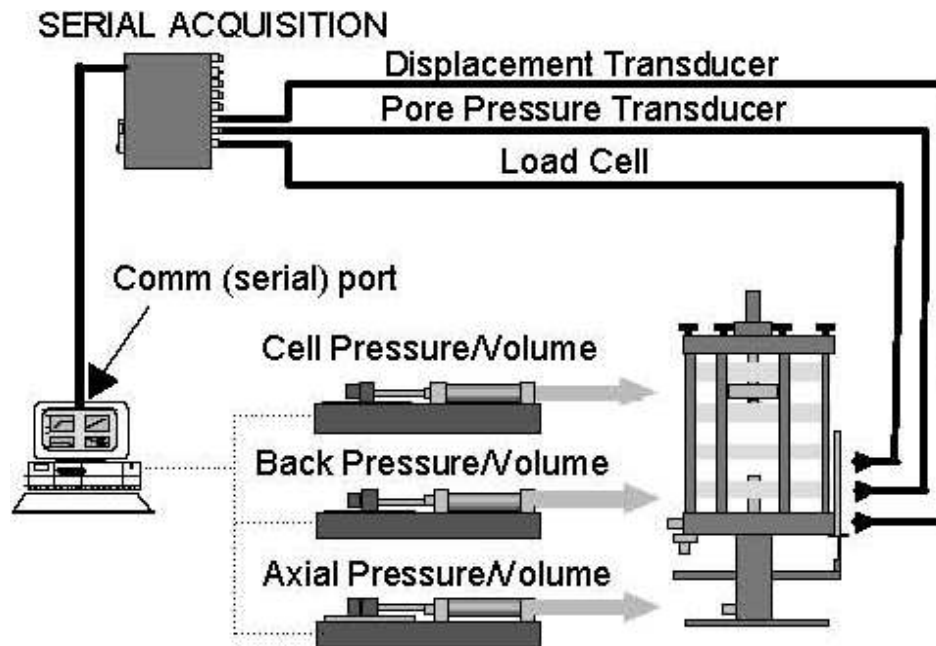


Figure 3.6 The complete triaxial test system (up to 1.7 MPa) (after Hooker 2002)

This conventional system can only provide confining pressure up to 1.7MPa and chamber pressure up to 3MPa. Its capacity is not enough to investigate the behaviour of cemented specimens or dense specimens which diameter are larger than 50mm. Hence the high pressure triaxial system is essential in this project.

3.4.2 High pressure triaxial testing system

In Nottingham Centre of Geomechanics (NCG), there is a GDS high pressure triaxial cell which is an advanced design for high quality high pressure triaxial testing. In order to apply high confining pressure and provide higher load range, the cell needs to be designed to resist high pressure and the axial load providing system also need to provide higher force. Controlling and measuring system have to be modified as well. The control system is shown in figure 3.7. The cell and back pressure/volume controllers are connected to the triaxial cell via steel pipes and linked to the computer by cables. The axial pressure/volume controller, load cell, pore pressure transducer and displacement transducer connected to the loading frame are connected to the serial acquisition. The serial acquisition is connected to computer via Comm port for

transferring data.

The overall setup of high pressure triaxial apparatus is shown in figure 3.8. Detailed description of the high-pressure triaxial cell, the loading frame, and the advanced digital pressure/volume controller is given in following section.

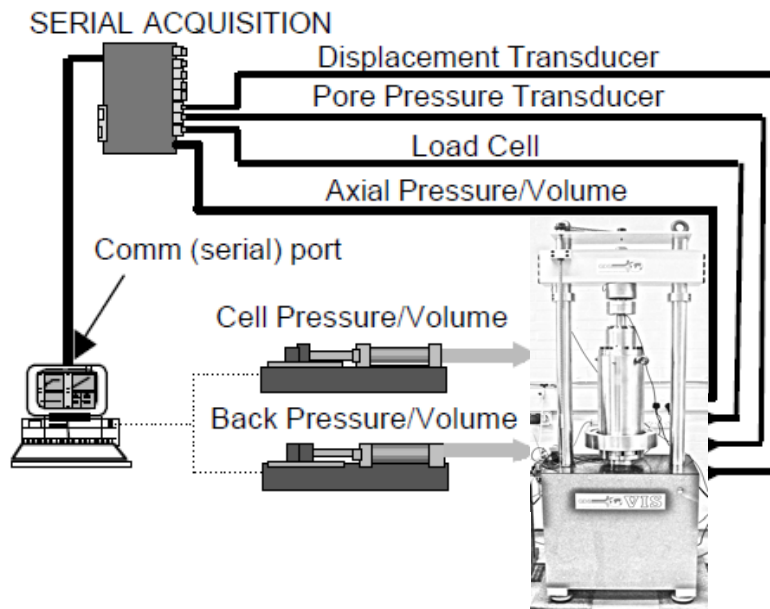


Figure 3.7 Schematic diagram of the high pressure apparatus (modified after GDS 2003)

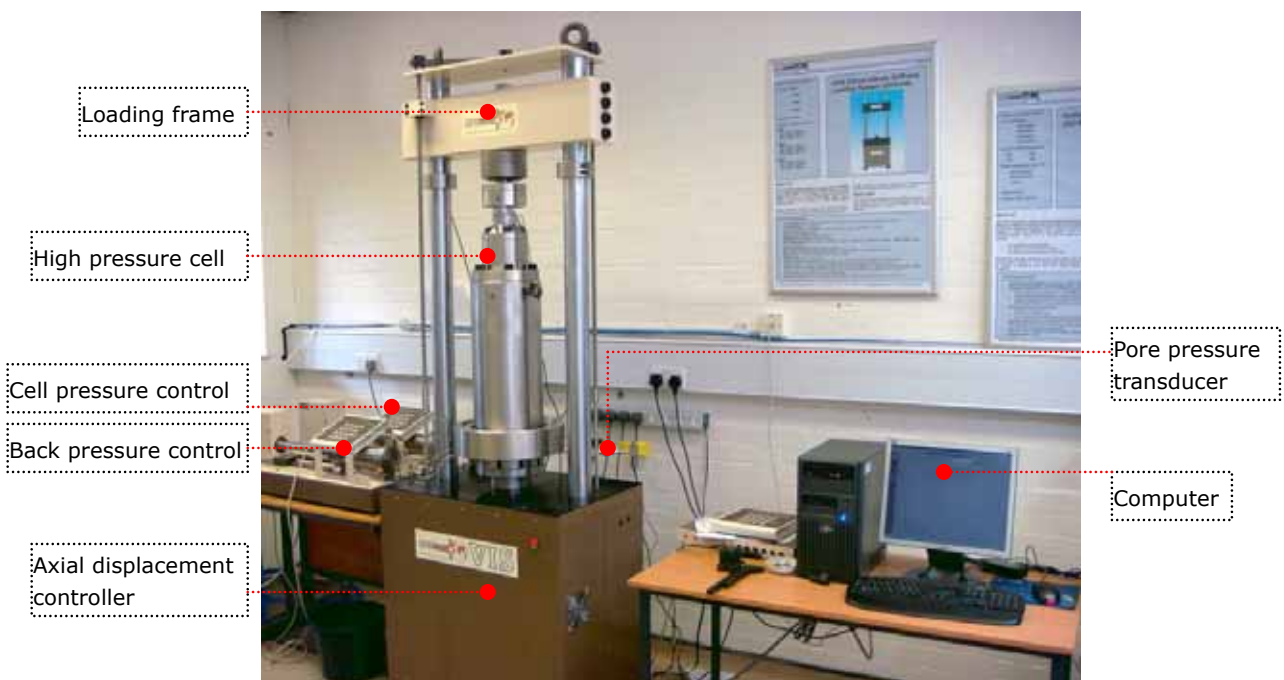


Figure 3.8 Overall setup of high pressure triaxial system.

3.4.3. High Pressure Triaxial Cell

This GDS high pressure triaxial cell is different from conventional triaxial cell in two major aspects. One is that high pressure triaxial cell can provide confining pressure up to 64 MPa. The other is that high pressure triaxial cell is made by metal, so alteration of the specimen does not be observed during the test. The high-pressure triaxial cell and its cross section are shown in figure 3.9. The high-pressure triaxial cell is assembled with seven parts. These are cell top, cell base, pedestal, topcap, clamping ring, retaining ring and two load cell spacers. The cell top includes the main chamber, balanced ram assembly and the ram slip coupling and the clamp ring, which could be split into three parts and retaining ring are used to combine the cell top and cell base. The cell base and its connections are shown in figure 3.10, around the outside of the cell base, swagelok connectors are built for steel pressure pipe connections.

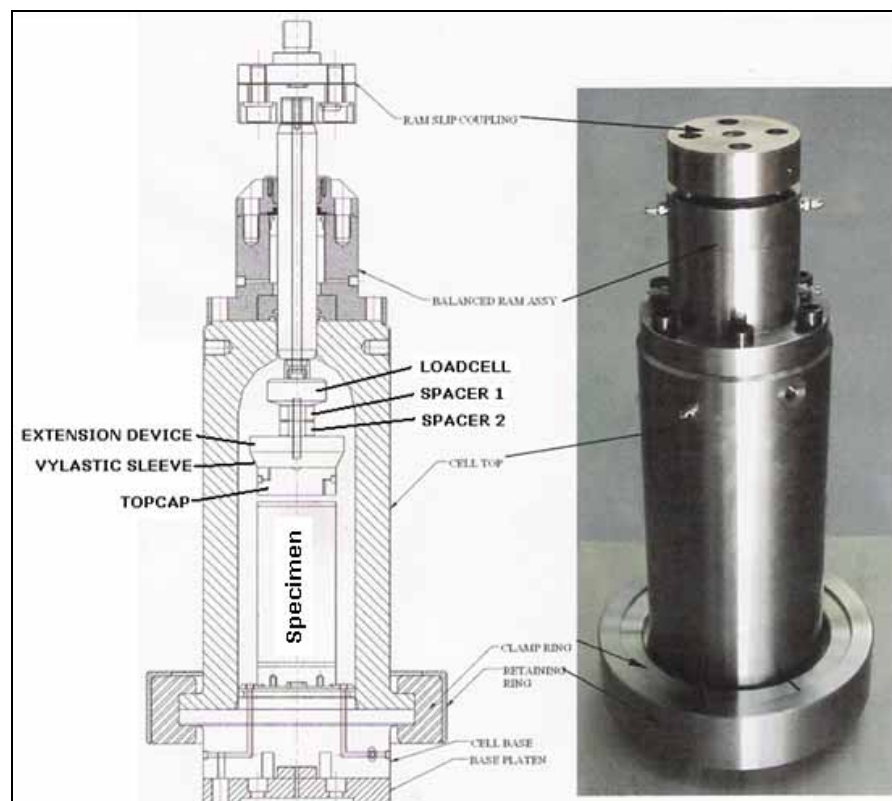


Figure 3.9 Cross-section of high pressure triaxial cell (after GDS 2003).

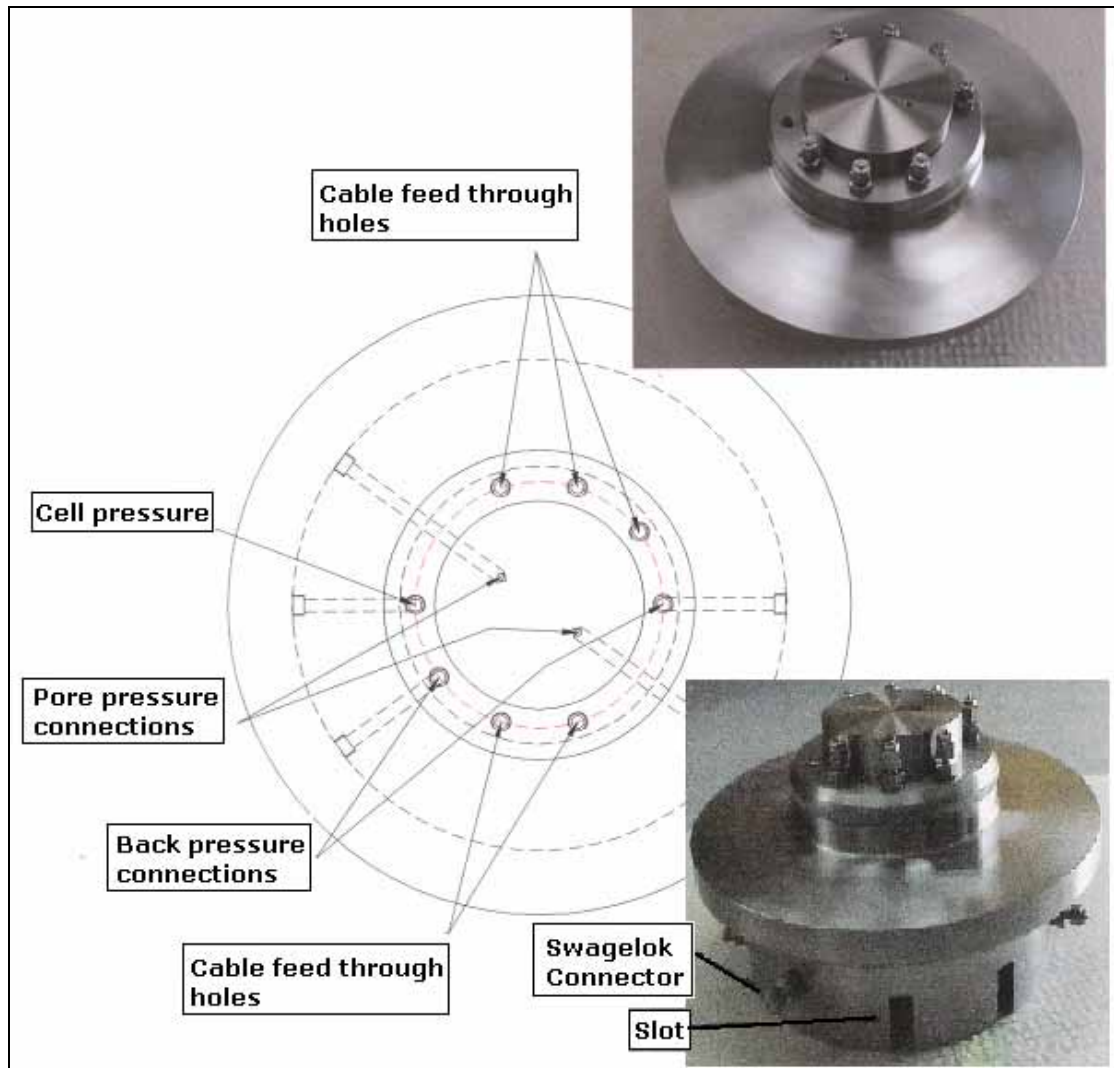


Figure 3.10 Cell base connections (after GDS 2003)

3.4.4 Loading frame

The GDS Virtual Infinite Stiffness Loading System (GDSVIS) is used as loading system to apply the axial loads onto the triaxial cell as shown in figure 3.11. It could apply the axial load up to 400kN. For the entire loading range, both the measurement and control of platen displacement is automatically corrected so that it corresponds to the deformation that occurs between the platen and the load button of the load cell. In this way, the platen displacement is corrected for strain in the load cell and side columns, bending flexure of the cross beams, and distortion within the motorised mechanical transmission. Therefore, in terms of the test specimen, it allows the axial

loading system to appear to have infinite stiffness.

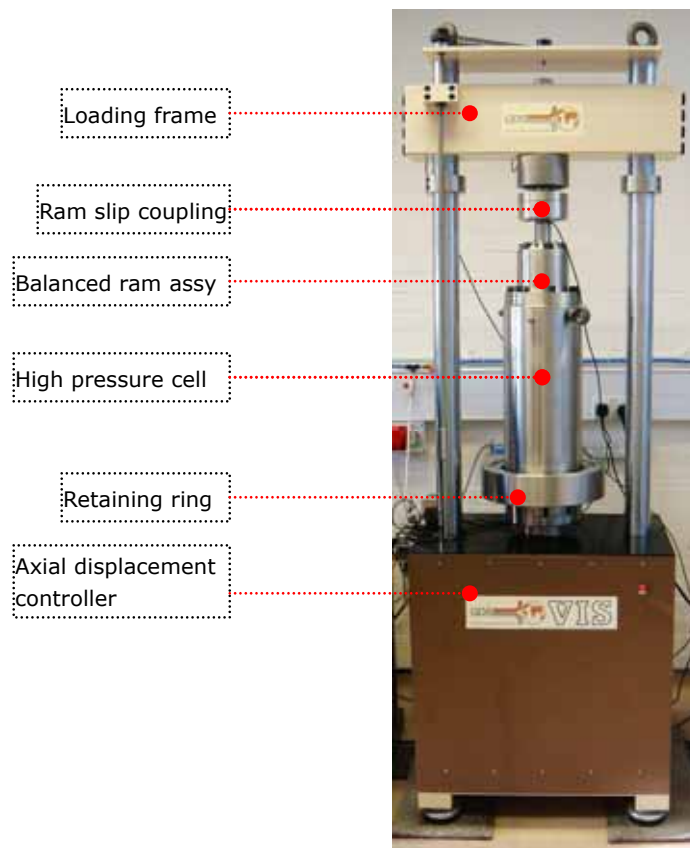


Figure 3.11 Overall setup of high pressure triaxial apparatus in the loading frame.

3.4.5 Advanced Digital Pressure/Volume Controller

Advanced Digital Pressure/Volume Controller (ADPVC) (see figure 3.12) generates, measures and logs both liquid pressure and volume change. The ADPVC has a pressure range up to 64MPa and volume ranges up to 1000cc. The device has its own computer interface and can be controlled directly from a computer. In stand alone mode it can be a constant pressure source, a volume change gauge, a pore pressure measuring system and it also can be programmed through its own control panel to ramp and cycle pressure and volume change linearly with respect to time. In computer control mode, it is a computer peripheral enabling computer-automated test control and data logging via computer interface.



Figure 3.12 Advanced Digital Pressure/Volume Controller

Liquid in a cylinder is pressurised and displaced by a piston moving in the cylinder. The piston is actuated by a ball screw turned in a captive ball nut by an electric motor and gearbox that move rectilinearly on a ball slide (see figure 3.13). Pressure is measured by an integral solid state transducer. Control algorithms are built into the onboard microprocessor to cause the controller to seek to a target pressure or step to a target volume change. Volume change is measured by counting the steps of the incremental motor (GDS 2003).

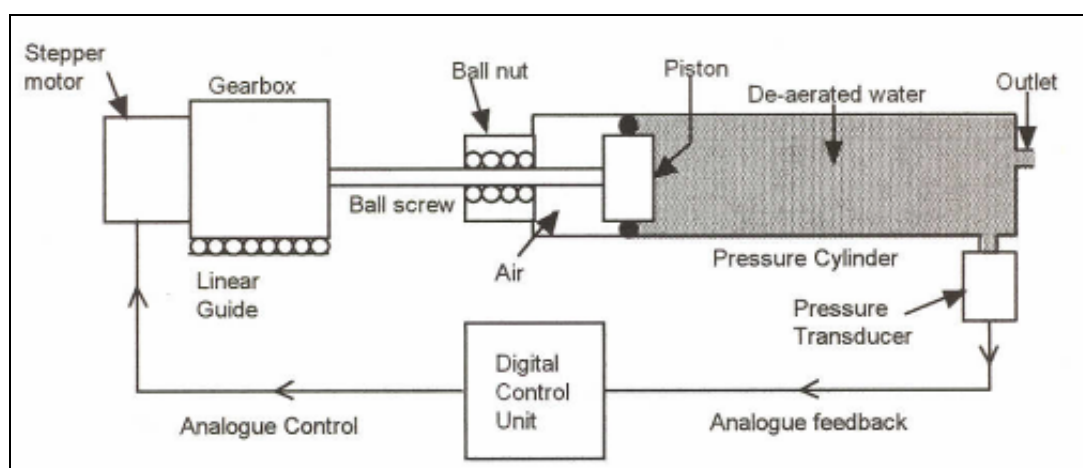


Figure 3.13 Control of Advanced Digital Pressure/Volume Controller (after GDS 2003)

3.5 Testing procedures

Isotropically consolidated undrained triaxial test procedures are similar in high pressure triaxial test system and conventional triaxial test system. Therefore, this section will mainly describe the procedures in high pressure test. Firstly, before the specimen is placed into high pressure cell, the specimen preparation will be divided into two parts. One is uncemented specimen preparation and the other is cemented specimen preparation. Secondly, the high pressure cell assembling processes are introduced. Finally, the stages of sample flushing, saturation, consolidation, and shearing stage are described.

3.5.1 Uncemented specimen preparation

Firstly, the membrane was placed on the pedestal which grease had applied on the surface, and then the O-ring stretcher was used to fix one end of membrane. The function of membrane is crucial, because it separate cell pressure and back pressure to create specific confining pressure. Therefore, careful check was taken to ensure there was no cut on its surface is indispensable before the membrane is employed. Following this, the porous disc which was saturated was placed onto the pedestal and then, the filter paper was placed on the porous stone. The filter paper and porous disc were used to prevent sand particles causing blockages inside the valves.

Secondly, the membrane was stretched in a split membrane stretcher. It has a pipe connection at its mid-height to enable a suction to be applied to the air gap between the membrane and the membrane stretcher. Next, the diameter and height of mould with membrane was measured and recorded to calculate the volume. Afterward, required Portaway sand was collected and separated into 3 layers. Then the specimen was dynamically compacted in three layers in side the membrane with hammer and the height of each layer was controlled to $1/3$ of the required height of specimen. In order to increase the specimen consistency, the top of first and second layer was slightly scarified to avoid discontinuity.

Once the sand was placed into the membrane, the filter paper was placed on the sample and put the porous disc on the filter paper. Following this, the top part membrane was rolled up from the split mould and then the O-ring stretcher with O-ring seals stretched on the mould. Then, the top cap which grease applied on the surface, was carefully placed into the membrane and onto the top of the porous stone. O-ring seals were rolled from the mould to hold the top cap. The top cap was kept horizontally and its top drainage pipe tightened on the top drainage connection which was on the cell base. After the vylastic sleeve was applied onto the top cap which is shown in figure 3.16, the bottom drainage connection was closed, and then suction was applied from the top drainage valve to keep the specimen intact during the setting of high pressure cell. In the end, the mould was removed carefully to avoid disturbance of specimen.

3.5.3 Cemented specimen preparation

Before specimen preparation, cemented specimen was moulded and cured 13 days. After curing, the specimens were submerged in water for 24 hours for saturation, bringing the total curing time to 14 days. Immediately before the test, the specimen was taken out of the water and dried superficially with an absorbent cloth.

To begin with, the porous disc (bottom), filter paper (bottom), cemented specimen, filter paper (top), and porous disc (top) were placed on the pedestal in sequence. Next, after checking two membranes to ensure there was no cut on its surface, they were stretched in membrane stretcher, which was simply a tube with a pipe connection at its mid-height to enable a suction to be applied to the air gap between the membranes and the membrane stretcher. Afterward, the membranes were applied onto the specimen. Following this, 2 O-ring seals were used to tight the membranes on the pedestal. After the top cap was placed on the top of porous disc horizontally, its top drainage pipe was tightened on the top drainage connection which was on the cell base. Finally, the vylastic sleeve was applied onto the top cap, the bottom drainage

connection was closed, and then suction was applied from the top drainage connection to keep the specimen intact during the setting of high pressure cell. Figure 3.14 and figure 3.15 show the specimen before removing the split membrane stretcher and prepared cemented specimen on the cell base respectively.

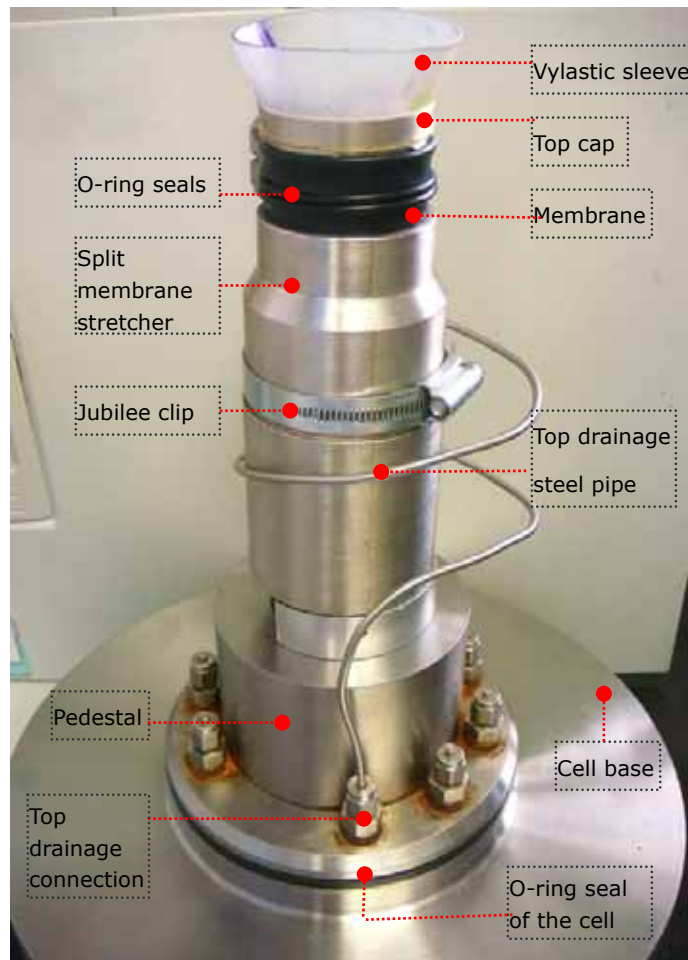


Figure 3.14 Uncemented specimen preparation before removing the split membrane stretcher



Figure 3.15 Prepared cemented specimen.

3.5.3 Setting up the high pressure cell

Before assembling the high pressure cell, there were several things which should be checked. First, base plate was cleaned and the grease applied on its O-ring seal. Next, the ram height was checked that it would not disturb the specimen during assembling the cell. Then, the direction of cell base was confirmed that the top drainage connection was in the front.

After the top cell was lifted, the cell base was moved to the proper place where was below the lifted top cell. Following this, the top cell was lowered slowly and vertically onto the cell base. Extreme care was taken to ensure no disturbance was applied on the specimen. Next, the three parts of the clamp ring were placed as shown in figure 3.16(a), and then the remaining rings as shown in figure 3.16(b) was placed over the assembled clamping ring.



(a)

(b)

Figure 3.16 Assemble the Clamp Ring(a) and retaining ring(b) (after GDS 2003)

Due to a large mass of the cell, a trolley was designed and used to transport the high pressure cell onto the loading frame, as shown in figure 3.17 and figure 3.19. The trolley was made together with two rails on each side, so that, once the triaxial cell was loaded onto the trolley, the cell could be rolled on the rails. The cell was moved slowly and carefully to avoid disturbing the specimen or slipping out of the rails.

After placing the high pressure cell into the loading frame, two bolts were used to connect the ram to the loading frame diagonally. Then, the cable was connected to serial acquisition and the power of loading frame was turned on. Afterward, the GDS testing control software was executed to move the base plate of loading frame to lift cell from the rails of the trolley. Then, the trolley was removed from the bottom of the cell. The overall setup of high pressure triaxial apparatus in a loading frame is shown in figure 3.11. Before filling water in the cell, the steel pipes of providing cell pressure and linking between balance ram and cell were connected. When the cell was filled with water, the air valve was tightened. In the end, the confining pressure was increased to 150 kPa, then the suction applied on the specimen was released.

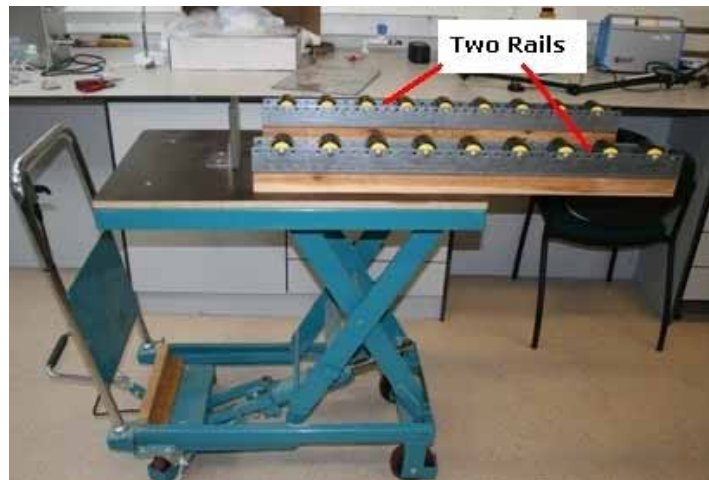


Figure 3.17 The Trolley



Figure 3.18 Fitting the triaxial cell into the loading frame

3.5.4 Procedures of triaxial test

After specimens had been prepared and placed into the triaxial cell, together with all the testing equipments were also set up, saturation and isotropical consolidation would be conducted before triaxial compression test. Detailed description of these procedures is given below.

3.5.4.1 Saturation

All the specimens were saturated by flushing with de-aired water. For expelling the air from specimens, back pressure was applied from the bottom drainage to let the void inside filled with water. In the meanwhile, the top drainage was open to let air discharge with water. The back pressure was adjusted to 100 kPa which was lower than the cell pressure. It took at least an hour, and was longer in cemented specimen or dense specimen.

The process of saturation was followed by increasing back pressure until the B value was greater than 0.95. The B value, Skempton's pore water parameter, can be expressed by equation 3.1.

$$B = \frac{\Delta u}{\Delta \sigma_3} \quad (3.1)$$

Where the Δu = change in pore pressure and $\Delta \sigma_3$ = change in cell pressure.

During the process, an effective confining pressure 100 kPa was maintained on the specimen and drainage was not allowed. This process was controlled by GDS software. In this project, the targets of saturation ramp were 2100 kPa in cell pressure and 2000 kPa in back pressure and took 12 hours to reach. Real time monitor was also provided by GDS software.

After completing the saturation ramp, B-check was carried out to ensure that the specimen was sufficiently saturated. Before starting the check, the current cell pressure and pore pressure were recorded. Then, the cell pressure was increased to the specified value, then at the same time, the back pressure remained the same. In this project, the target cell pressure is set to 2200kPa. When the cell pressure reached the target, the pore pressure was recorded to calculate the B value according to equation (3.1). In this project, the pore pressure was increased greater than 2095kPa and the B values reached 0.95. During the process, the top drainage valve and back

pressure valve are closed. Following this, the cell pressure and back pressure were adjusted to 2100kPa and 2000kPa, respectively.

3.5.4.2 Isotropic consolidation

Isotropic consolidation was carried out to ensure the specimen was at the state of the required boundary stress conditions and had no excess pore pressure. Hence, the process was followed by increasing cell pressure to specific confining pressure. For example, if the backpressure was 2000kPa and specific confining pressure was 4000 kPa, so the target cell pressure was increased to 6000kPa. The consolidation was continued until there was no further volume change and all the excess pore pressure dissipated. During the procedure, the top drainage valve was open and the back pressure valve closed. This process was controlled and monitored by GDS software. The typical back volume against time during the process of consolidation is shown in figure 3.19.

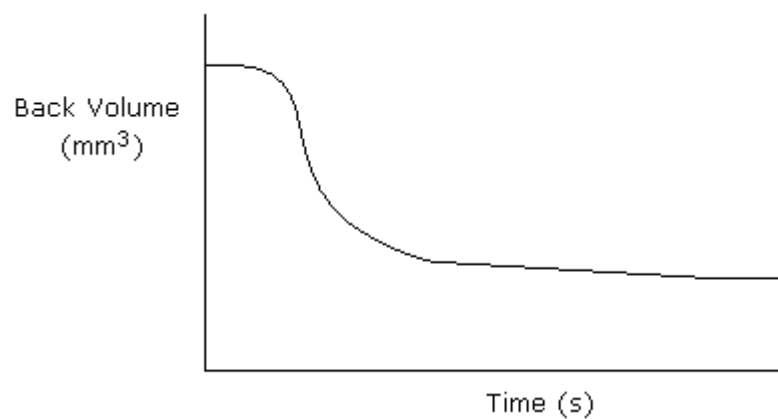


Figure 3.19 Typical back volume against time during the process of consolidation

3.5.4.3 Undrained Shearing

During the undrained shearing test, a compression took place by applying an axial load onto the specimen. The cell pressure was maintained at a specific value while the specimen was sheared at a constant rate of axial deformation until failure occurred. Drainage was not allowed through the entire test, so that the volume of the specimen

was remained constant during compression. The top drainage valve and back pressure valve were closed. The measurement of changes in pore pressure was done at the base of the specimen by a pore pressure transducer. The rate of axial deformation was applied slowly to the specimen at the rate of 0.2 mm per minute or strain rate 0.2% per minute in specimen of 100mm in height or 0.26% per minute in specimen of 76 mm in height.

During all the tests, parameters such as axial strain (ϵ_a), pore pressure (u), axial stress (σ_1) and radial stress (σ_3) were recorded and used for plotting results.

3.6 Experimental Program

In order to understand the effect of cementation, effective confining pressure and drainage on the behaviour of the cemented granular material, a detailed experimental program was planned. Portland cement in amounts of 5%,10% and 15% by weight of dry soil was used to prepare artificially cemented specimens. All the cemented specimens were prepared at dry unit weights of 17.4kN/m³. They moulded and cured as described in Section 3.3. The triaxial tests were carried out at three different effective confining pressures of 500,1000,4000 kPa. A summary of all the tests is given in table 3.6

Table 3.6 Summary of test conducted

NO	Cement Content	σ_3' (Mpa)	Specimen size	Comment
1	0%	0.5	D=50mm, H=100mm	Dr=47%
2	0%	0.5	D=38mm, H=76mm	Dr=81%
3	0%	1	D=50mm, H=100mm	Dr=82%
4	0%	4	D=50mm, H=100mm	Dr=81%
5	5%	0.5	D=38mm, H=76mm	
6	5%	4	D=50mm, H=100mm	
7	10%	4	D=50mm, H=100mm	
8	15%	4	D=50mm, H=100mm	

3.7 Summary

In this chapter, the material properties, high pressure triaxial testing system, and detailed experimental procedures including moulding and curing of cemented specimens, and isotropically consolidated undrained triaxial test procedures have been introduced. The following chapters describe the results and the associated interpretations based on the outcome from experimental program.

Chapter 4 Experimental results and discussion

4.1 Introduction

A total of 8 consolidated undrained triaxial tests on uncemented and artificially cemented sand have been carried out. Test results are presented as including stress–strain curves, stress paths, excessive pore pressure versus strain and effects of density, cementation, and drainage effects are discussed. The test results from this research have been compared with the results of a parallel study, which used the same base soil but conducted in isotropically consolidated drained condition.

The test results have been analysed using σ_1' , σ_3' , ϵ_1 , ϵ_v , u , q and p' , where

σ_1' and σ_3' are, respectively, the effective axial stress and effective confining stresses on a cylindrical sample, ϵ_1 and ϵ_v are respectively the axial and volumetric strains, u is excessive pore water pressure, q and p' are respectively deviatoric and mean effective stresses. q and p' are defined as:

$$q = \sigma_1' - \sigma_3' \quad (4.1)$$

$$p' = (\sigma_1' + 2\sigma_3')/3 \quad (4.2)$$

4.2 Undrained behaviour of uncemented sand

This section will focus on the undrained behaviour of uncemented sand. There are two parts: effect of density and effect of confining pressure. The detailed description is given below.

4.2.1 Effect of density

The results on two different relative densities of specimens in undrained triaxial test are shown in figure 4.1. Deviatoric stress (q), excess pore water pressure (u),

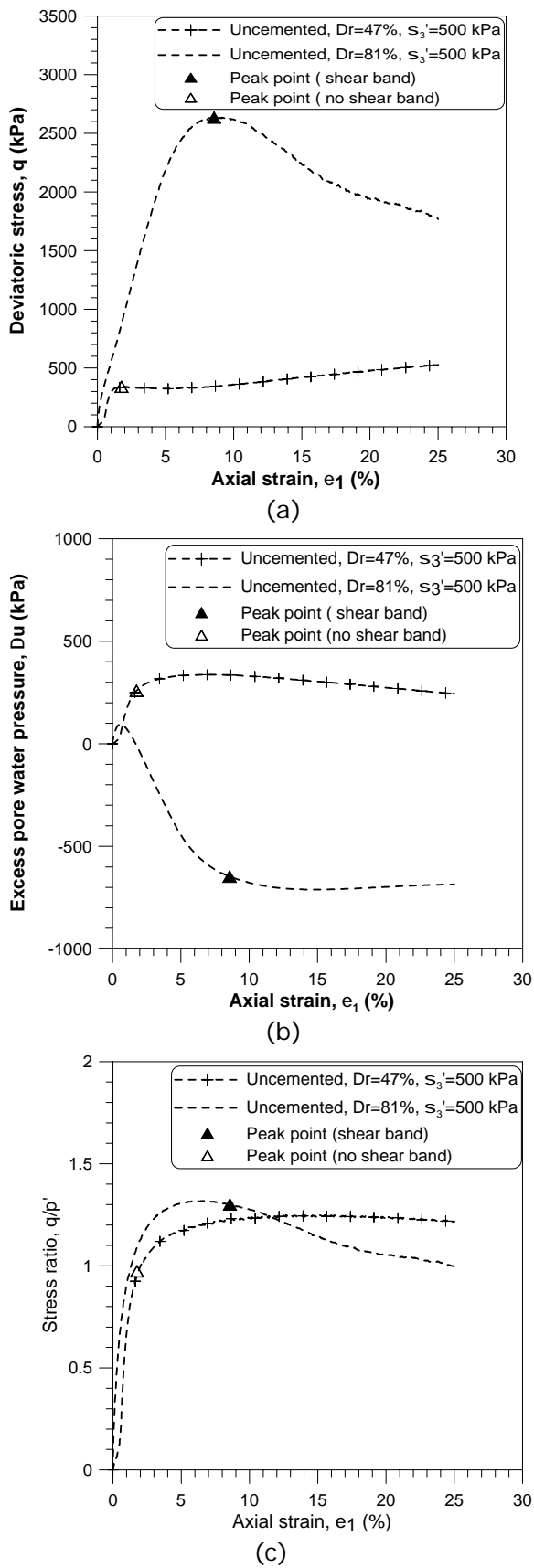
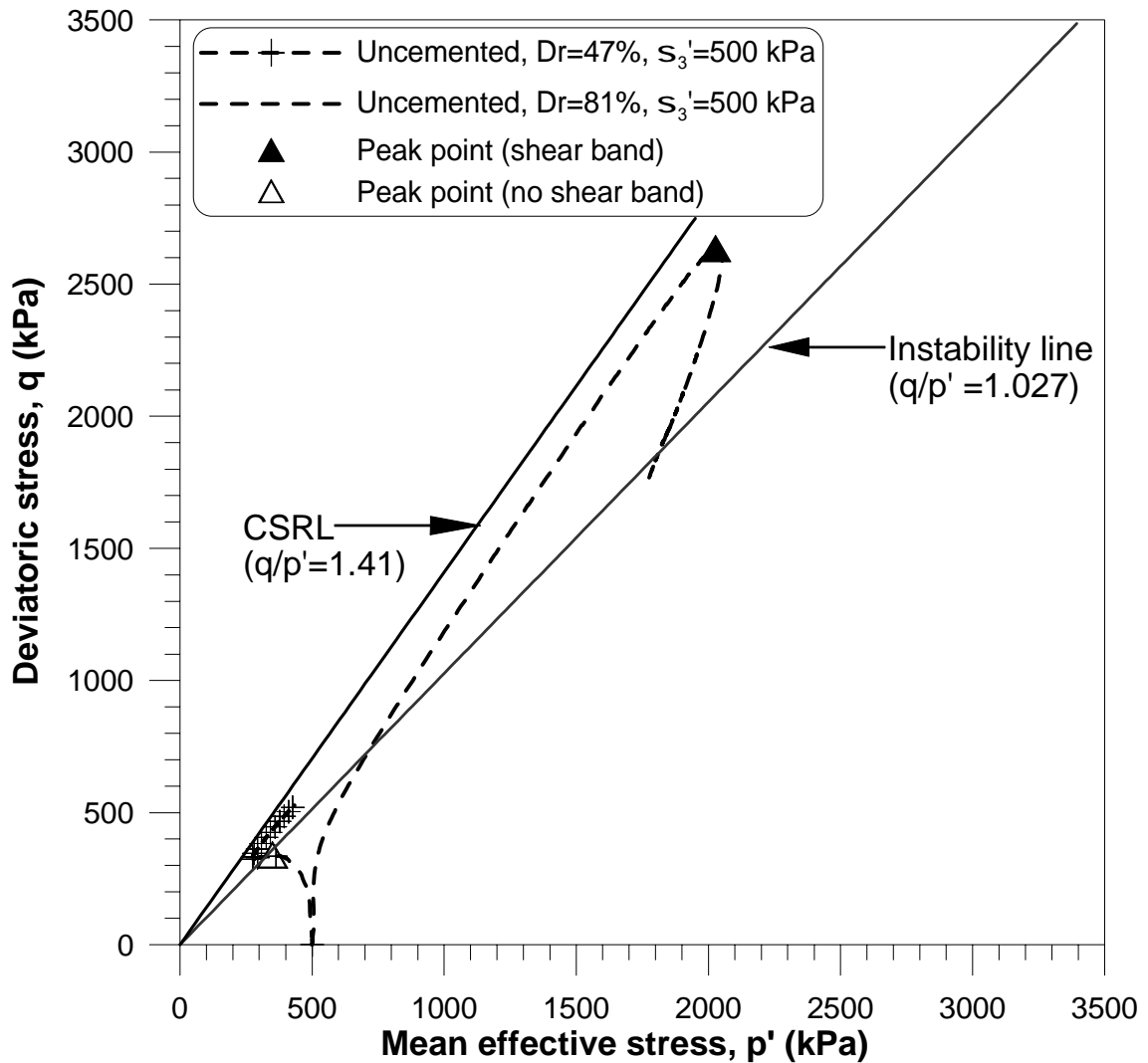


Figure 4.1 Results of CIU triaxial test on medium dense and dense sand: (a) stress-strain behaviour; (b) u versus e_1 curves; (c) q/p' versus e_1 curves; (d) effective stress paths.



(d)

Figure 4.1 Continued.

and stress ratio (q/p') plotted against axial strain (ϵ_1), and the effective stress paths are shown as well.

In figure 4.1 (a), the initial slopes of stress-strain curve of dense specimen is steeper than medium dense as expected. In medium dense specimen, shows the deviatoric stress increasing to a peak, followed by a decrease, but it rises again to its maximum value at failure. After the first peak is reached, the drop in the deviatoric stress is caused by the tendency of the specimen to compress volumetrically, causing the pore pressure to rise, thus decreasing the effective stress. The test of dense sample shows

the different behaviour. It increases to a peak, then following by a decrease with increasing strain to the end of test.

The excess pore water pressures shown in figure 4.1 (b) indicate that dense and medium dense specimens show different tendencies. The generated pore water pressure of the medium dense specimen is positive, which displays tendency for overall net compressive volumetric behaviour. At larger strain, the effective confining pressure has declined sufficiently to allow the specimen to show volumetrically dilatant tendencies, causing the pore pressure to drop. However, the positive excess pore water pressure in dense specimen is found at beginning of shearing with small magnitude, followed by a rapid decrease to about relative large negative value at about 10% axial strain, and then keeps steady to the end.

In figure 4.1 (c), the stress ratios against axial strain are presented. The dense specimen has higher value of maximum stress ratio than medium dense specimen. However, the ultimate stress ratio of medium dense specimen is higher than dense specimen. Both of them may approach a constant value at high strain levels.

In figure 4.1 (d), the CIU triaxial test in medium dense specimen indicates an effective stress path that increases upward, followed moving slightly to the left. Then, the specimen continues to strengthen, and it causes the stress path to continue upward with increasing deviatoric stress and effective mean stress. In the end, it reaches the maximum deviatoric stress. Lade (1992) indicates that the stress state at instability would occur corresponds to the top of the current yield surface which is slightly before, but very close to the top of the undrained effective stress path. The location of instability line is shown in figure 4.2. Therefore, the instability line can be determined experimentally by a line connecting the peaks of a series of effective stress paths obtained from undrained test. In figure 4.1 (d), the instability line is plotted by a line connecting the peak and the origin. However, more results are needed to determine the instability line. The stress path of dense specimen, it increases upward at the beginning, and then it inclines to follow the constant stress ratio line (CSRL) with the

slope of 1.323 until the maximum deviatoric stress reached. Following this, it turns to opposite direction to the end.

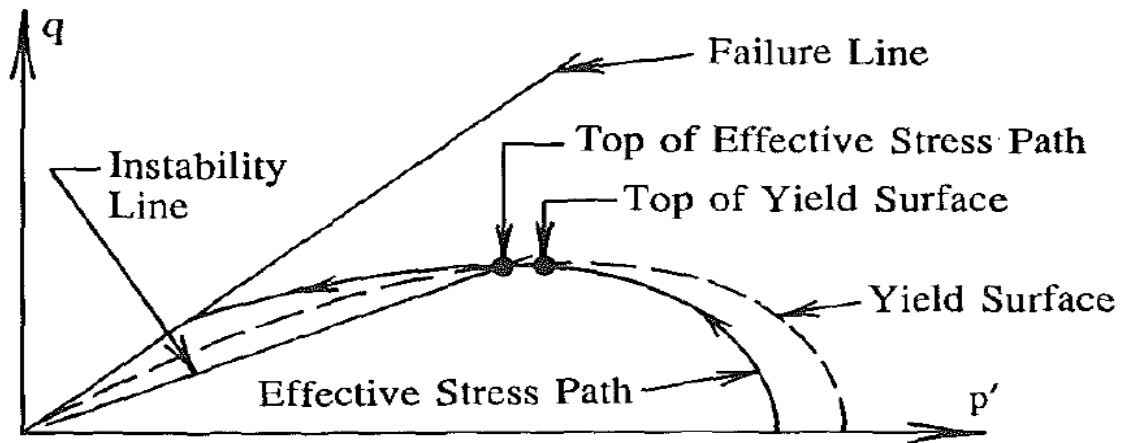


Figure 4.2 Location of instability line for loose sand (after Lade 1992)

4.2.2 Effect of confining pressure

The results on three different confining pressure specimens in undrained triaxial test are shown in figure 4.3. Deviatoric stress (q), excess pore water pressure (u), and stress ratio (q/p') plotted against axial strain (ϵ_1), and the effective stress paths are shown as well.

As shown in figure 4.3 (a), as the effective confining pressures increase the peak deviatoric stresses increase. Table 4.1 shows peak deviatoric stresses, peak effective mean stresses and peak stress ratios of three confining pressure. For the confining pressure of 500kPa the maximum deviatoric stress is 2635kPa, and for the confining pressures of 1000kPa and 4000kPa the maximum deviatoric stresses are 5529kPa and 6597kPa. The confining pressure increase twice from 500kPa to 1000kPa and the deviatoric stress increase about 2.1 times from 2635kPa to 5529kPa. However, the confining pressure increase four times from 1000kPa to 4000kPa and the deviatoric stress increase about 1.19 times from 5529kPa to 6597kPa. It appears that the effect

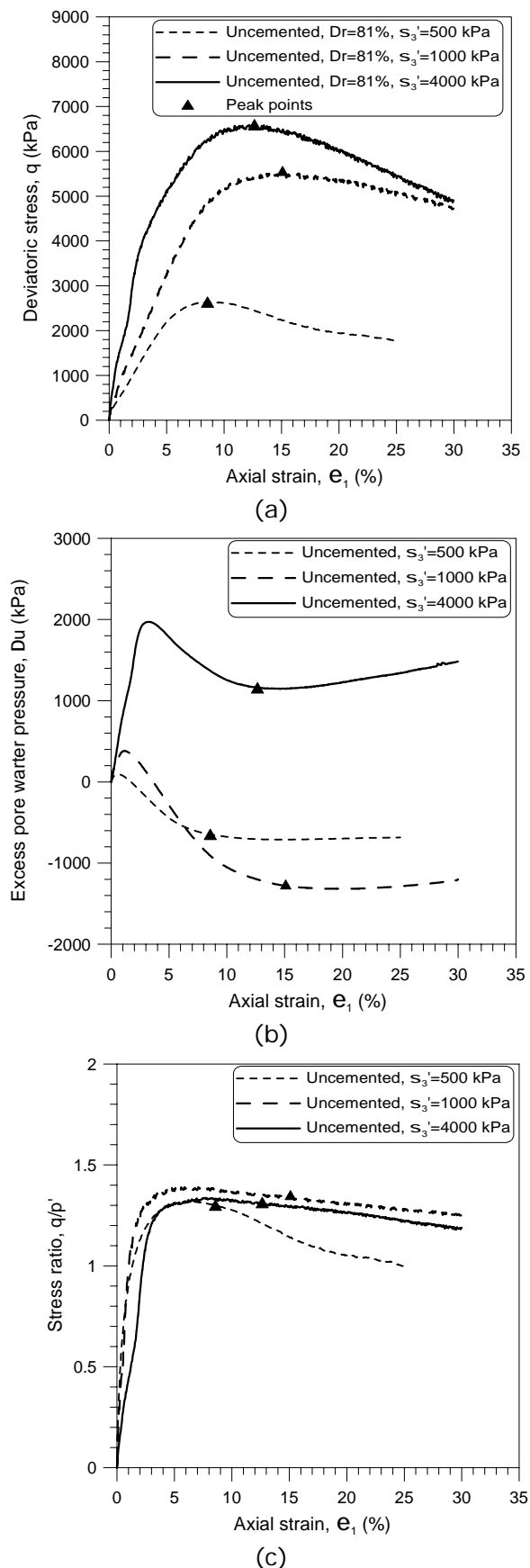
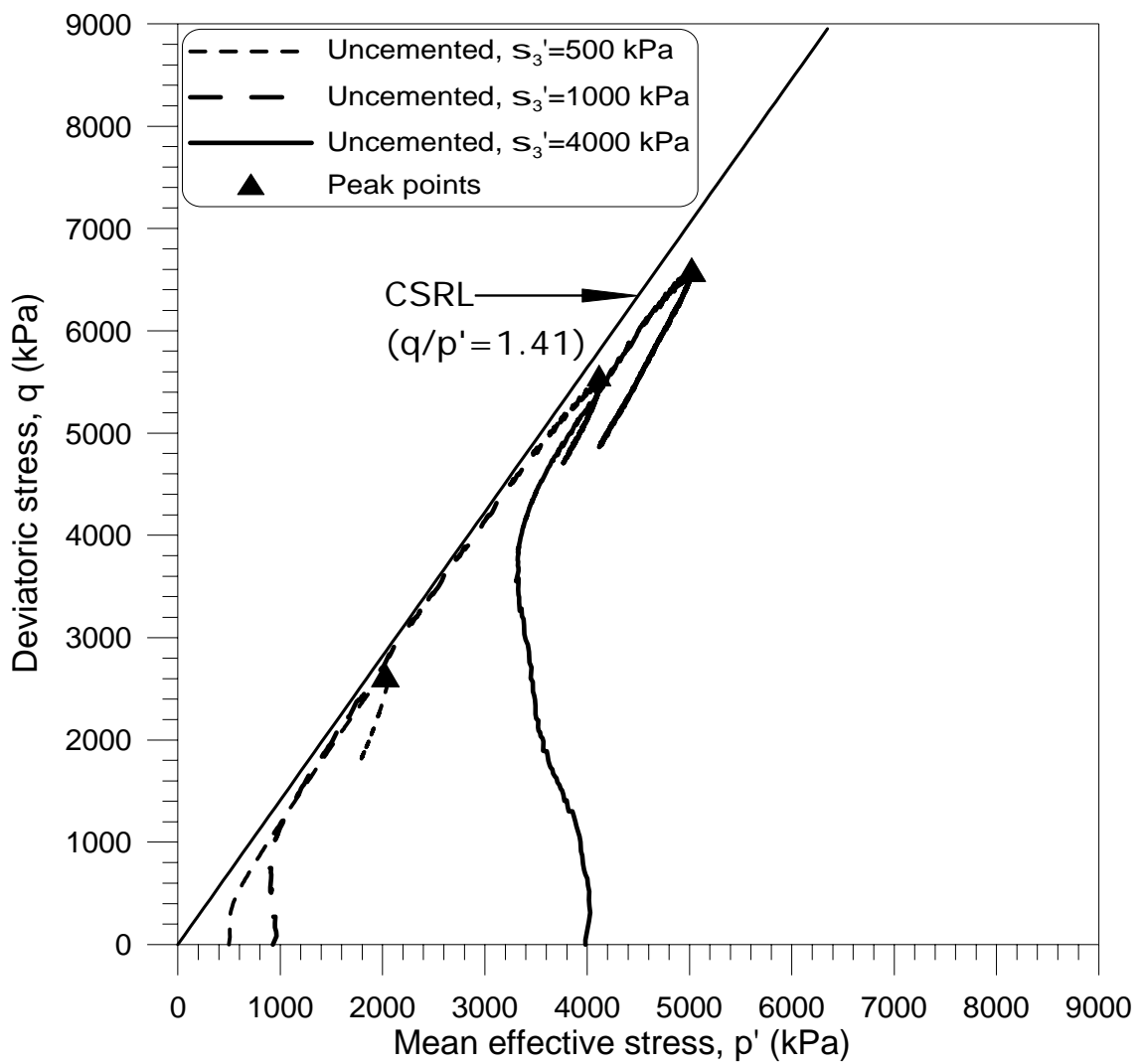


Figure 4.3 Results of CIU triaxial test in uncemented specimens at different confining pressures: (a) stress-strain behaviour; (b) u versus ϵ_1 curves; (c) q/p' versus ϵ_1 curves; (d) effective stress paths.



(d)

Figure 4.3 Continued.

Table 4.1 Peak deviatoric stresses, Peak effective mean stresses and peak stress ratios of three confining pressure.

Effective confining pressure (kPa)	Peak Deviator stress (kPa)	Peak effective mean stress (kPa)	Peak stress ratio
500	2635	2026	1.300
1000	5529	4117	1.343
4000	6600	5022	1.314

of confining pressure to deviatoric stress declines with the increase of confining pressure.

In figure 4.3 (b), the induced excess pore pressures of three different confining pressures show the similar tendencies. The positive excess pore water pressure is generated at the beginning, following with a decrease and then keeps steady to the end. However, higher confining pressure induces higher positive excess pore water pressure at beginning. The higher maximum positive excess pore pressure occurs at larger confining pressure.

The stress ratios against axial strains are plotted in figure 4.3 (c). The maximum stress ratios in three confining pressures of 500kPa, 1000kPa and 4000kPa are 1.3, 1.343 and 1.314 respectively. They seem close.

As figure 4.3 (d) shown, the stress paths in three confining pressure are similar. The stress paths increase upward at the beginning, and then they incline to follow the constant stress ratio line (CSRL) until the maximum deviatoric stress reached. Following this, it turns to opposite direction to the end. The CSRL can be determined by fit the three maximum deviatoric stresses from the origin.

4.3 Undrained behaviour of cemented sand

This section will focus on the undrained behaviour of cemented sand. There are two parts: effect of cement content in conventional and high conventional pressure and effect of confining pressure. The detailed description is given below.

4.3.1 Effect of cement content

The results of uncemented and 5% cement content under conventional confining pressure specimens in undrained triaxial test are shown in figure 4.4. Deviatoric stress (q), excess pore water pressure (u), and stress ratio (q/p') plotted against

axial strain (ϵ_1), and the effective stress paths are shown as well.

As shown in figure 4.4 (a), the deviatoric stress of the cemented specimen is higher than uncemented specimen in conventional confining pressure. The initial slope of stress-strain curve of cemented specimen is steeper than uncemented specimen and the maximum deviatoric stress of cemented specimen occurs earlier than uncemented specimen.

In figure 4.4 (b), the excess pore pressures of uncemented and cemented specimens show similar tendencies in CIU tests. The positive excess pore water pressure is induced at small axial strain ($< 1\%$) and small magnitude, then following with a significant decrease and then keeps steady to the end.

The stress ratios against axial strains are plotted in figure 4.4 (c). The maximum stress ratios in uncemented and cemented specimens are about 1.3, 1.7 respectively. The maximum stress ratio of cemented specimen occurs earlier than uncemented sample. It appears that the cementing agent shows obvious influence in stress ratio.

In figure 4.4 (d), the stress paths of 5% cement content specimen and uncemented specimen show different routes. The stress path of uncemented specimen is described in Section 4.2.2. The stress path of cemented specimen increase upward at the beginning, and then they incline to follow the constant stress ratio line (CSRL) until the maximum deviatoric stress reached. Following this, it turns to opposite direction to the end. If the CSRL of cemented specimen assumes that it has the same slop with the CSRL of uncemented specimen, the CSRL of cemented specimen can be determined by shifting the CSRL of uncemented specimen to fit the maximum deviatoric stress of cemented specimen. Therefore, the CSRL of 5% cement content specimen can be expressed as:

$$q=1.41p'+600 \quad (4.3)$$

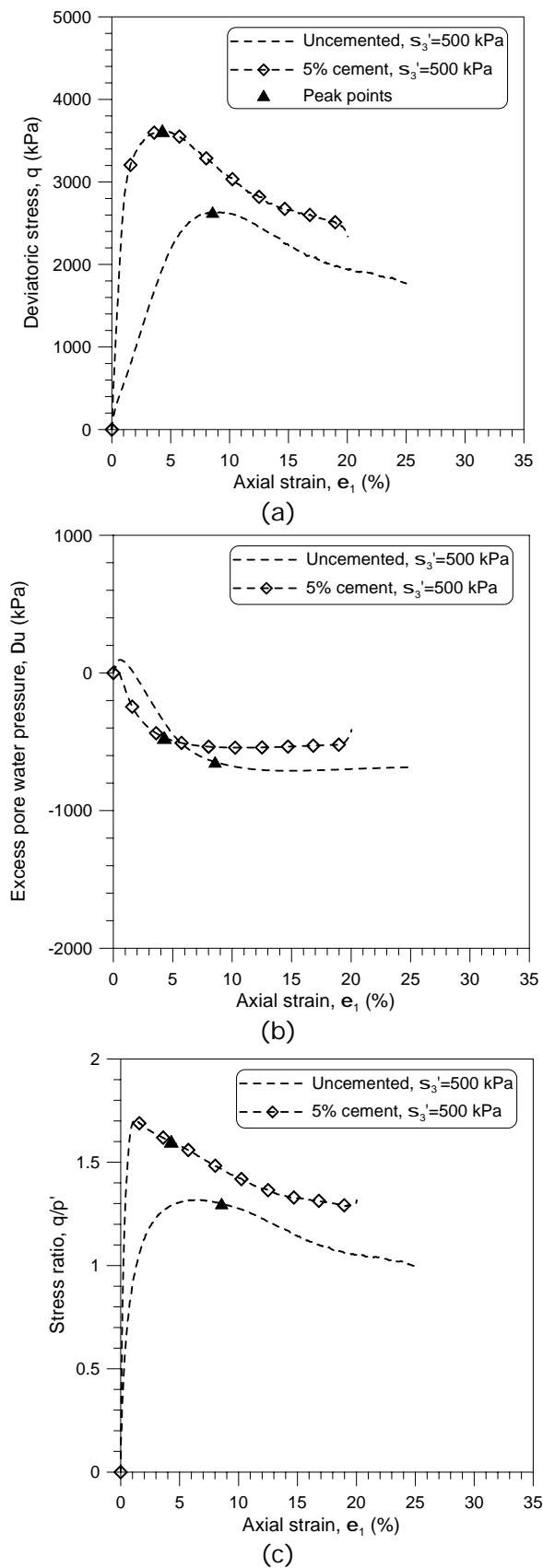


Figure 4.4 Results of CIU triaxial test in of different cement content at conventional confining pressure(500 kPa): (a) stress-strain behaviour; (b) u versus e_1 curves; (c) q/p' versus e_1 curves; (d) effective stress paths.

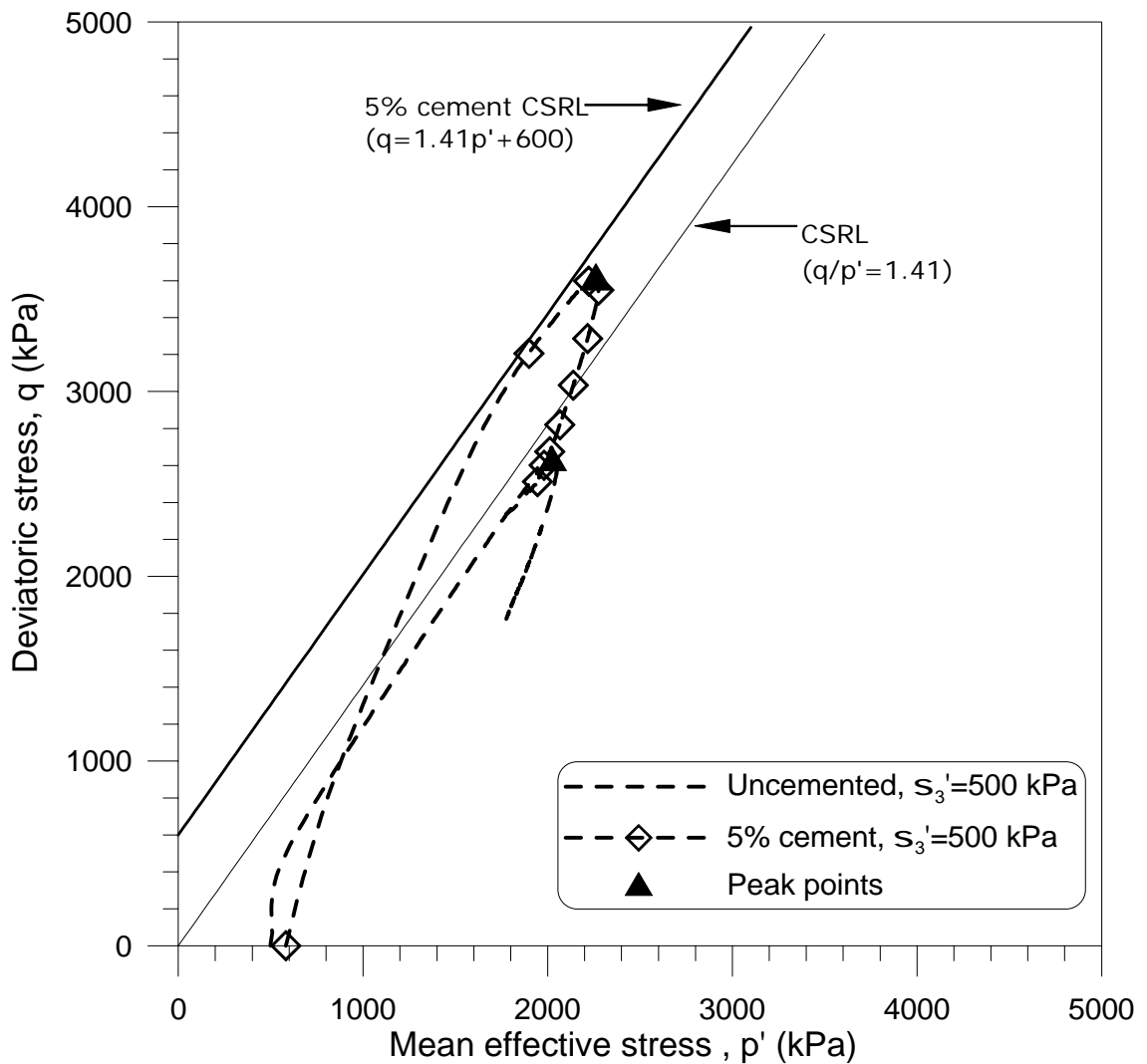


Figure 4.4 Continued.

The results of uncemented, 5%, 10%, and 15% cement content under high confining pressure (4MPa) specimens in undrained triaxial test are shown in figure 4.5. Deviatoric stress (q), excess pore water pressure (u), and stress ratio (q/p') plotted against axial strain (ϵ_1), and the effective stress paths are shown as well.

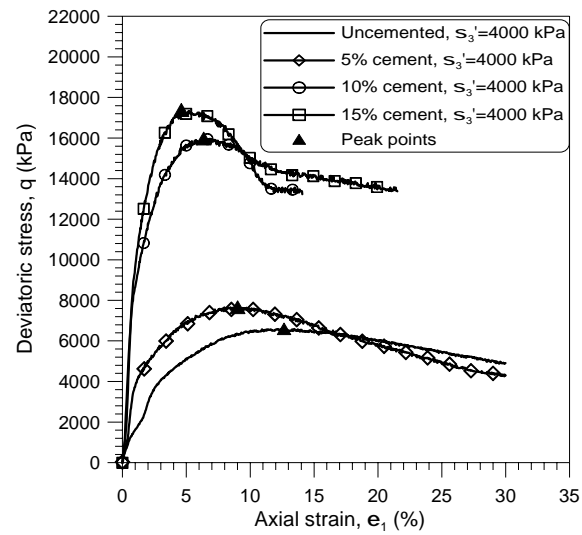
As shown in figure 4.5 (a), the higher cement content leads to higher maximum deviatoric stress. The peak deviatoric stresses of uncemented, 5%, 10%, and 15% occurs in 12.6%, 9.0%, 6.4%, and 4.6% respectively. It appears that higher cement content let the peak deviatoric stress show earlier and the initial slope of stress-strain

curve be steeper. The behaviours of uncemented and 5% cemented specimen are different from 10% and 15% cemented specimen. 10% and 15% cemented specimens show clear peaks and their maximum deviatoric stresses are 15975kPa and 17384kPa, respectively. However, the peak deviatoric stress of uncemented and 5% cemented specimens is not so obvious and their maximum deviatoric stresses are 6597kPa and 7661kPa, respectively. It appears that the deviatoric stress in high confining pressure may be sensitive when cement content between 5% and 10%. Anyway, it needs more results to confirm.

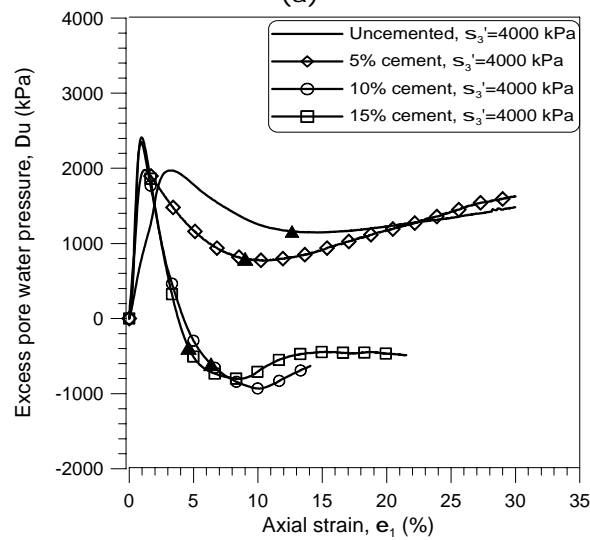
In figure 4.5 (b), the positive excess pore water pressure is induced at small axial strain which is about 1% in cemented specimen and about 3% in uncemented specimen. The generated maximum excess pore water pressure is larger in higher cement content. The excess pore pressures show similar tendencies to deviatoric stresses shown in figure 4.5 (a). The behaviours of uncemented and 5% cemented specimen are different from 10% and 15% cemented specimen. The excess pore water pressure of uncemented and 5% cemented keep positive during the test. However, the induced excess pore water pressure in 10% and 15% cemented specimen are positive at beginning, and then declined sharply to the negative values.

As figure 4.5 (c) shown, the specimen of higher cement content has higher maximum stress ratios. It appears that stress ratios of uncemented and 5% cemented specimens show different tendency from 10% and 15% cemented specimen. The stress ratios of 10% and 15% cemented specimen have noticeable peaks.

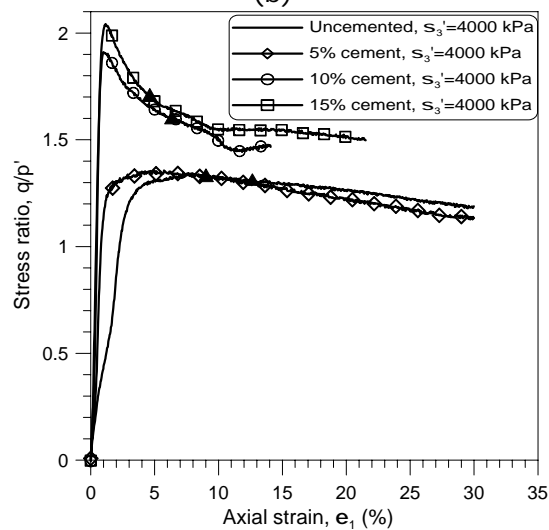
In figure 4.5 (d), the specimen of different cement contents show similar type of stress paths which increase upward at the beginning, and then they incline to follow the constant stress ratio line (CSRL) until the maximum deviatoric stress reached. Following this, it turns to opposite direction to the end. If the CSRL of cemented specimen assumes that it has the same slop with the CSRL of uncemented specimen, the CSRL of cemented specimen can be determined by shifting the CSRL of uncemented specimen to fit the maximum deviatoric stress of cemented specimen.



(a)



(b)



(c)

Figure 4.5 Results of CIU triaxial test in of different cement content at high confining pressure(4000 kPa): (a) stress-strain behaviour; (b) u versus e_1 curves; (c) q/p' versus e_1 curves; (d) effective stress paths.

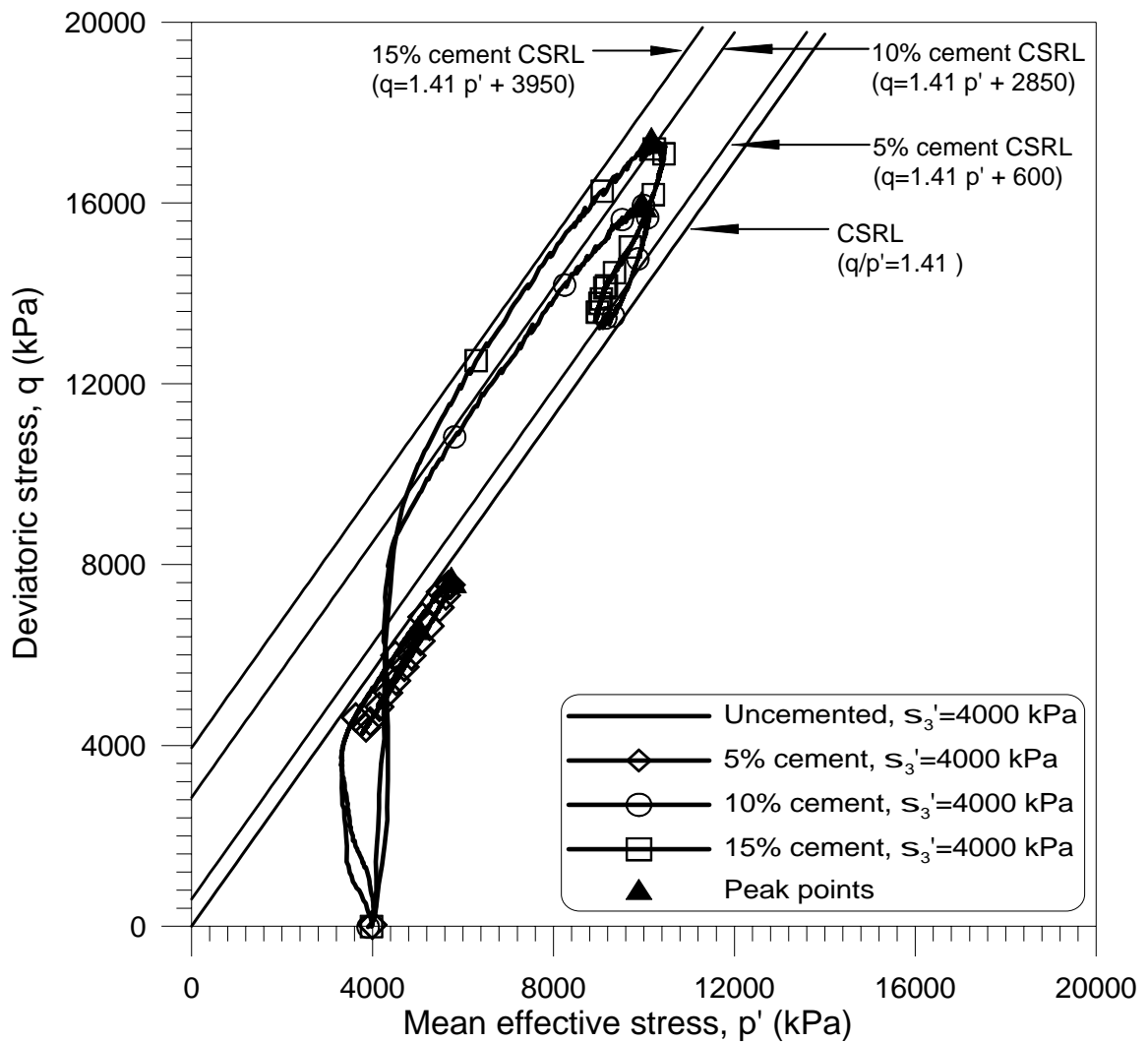


Figure 4.5 Continued.

Therefore, the CSRL of 10% and 15% cement content specimen can be expressed as:

$$q=1.41p'+2850 \quad (4.4)$$

$$q=1.323p'+3950 \quad (4.5)$$

In figure 4.6 the cement contents and cohesion intercepts of equation (4.3), (4.4) and (4.5) are plotted. It appears that cohesion intercepts increase to power 1.77 of cement content. It means that non-linear relationship between the cohesion intercept of CSRL.

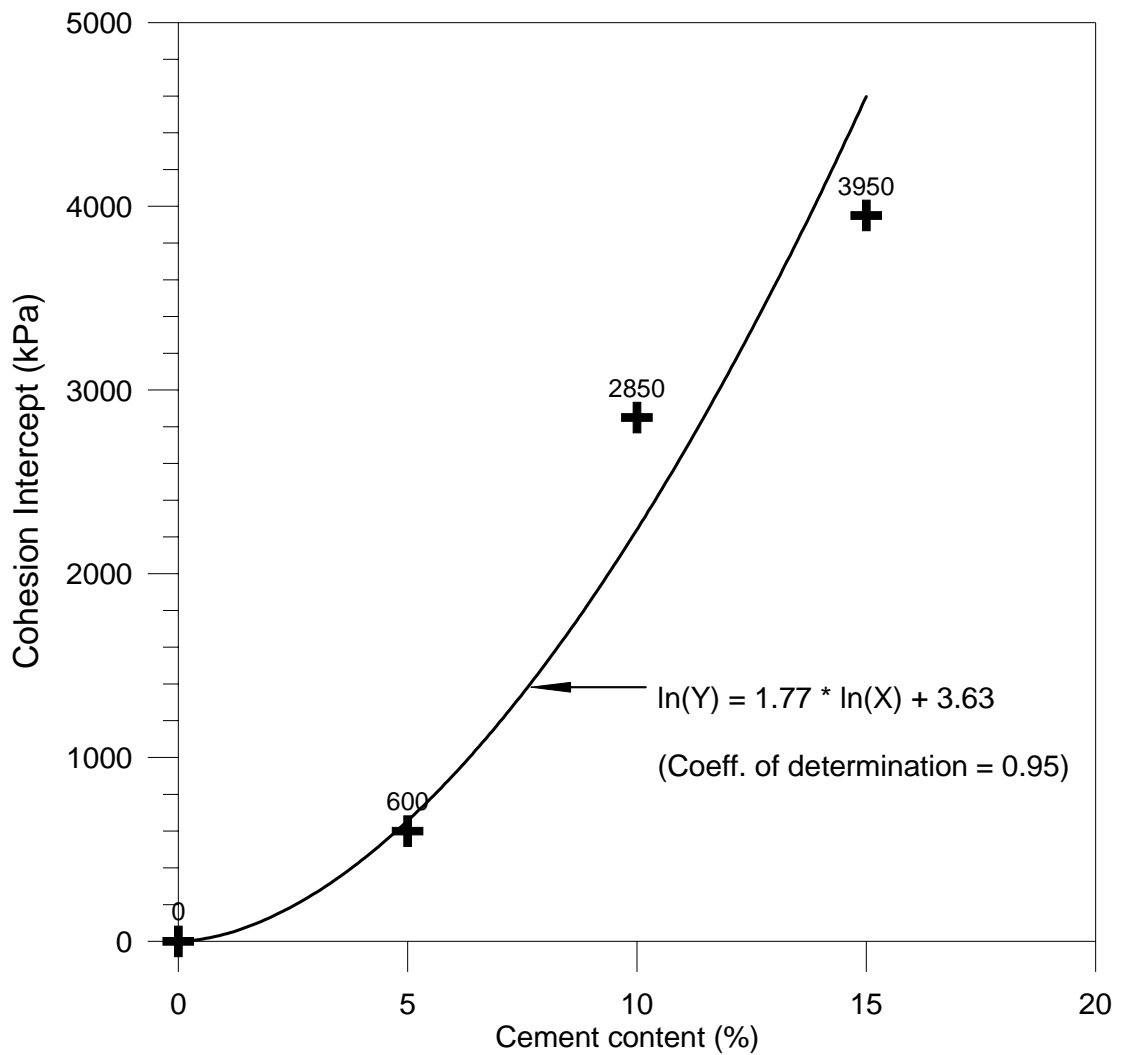


Figure 4.6 The relationship between cement content and intercept

4.3.2 Effect of confining pressure

The results of 5% cement content under conventional confining pressure (500kPa) and high confining pressure (4000kPa) specimens in CIU tests are shown in figure 4.7. Deviatoric stress (q), excess pore water pressure (u), and stress ratio (q/p') plotted against axial strain (ϵ_1), and the effective stress paths are shown as well.

In figure 4.7 (a), the peak deviatoric stress in high confining pressure and conventional confining pressure occurs in 9.00% and 4.29% axial strain respectively. It appears that high confining pressure let peak stress occurs later than conventional confining pressure. In other words, the high confining pressure seems to let behaviour

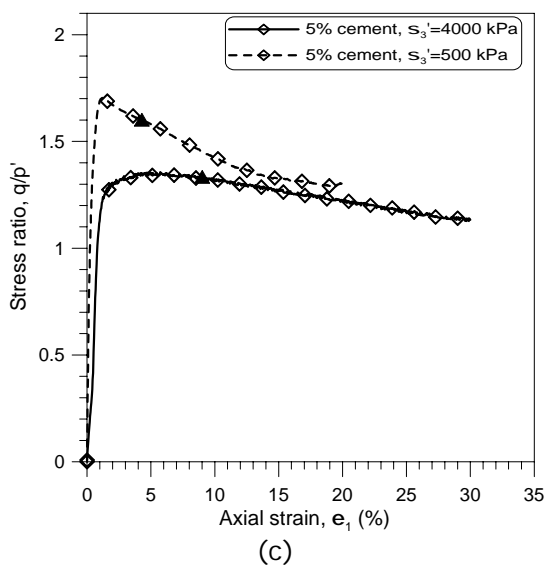
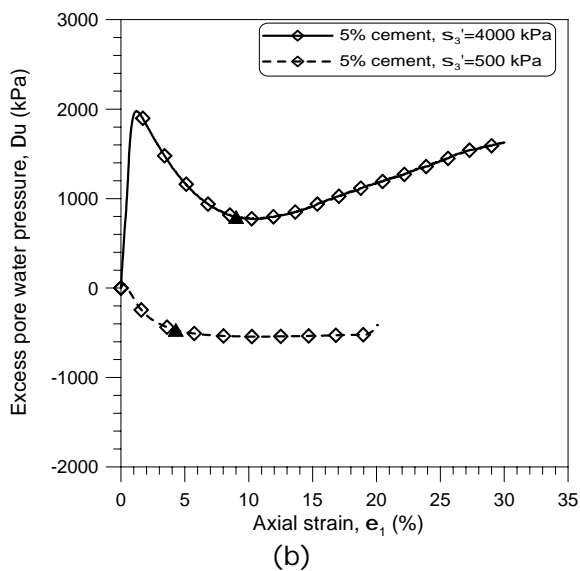
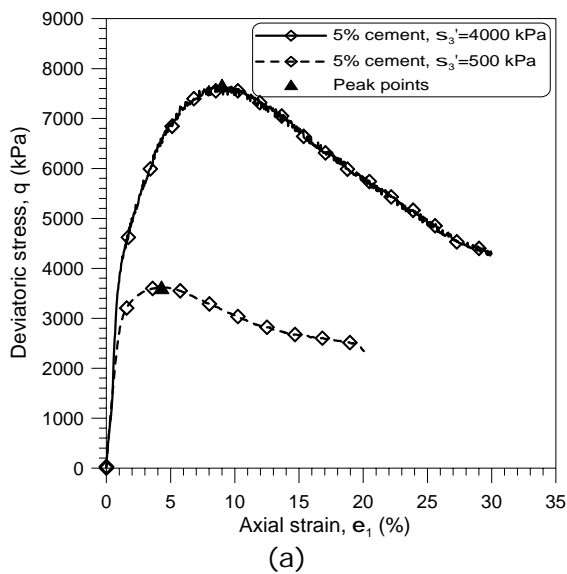
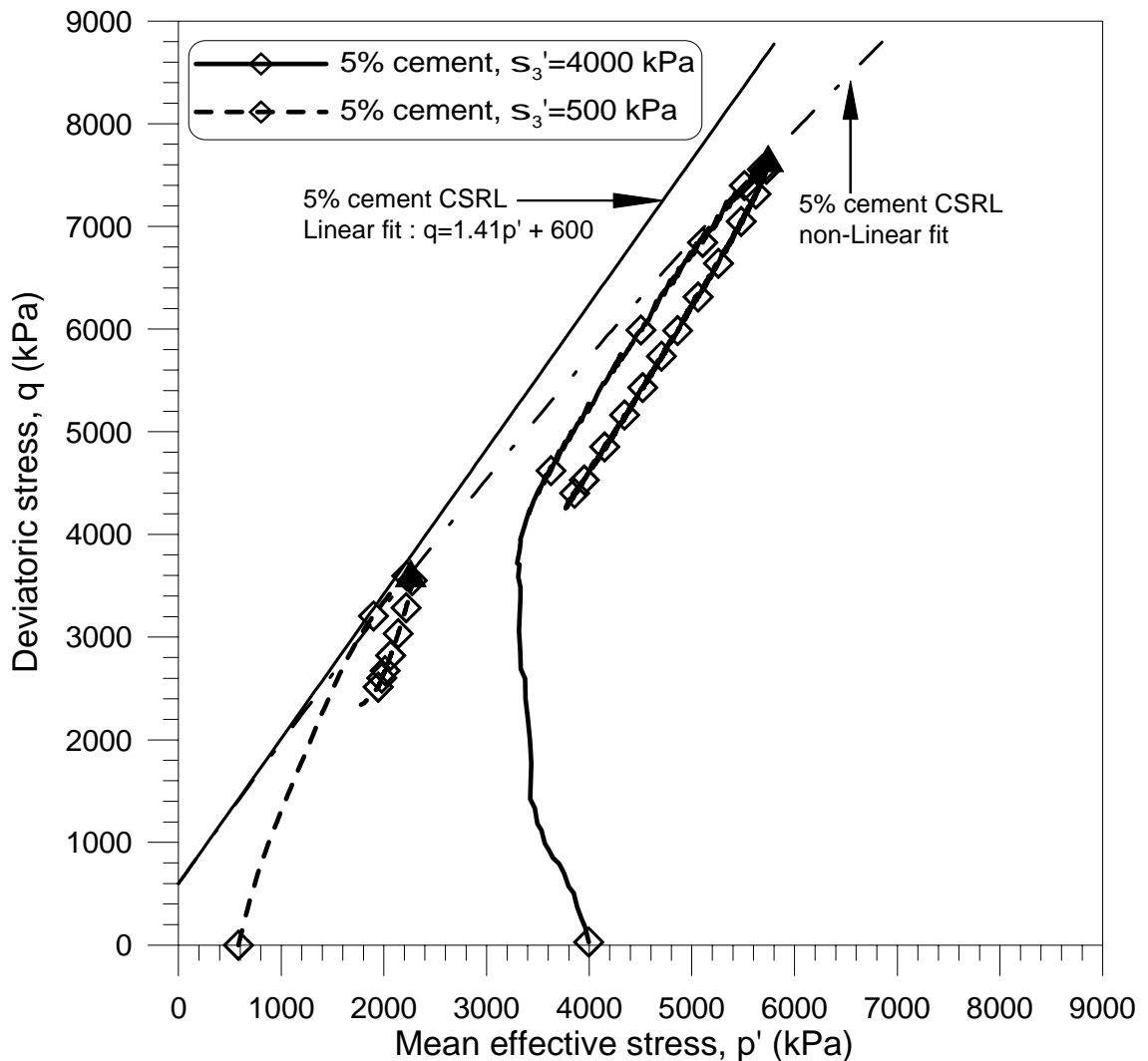


Figure 4.7 Results of CIU triaxial test in different confining pressure : (a) stress-strain behaviour; (b) u versus σ_1 curves; (c) q/p' versus σ_1 curves; (d) effective stress paths.



(d)

Figure 4.7 continued

of cemented soils show similar characteristics of looser sand in stress-strain behaviour. However, the maximum deviatoric stress in high confining pressure is higher than conventional confining.

As shown in figure 4.7 (b) the excess pore water pressures in high pressure and conventional pressure both described in Section 4.3.1 show different behaviours. It appears that high confining pressure let the 5% cemented specimen has positive

excess pore water pressure during the test and induced excess pore water pressure has noticeable peak and higher value.

In figure 4.7 (c) the stress ratios against strain of 5% cemented specimen in high pressure and conventional pressure both described in Section 4.3.1 are presented. In high confining pressure, the maximum stress ratio shows obvious peak and high than conventional confining pressure. However, they seem to approach a constant value at ultimate state (high strain levels).

As shown in figure 4.7 (d), the stress paths in high and conventional confining pressure approach the same CSRL to reach their maximum deviatoric stress. It seems that CSRL can be a curve. However, more results are needed to clarify which type is rational.

4.4 Comparison between drained and undrained behaviour

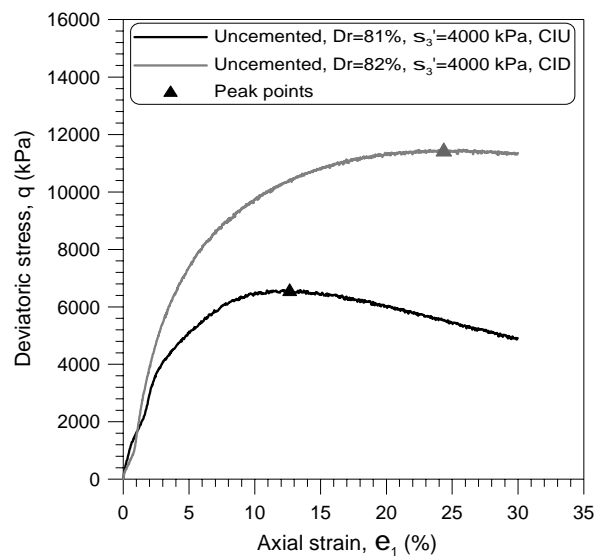
This section will compare undrained behaviour with drained behaviour of uncemented and cemented sand at high pressure. The detailed description is given below.

4.4.1 Uncemented sand

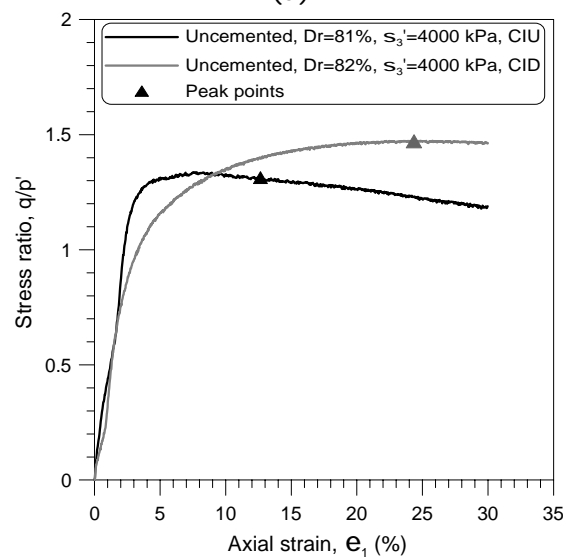
The results of uncemented content under high confining pressure (4000kPa) specimens in CIU and CID tests are shown in figure 4.8. Deviatoric stress (q), excess pore water pressure (u), and stress ratio (q/p') plotted against axial strain (ϵ_1), and the effective stress paths are shown as well.

As shown in figure 4.8 (a), the deviatoric stresses against strain in CID and CIU tests shows different behaviour. In CID and CIU test, the peak deviatoric stresses which occur at 24.35% and 12.65% axial strain are 11479kPa and 6597kPa, respectively. The peak deviatoric stress of CID test is 1.74 times than CIU test, and occurs at very large strain. However, the deviatoric stress against strain in CIU test has noticeable peak. Furthermore, the initial slope of CID test is steeper than CIU test.

In figure 4.8 (b), the maximum stress ratio in CID test is higher than CIU test and it occurs large axial strain. As shown in figure 4.8 (c), the stress paths of CID and CIU tests show different routes. In CIU test, the stress path which increase upward at the beginning, and then they incline to follow the constant stress ratio line (CSRL) until the maximum deviatoric stress reached. Following this, it turns to opposite direction



(a)

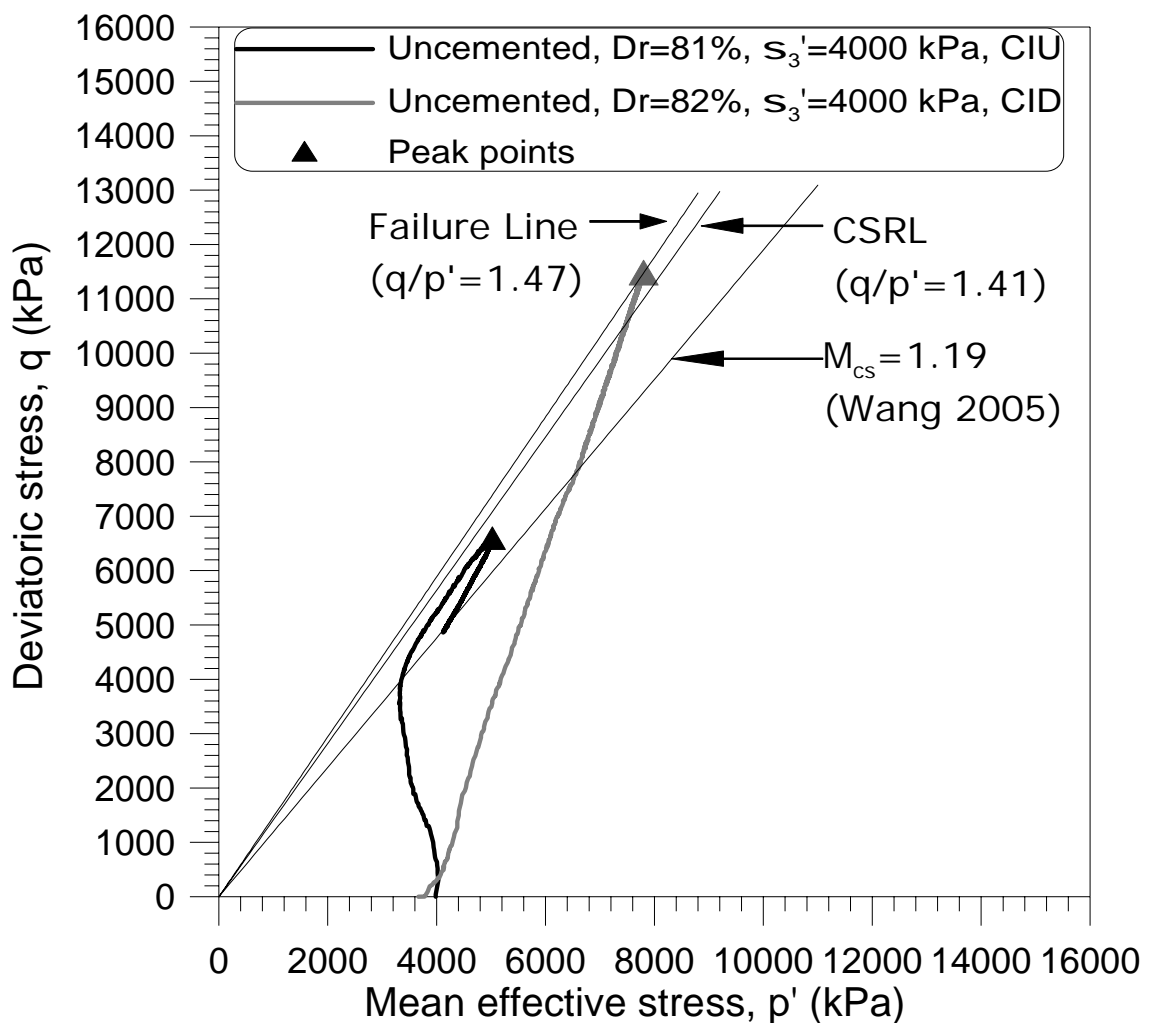


(b)

Figure 4.8 Results of uncemented specimens in CIU and CID triaxial test: (a) stress-strain behaviour; (b) q/p' versus e_1 curves; (c) effective stress paths.

to the end. In CID test, the total stress path which expect to increase in slop 1:3 to approach the failure line. However, the result seems not to follow the expectation and

the peak point is above the CSRL. This may cause by the difference of the relative density or the fit of CSRL. Nevertheless, It appears that more test should be conducted to clarify this. In CIU test, the stress path which increase upward at the beginning, and then they incline to follow the constant stress ratio line (CSRL) until the maximum deviatoric stress reached. Following this, it turns to opposite direction to the end. In CID test, the total stress path which expect to increase in slop 1:3 to approach the failure line. However, the result seems not to follow the expectation and the peak point is above the CSRL.



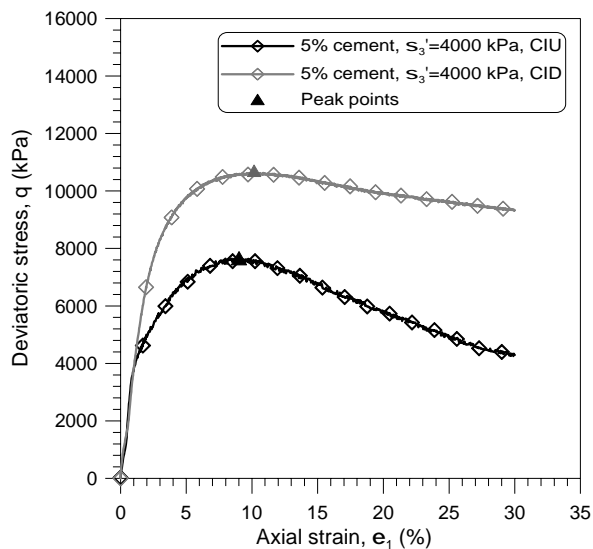
(c)

Figure 4.8 Continued

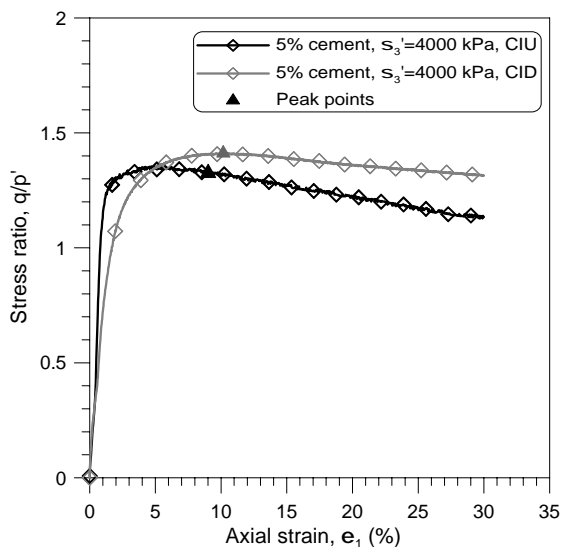
4.4.2 Cemented sand

The results of cemented content under high confining pressure (4000kPa) specimens

in CIU and CID tests are shown in figure 4.9. Deviatoric stress (q), excess pore water pressure (u), and stress ratio (q/p') plotted against axial strain (ϵ_1), and the



(a)



(b)

Figure 4.9 Results of cemented specimens in CIU and CID triaxial test: (a) stress-strain behaviour; (b) q/p' versus ϵ_1 curves; (c) effective stress paths.

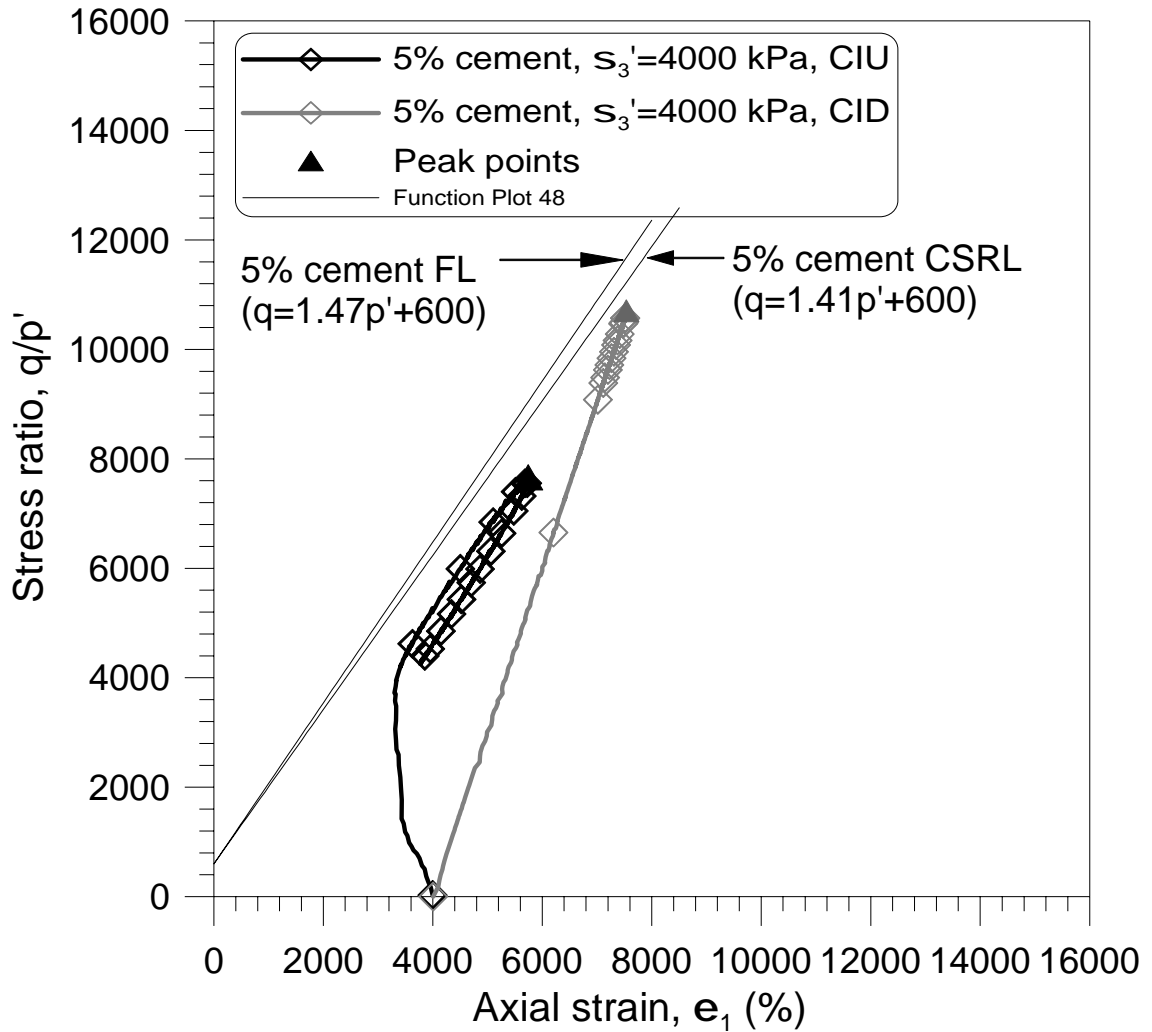


Figure 4.9 continued.

effective stress paths are shown as well.

As shown in figure 4.9 (a), the deviatoric stresses against strain in CID and CIU tests shows the same tendency as uncemented specimen. In CID and CIU test, the peak deviatoric stresses which occur at 10.17% and 9.01% axial strain are 10637kPa and 7661kPa, respectively. The peak deviatoric stress of CID test is higher than CIU test, and occurs at larger strain.

In figure 4.9 (b), the maximum stress ratio in CID test is higher than CIU test and it occurs large axial strain. As shown in figure 4.9 (c), the stress paths of CID and CIU tests show different routes. In CIU test, the stress path which increase upward at the

beginning, and then they incline to follow the constant stress ratio line (CSRL) until the maximum deviatoric stress reached. Following this, it turns to opposite direction to the end. In CID test, the total stress path which increase in slop 1:3 to approach the failure line. It appears that FL and CSRL can be curves. However, more results are needed to verify these.

Chapter 5 Conclusions and recommendations for further research

5.1 Conclusions

A series of laboratory tests including uncemented and cemented Portaway sand CIU triaxial tests of at high pressures and conventional pressure has been carried out to understand the behaviour of cemented sand. Portland cement was used as cementation agent for preparing artificially cemented specimens. The results provide the following main conclusion:

1. Stress-strain curves show that maximum deviatoric stresses and stiffness increases with an increase in cement content, density, and the confining pressure. The effect of confining pressure to peak deviatoric stress declines with the increase of confining pressure in uncemented specimens.
2. The drainage conditions influence maximum deviatoric stresses, stress ratios and stiffness in both cemented and uncemented specimens. The stress-strain curves in CID tests have higher maximum deviatoric stresses, stress ratios and stiffness than CIU ones. The Failure line and CSRL can be curves in p' - q space.
3. Stress ratio against strain curves show that peak stress ratios increase with an increase in cement content and density. Each curves approaches to a constant value at large strain level.
4. The excess pore water pressures for both uncemented specimen of medium dense density and 10% and 15% cement content specimens at high pressure are positive during the tests.
5. The excess pore water pressure for uncemented specimens of dense density, 5% cement content specimens at high confining pressure and cemented specimens at conventional confining pressures are positive at beginning of the test, and

then the values change to negative as axial strains increase. The transition from positive excess pore water pressure to negative in uncemented and 5% cement content specimens are gradually, while it is extremely sharp in 10% and 15% cement content at high confining pressure.

6. The effective stress paths in dense and cemented specimens at conventional and high confining pressure are similar. They all increase upward at the beginning, and then they incline to approach the CSRL with the slope of 1.41 until the maximum deviatoric stress is reached. It appears that cohesion intercepts increase to a power of 1.77 of cement content. It means that there is a non-linear relationship between the cohesion intercept of CSRL.
7. The effective stress path of medium dense sand can be used to determine the instability line.
8. The effect of confining pressure to peak deviatoric stress declines with the increase of confining pressure in uncemented specimens.
9. The higher cement content leads to higher maximum deviatoric stress and lets the peak deviatoric stress occur earlier. The behaviours of uncemented and 5% cemented specimens are different from 10% and 15% cemented specimens. 10% and 15% cemented specimens show clear peaks and their maximum deviatoric stresses. However, the peak deviatoric stress of uncemented and 5% cemented specimens is not so obvious. The deviatoric stress in high confining pressure may be more sensitive when cement content is between 5% and 10%. However, it needs more results to clarify.

5.2 Recommendations for future research

This project has provided some understanding of the stress-strain behaviour of cemented and uncemented sands at high pressures. However, more experimental studies are still essential for further understanding. Further experiments and ideas

are outlined below.

- CIU tests conducted in higher confining pressure, i.e. the confining pressure over 20MPa to investigate the influence of the high confining pressure.
- CIU tests for lower cement content, i.e. 1%, 3%, 7% to clarify the effect of cement content.
- Relative CID tests should be carried out to explore the effect of drainage.
- With more data obtained could be used to examine or improve existing constitutive models to simulate behaviour of cemented materials more accurately.

References

- Airey, D.W. (1993), "Triaxial testing of naturally cemented carbonate soil", *Journal of Geotechnical Engineering*, 119, 1379.
- Asghari, E., Toll, D.G. and Haeri, S.M. (2003), "Triaxial behaviour of a cemented gravely sand, Tehran alluvium", *Geotechnical and Geological Engineering*, 21(1), 1-28.
- Boey, C.F. (1990), "Modelling of the behaviour of natural calcarenite. Ph.D. thesis, University of Sydney.
- Clough, G. W., Sitar, N., & Bachus, R. C. (1981). "Cemented sands under static loading. *J. Geotech. Engrg.*", ASCE, Vol. 107, No. 6, pp. 799-817.
- Consoli, N.C., Foppa, D., Festugato, L. and Heineck, K.S. (2007), "Key Parameters for Strength Control of Artificially Cemented Soils", *Journal of Geotechnical and Geoenvironmental Engineering*, 133, 197.
- Coop, M.R. and Atkinson, J.H. (1993), "The mechanics of cemented carbonate sands", *Geotechnique*, 43(1), 53-67.
- Cuccovillo, T., & Coop, M. R. (1999), "On the mechanics of structured sands", *Géotechnique*. Vol. 49, No. 6, pp. 741-760.
- Das, B.M., Yen, S.C. and Dass, R.N. (1995), "Brazilian tensile strength test of lightly cemented sand", *Canadian Geotechnical Journal*, 32(1), 166-171.
- Haeri, S.M., Hosseini, S.M., Toll, D.G. and Yasrebi, S.S. (2005), "The behaviour of an artificially cemented sandy gravel", *Geotechnical and Geological Engineering*, 23(5), 537-560.
- Hooker, P. (2002). "The development of automated testing in geotechnical engineering", *Proc. of the Indian Geotechnical Conference*, December 2002.

- Huang, J.T. and Airey, D.W. (1993), "Effects of cement and density on an artificially cemented sand", *Geotechnical engineering of hard soils–soft rocks*. Edited by A. Anagnostopoulos, F. Schlosser, N. Kalteziotis, and R. Frank. AA Balkema, Rotterdam, 553–560.
- Huang, J.T. and Airey, D.W. (1998), "Properties of artificially cemented carbonate sand", *Journal of Geotechnical and Geoenvironmental Engineering*, 124(6), 492-499.
- Ismail, M.A., Joer, H.A., Sim, W.H. and Randolph, M.F. (2002), "Effect of cement type on shear behavior of cemented calcareous soil", *Journal of Geotechnical and Geoenvironmental Engineering*, 128, 520.
- Lade, P.V. and Yamamuro, J.A. (1996), "Undrained Sand Behavior in Axisymmetric Tests at High Pressures", *Journal of Geotechnical and Geoenvironmental Engineering*, 122(2), 120.
- Leroueil, S. & Vaughan, P. R., (1990). The general and congruent effects of structure in natural soils and weak rocks. *Géotechnique*. Vol. 40, No. 3, pp. 467-488.
- McLelland, B. (1988). *Calcareous sediments: an engineering enigma*. Proc. Int. Conf. on Calcareous Sediments, 2, pp. 777-786.
- Powrie, W. (2004). "Soil mechanics : concepts and applications" E&F Spon Press, London
- Rotta, G.V., Consoli, N.C., Prietto, P.D.M., Coop, M.R. and Graham, J. (2003), "Isotropic yielding in an artificially cemented soil cured under stress", *Geotechnique*, 53(5), 493-501.
- Schnaid, F., Prietto, P.D.M. and Consoli, N.C. (2001), "Characterization of cemented sand in triaxial compression", *Journal of Geotechnical and Geoenvironmental Engineering*, 127(10), 857-868.

Wanatowski, D. and Chu, J. (2008), "Undrained behaviour of Changi sand in triaxial and plane-strain compression", *Geomechanics and Geoengineering*, 3(2), 85-96.

Wang, J. (2005), *The Stress-Strain and Strength Characteristics of Portaway Sand*, The University of Nottingham, Nottingham.

Yamamuro, J.A. and Lade, P.V. (1996), "Drained sand behavior in axisymmetric tests at high pressures", *Journal of Geotechnical Engineering*, 122, 109.

Yu, H.S., Tan, S.M. and Schnaid, F. (2007), "A critical state framework for modelling bonded geomaterials", *Geomechanics and Geoengineering*, 2(1), 14.